Characterisation of Syncoilin

William Thomas Clarke

Merton College
University of Oxford

Submitted for the degree of Master of Science, 2009

Abstract

Characterisation of syncoilin

William Thomas Clarke

Merton College
University of Oxford

A thesis submitted for the degree of Master of Science

Hilary term, 2009

Syncoilin is a 64kDa intermediate filament protein (IF) first studied because it binds to the dystrophin associated protein complex (DAPC) through α-dystrobrevin. Syncoilin is highly expressed in skeletal and cardiac muscle, but the function of syncoilin in muscle remains largely unknown. A recently generated syncoilin null (*sync*-/-) mouse has almost no muscle phenotype. This thesis makes significant progress in characterising the function of syncoilin in muscle and nerve and discovering a phenotype in the *sync*-/- mouse.

The first half of this thesis attempts to further elucidate the function of syncoilin in muscle. Two new syncoilin isoforms were discovered in muscle, and syncoilin was shown to be upregulated in muscle during atrophy and regeneration. *Sync*+/+ and *sync*-/- primary muscle cell lines were generated in an attempt to elucidate a signalling role for syncoilin in muscle, but no difference was discovered between the two cell lines in cell growth, drug resistance or protein synthesis.

Recent discoveries from this laboratory reveal that syncoilin is also expressed in neurons. The second half of this thesis is an attempt to characterise the function of syncoilin in neurons. Two potential syncoilin neuronal binding partners were examined. Syncoilin and α-tubulin bind via co-immunoprecipitation, but there is no co-localisation between the two proteins in sciatic nerve. Peripherin was shown to co-localise with syncoilin in sciatic nerve, and co-transfections suggest that syncoilin acts to regulate peripherin filament formation.

Finally, a neuronal analysis of the *sync*-/- mouse shows decreased motor function in a range of behavioural tests. This observation is confirmed with the discovery that motor neurons in the *sync*-/- mouse have decreased axon calibre when compared to the *sync*+/+ mouse. The possibility that syncoilin plays a vital role in neuronal function is a significant discovery and opens an exciting new avenue of research.

Declaration

The work in this thesis was performed in the Department of Physiology, Anatomy & Genetics. Except where acknowledgement is made, all of the work presented is my own and has not been submitted for any other degree in this or any other University or institute of learning.

Acknowledgements

I would first like to thank Professor Dame Kay Davies for all of her support, guidance and advice. Not only am I indebted to Kay for allowing me to be a part of her group, but her assistance in my scholarship application process was critical to me being able to spend these past two years in the UK.

I am extremely grateful to the British government and the Marshall Aid Commemoration Commission for giving me the opportunity to live and study in Britain. I cannot imagine it would be possible for me to leave the UK with a more favourable impression.

Ben Edwards, Dr. Matt Kemp, Matthew Burgess and Dr. Catherine Moorwood taught me everything there is to know about syncoilin and never stopped answering my questions. Ben picked me up from Anatomy reception on my first day and has been a constant support ever since. He has been involved in all of my experiments and has helped me review every page of this thesis. There are many people who have worked on the syncoilin project before me. Their work is greatly appreciated and is regularly cited throughout this thesis.

In the lab, Dr. Peter Oliver, Dr. Dirk Baumer, Dr. Justin Moore and Dr. Esther Becker gave me a crash course in neurology and provided excellent advice on all of the neuronal work in this thesis. Mohan Masih provided fantastic technical assistance.

Arran, Akshay, Sarah, Aurelie, Carmen, Dave, Ally, Rebecca and those already named plus everyone else in the lab have been fantastic friends and have kept me thoroughly entertained. Without them, my life would be much less fun and I would be much less British.

I am greatly indebted to many people in Arizona and at UCLA. Most of all, I am thankful for my family and all of their love and support.

Contents

Chapter 1: Introduction

1.1 Muscular dystrophy and the DAPC

1.1.1 The dystrophin associated protein complex

The dystrophin associated protein complex (DAPC) of proteins is found at the sarcolemma of muscle fibres (Ervasti, Ohlendieck et al. 1990). The DAPC is comprised of dystrophin (Koenig, Monaco et al. 1988), α- and β-dystroglycan (Ibraghimov-Beskrovnaya, Ervasti et al. 1992), α-dystrobrevin (Sadoulet-Puccio, Khurana et al. 1996), α-, β-, γ- and δ-sarcoglycan (Roberds, Anderson et al. 1993, Lim, Duclos et al. 1995, Noguchi, McNally et al. 1995b, Jung, Duclos et al. 1996), α1- and β1-syntrophin (Adams, Butler et al. 1993) and sarcospan (Crosbie, Heighway et al. 1997). The DAPC provides a structural link between the extracellular matrix (ECM) and internal cytoskeleton (Koenig, Monaco et al. 1988). Extracellular DAPC component α-dystroglycan binds laminin-2 and perlecan in the ECM (Ibraghimov-Beskrovnaya, Ervasti et al. 1992, Talts, Andac et al. 1999). Many intracellular DAPC components directly or indirectly interact with the cytoskeleton. Most notably, dystrophin binds filamentous actin (Levine, Moir et al. 1992). Dystrophin and β-dystroglycan both bind plectin, a protein that links to all three types of cytoskeletal proteins including intermediate filaments (IFs) desmin (Hijikata, Murakami et al. 2003, Rezniczek, Konieczny et al. 2007), vimentin (Svitkina, Verkhovsky et al. 1996) and synemin (Hijikata, Nakamura et al. 2008), γ- and α-actin (Svitkina, Verkhovsky et al. 1996, Foisner, Bohn et al. 1995) and microtubules (Svitkina, Verkhovsky et al. 1996). The DAPC has several other links with desmin via intermediaries such as the synemins that bind dystrophin (Bhosle, Michele et al. 2006) and syncoilin that binds α-dystrobrevin (Newey, Howman et al. 2001, Poon, Howman et al. 2002). Dystrophin interacts directly with IF protein cytokeratin 19 and indirectly with cytokeratin 8 (Ursitti, Lee et al. 2004, Stone, O'Neill et al. 2005, Thompson, Chan et al. 2000).

1.1.2 The structural function of the DAPC

Tremendous amounts of force are generated in the muscle contractile apparatus. Ultimately, this force must then be transmitted from muscle to the skeletal system in order to produce movement. Some force is transmitted directly from muscle fibres to tendons at the myotendinous junction. However, most force is transmitted via the ECM. From the contractile apparatus, force is transmitted within the muscle fibre to Z-disks. Force is then transmitted to the DAPC at the sarcolemma by cytoskeletal components including desmin IFs and actin filaments. The DAPC transmits force to the ECM which ultimately results in force on the skeletal system and movement (Patel, Lieber 1997, Ervasti 2003, Monti, Roy et al. 1999).

The DAPC is essential for normal muscle strength and structural integrity, especially in its role as a physical link between the internal cytoskeleton and the external extracellular ECM. Patients and mouse models with mutations in different DAPC components that lead to the loss of the DAPC have similar muscle phenotypes. Mutations in dystrophin (Hoffman, H. et al. 1987), the sarcoglycans (Lim, Duclos et al. 1995, Noguchi, McNally et al. 1995a, McNally, Duggan et al. 1996, Roberds, Leturcq et al. 1994, Piccolo, Roberds et al. 1995, Bonnemann, Modi et al. 1995, Passos-Bueno, Terwilliger et al. 1991, Nigro, de Sa Moreira et al. 1996), laminin-α2 (ter Laak, Leyten et al. 1998) and desmin (Hoffman, Schwartz 1991, Goldfarb, Park et al. 1998, Munoz-Marmol, Strasser et al. 1998, Sjoberg, Saavedra-Matiz et al. 1999) all cause human muscular dystrophies.

1.1.3 Muscular dystrophies caused by DAPC mutations

All muscular dystrophies cause progressive muscular weakness, but the clinical manifestations of different forms of muscular dystrophy vary. In more severe forms of the disease, there can be a loss of muscle function and cardiac and respiratory failure.

At a histological level, muscular dystrophy is characterised by sarcolemmal damage, cycles of muscle degeneration and regeneration, hypertrophy and the gradual replacement of muscle with connective and adipose tissue (Hoffman, Schwartz 1991, Emery 2002).

In many cases, the absence of a single DAPC component results in the loss of all or part of the DAPC from the sarcolemma. Patients and mouse models with all or partial loss of the DAPC have similar muscle phenotypes including a reduced muscular force-generating capacity (Carlson, Makiejus 1990, Cox, Cole et al. 1993) and an increased susceptibility to sarcolemmal damage (Menke, Jockusch 1991, Weller, Karpati et al. 1990, Matsuda, Nishikawa et al. 1995). The loss of dystrophin, the cause of Duchenne muscular dystrophy (DMD), results in the loss of the entire DAPC from the sarcolemma (Ervasti, Ohlendieck et al. 1990, Ibraghimov Beskrovnaya, Ervasti et al. 1992, Ohlendieck, Campbell 1991, Compton, Cooper et al. 2005, Metzinger, Blake et al. 1997). Becker muscular dystrophy (BMD) is also caused by mutations in dystrophin, but BMD is less severe than DMD because BMD patients have only a partial reduction in functional dystrophin and therefore only a partial reduction of DAPC at the sarcolemma (Blake, Martin-Rendon 2002, Davies, Nowak 2006, Cohn, Campbell 2000).

In the dystroglycan knockout mouse model, the entire DAPC is usually lost, resulting in a mild phenotype that resembles *mdx* mice that have loss of dystrophin and the rest of the DAPC (Cohn, Henry et al. 2002, Cote, Moukhles et al. 2002). Mutations in α-, β-, γ- and δ-sarcoglycans cause limb-girdle muscular dystrophy types 2D, 2E, 2C and 2F, respectively (Lim, Duclos et al. 1995, Noguchi, McNally et al. 1995a, Roberds,

Leturcq et al. 1994, Piccolo, Roberds et al. 1995, Passos-Bueno, Terwilliger et al. 1991, Nigro, de Sa Moreira et al. 1996). In the absence of one of the sarcoglycans, dystrophin and dystroglycan normally remain at the sarcolemma, but the remainder of the sarcoglycans are lost or severely reduced (Hack, Ly et al. 1998, Hack, Lam et al. 2000, Barresi, Confalonieri et al. 1997, Araishi, Sasaoka et al. 1999).

The DAPC is retained at the sarcolemma in muscular dystrophies caused by mutations in proteins that are not part of the DAPC. It is believed that these muscular dystrophies are a result of protein mutations that create structural deficiencies in the link between the cytoskeleton and ECM (Sjoberg, Saavedra-Matiz et al. 1999, Draviam, Billington et al. 2001, Merlini, Villanova et al. 1999). IF protein desmin (Goldfarb, Park et al. 1998) and ECM component collagen VI (Jobsis, Keizers et al. 1996) are part of the extended DAPC support network, and mutations in either of these proteins can cause muscular dystrophies. A severe congenital muscular dystrophy is caused by mutations in laminin-2, an ECM ligand for α-dystroglycan (Xu, Wu et al. 1994, Helbling-Leclerc, Zhang et al. 1995). Mutations in proteins such as fukutin (Kobayashi, Nakahori et al. 1998), LARGE (Grewal, Holzfeind et al. 2001, Longman, Brockington et al. 2003) and POMT1 (Beltran-Valero de Bernabe, Currier et al. 2002, Balci, Uyanik et al. 2005) that glycosylate α-dystroglycan reduce the affinity of α-dystroglycan for its ECM ligands. Although the DAPC is still intact, its connection to the ECM is weakened and results in various muscular dystrophies such as Fukuyama congenital muscular dystrophy (FCMD), Walker-Warburg syndrome (WWS) and limb-girdle muscular dystrophy.

1.1.4 The signalling function of the DAPC

The structural importance of the DAPC has been well documented, but there is evidence that the DAPC is also involved in signal transduction. It is known that signalling is perturbed in muscular dystrophy, but it is unclear if this is due to the loss of the DAPC or a result of cell damage in dystrophic muscle. Many signalling molecules and pathways are associated with the DAPC. Some of these pathways are discussed below.

Calmodulin binds DAPC components dystrophin and α1-syntrophin (Madhavan, Massom et al. 1992). Calmodulin is known to play a role in the Akt-mediated cell survival signalling pathways that have been shown to induce skeletal muscle hypertrophy (Rando 2001, Rommel, Bodine et al. 2001). It is also hypothesised that calmodulin regulates the interaction between dystrophin and actin by competing with actin for dystrophin binding (Jarrett, Foster 1995).

Adaptor protein Grb2 binds DAPC components β-dystroglycan and α1-syntrophin (Oak, Russo et al. 2001, Russo, Di Stasio et al. 2000). Grb2 is involved in the MAP kinase (MAPK) cell growth and survival signalling pathway, (Chardin, Cussac et al. 1995) the PI3K/Akt survival signalling (Langenbach, Rando 2002) and the c-Jun cell proliferation pathway (Oak, Zhou et al. 2003). The loss or disruption of any of these signalling pathways could contribute to muscle disease.

Extracellular signal-related kinases (ERKs) 1 and 2 are involved in MAPK mechanical force signalling (Martineau, Gardiner 2001), cardiac sarcomere organisation (Hornberger, Armstrong et al. 2005) and anti-apoptotic pathways (Chang, Karin 2001). Muscle from *mdx* and γ-sarcoglycan-null mice have abnormal

ERK1 and ERK2 phosphorylation in response to eccentric contraction, suggesting an intact DAPC is necessary for proper ERK signalling (Barton 2006, Griffin, Feng et al. 2005). ERKs 1 and 2 could function in mediating a DAPC response to mechanical stress.

The DAPC has been shown to play an important structural role in muscle, and there is growing evidence that the DAPC has a role in signalling. Several DAPC components are implicated in muscular dystrophy, but many aspects of the DAPC and its role in muscle disease remain unclear. There currently exists no cure for DMD, so a better understanding of the DAPC and its associated proteins is important for the development of future therapies.

1.2 Syncoilin

A yeast two-hybrid experiment was performed to investigate the signalling role of α-dystrobrevin in the DAPC. In this screen of a skeletal muscle cDNA library, syncoilin was identified as a novel binding partner for α-dystrobrevin (Newey, Howman et al. 2001). Another yeast two-hybrid experiment using syncoilin as the bait protein identified the muscle-specific IF protein desmin (Poon, Howman et al. 2002). These discoveries were significant because they demonstrated a direct link between the DAPC and desmin. This link suggested that syncoilin might play an important role in structurally connecting the DAPC with the IF cytoskeletal network.

A sequence analysis identified syncoilin as an IF protein with the greatest homology to type III IF chains (Newey, Howman et al. 2001, Kemp, Edwards et al. 2008). However, syncoilin has never been observed to form filaments alone or with other IF proteins *in vivo* or *in vitro* (Poon, Howman et al. 2002). Furthermore, when co-

transfected with desmin in COS-7 cells, syncoilin disrupts the desmin IF network which forms when desmin is transfected alone (Poon, Howman et al. 2002). This suggests syncoilin might regulate the formation of desmin IFs *in vivo*.

Syncoilin is highly expressed in skeletal and cardiac muscle (Newey, Howman et al. 2001). In skeletal muscle, syncoilin is expressed at the sarcolemma and enriched at neuromuscular junctions (NMJs) and myotendinous junctions (MTJs). Additional syncoilin expression is also seen in the perinuclear space, at the Z-lines and in low levels in the cytoplasm (Newey, Howman et al. 2001, Poon, Howman et al. 2002, McCullagh, Edwards et al. 2007).

Syncoilin has altered localisation and expression in a number of muscle diseases. Increased syncoilin expression is seen at the sarcolemma of patients with DMD and congenital muscular dystrophy as well as in *mdx* mice null for dystrophin and more severe double knockout mice null for dystrophin and utrophin (Newey, Howman et al. 2001, Howman, Sullivan et al. 2003, Brown, Torelli et al. 2005). In DMD patients, syncoilin immunolabelling was high in small, immature regenerating muscle fibres (Brown, Torelli et al. 2005). The upregulation of syncoilin leads to the hypothesis that syncoilin has a specific function in regenerating muscle fibres and muscular dystrophy.

Syncoilin is known to bind both α-dystrobrevin and desmin, so it was investigated how syncoilin is affected in the absence of either of those proteins. In the desmin-null mouse, syncoilin was lost from the sarcolemma, but in the α-dystrobrevin-null mouse, syncoilin maintained its normal localisation at the sarcolemma with increased

expression. The α-dystrobrevin-null mouse has skeletal and cardiac myopathies, and increased syncoilin immunostaining was especially seen in small, immature muscle fibres indicative of regenerating myopathic muscle (McCullagh, Edwards et al. 2007, Grady, Grange et al. 1999). Furthermore, changes in syncoilin protein levels in both null mice were not seen at the mRNA level, suggesting the loss of syncoilin is due to protein instability or translation rate (McCullagh, Edwards et al. 2007). This information shows that syncoilin localisation is dependent on desmin but not α-dystrobrevin for proper localisation and that syncoilin is upregulated in myopathic regenerating muscle.

Two separate syncoilin-null mice have been generated, yet neither displays an overt phenotype. Extensive muscle analysis suggests that syncoilin is dispensable for skeletal and cardiac muscle development. Loss of syncoilin results in a slight decrease of maximum muscle strength and resilience and may cause an increased susceptibility to muscle damage (Zhang, Bang et al. 2008, McCullagh, Edwards et al. 2008).

Syncoilin has been shown to be upreguated in diseased muscle and is known to interact with both the DAPC and desmin IF network. This information makes syncoilin an interesting subject for future research, and the work presented in this thesis will aim to advance the knowledge of the function of syncoilin.

1.3 Intermediate filaments

Intermediate filaments (IFs) are a family of proteins that share similar sequence and structural features. IFs are one of three primary components of the cytoskeleton along with microtubules and actin microfilaments. In Section 1.2, syncoilin was identified as an intermediate filament (IF) protein with homology to type III IF chains. This

section will describe the structure and function of IF proteins and give examples of IF proteins and associated diseases.

1.3.1 Structure of intermediate filament proteins

IFs are characterised by their specific structural features and domain functions. IFs have an average diameter of 10 nm and a hollow cylindrical shape. The conserved IF domain structure consists of head and tail globular domains at the N- and C-terminal ends surrounding an α-helical rod domain. The rod domain consists of coiled-coil domains 1A, 1B, 2A and 2B that are connected by short linker regions L1, L12 and L2. The coiled-coil domains and linker region L2 are highly conserved with a defined number of amino acids. Coiled-coil domains also have a heptad repeat in their amino acid structure. A conserved characteristic of IF proteins is an interruption of the heptad repeat called a "stutter" in helix 2B (Parry, Steinert 1999). The head and tail domains are more variable in their size, sequence and structure and are important for distinguishing different IF proteins (Parry, Strelkov et al. 2007). These differences affect the ability of IFs to interact with other proteins including other IF proteins for filament formation.

1.3.2 Classes of IF proteins

IF proteins are divided into six classes based on their domain structure, ability to self-assemble or dimerise and expression pattern. Types I and II are keratins with acidic keratins classified as type I and basic keratins as type II (Schweizer, Bowden et al. 2006). Type III IFs, which share the most homology with syncoilin, include vimentin, glial fibrillary acidic protein (GFAP), desmin and peripherin. Type IV IF proteins consists of the neurofilaments and α-internexin, type V consists of the nuclear lamins and type VI includes synemin, paranemin and nestin (DePianto, Coulombe 2004, Toivola, Tao et al. 2005).

1.3.3 Assembly of intermediate filament networks

The different classes of IF proteins vary in their filament formation. Type III and IV proteins form dimers through parallel coiled-coil associations. These dimers form tetramers using staggered antiparallel associations. Tetramers bind end-to-end to form unit length filaments (ULFs) that are approximately 55 nm in length. ULFs bind end-to-end and rearrange tetramers before forming immature filaments approximately 16 nm in width and several μm in length. Another rearranging takes place when the proteins condense from 16 nm in width to approximately 10 nm in width, creating mature IFs (Parry, Strelkov et al. 2007, Herrmann, Aebi 2004).

Filaments can be formed either by homopolymerisation of the same IF protein or by heteropolymerisation of multiple IF proteins. Keratins only form dimers comprised of one type I acidic keratin and one type II basic keratin. All type III IF proteins can self-assemble into homopolymers, but type III IFs are more likely to form heteropolymers. For example, type III IF protein vimentin can form filaments with type III IF proteins such as desmin, peripherin and GFAP and with type IV IF proteins NF-L and α-internexin (Herrmann, Aebi 2000). Syncoilin, which shares the most homology with type III filaments, has not been shown to be able to form filaments. Type IV IF proteins neurofilaments form heteropolymers containing all three neurofilaments (Lee, Xu et al. 1993) while α-internexin self-assembles (Ching, Liem 1998),

Intermediate filaments are dynamic in ways that actin filaments and microtubules are not. Actin filaments and microtubules can only grow or contract by adding to the ends, but IF subunits can grow or contract from the sides of the filament in addition to the ends. By growing or contracting from the sides, the number of subunits per filament cross-section can vary even in the same type of filament (Parry, Strelkov et

al. 2007, Herrmann, Aebi 1999, Engel, Eichner et al. 1985). IFs are known to form three different structures of varying sizes including extended filamentous networks, short filaments known as “squiggles” and particles that range from 0.1 – 1 μm in length (Chou, Flitney et al. 2007).

1.3.4 Functions of intermediate filaments

Intermediate filament networks are cytoskeletal components found throughout the cytoplasm. IFs are unique because of their flexibility, including the ability to stretch to more than three times their normal length and their ability to reassemble after acute damage (Wagner, Rammensee et al. 2007). IFs provide mechanical strength including intracellular structure and organelle positioning. For example, the disruption of the vimentin IF network results in a loss of normal cell morphology and nuclear invaginations (Goldman, Khuon et al. 1996, Sarria, Lieber et al. 1994). Desmin is necessary for the proper distribution and morphology of mitochondria and nuclei (Paulin, Li 2004), and mutations in lamin A/C result in abnormal mitochondria, rough endoplasmic reticulum and nuclei (Mounkes, Kozlov et al. 2005, Nikolova, Leimena et al. 2004).

Mutations in IF proteins cause structural and mechanical defects, resulting in a variety of diseases (Pekny, Lane 2007). In epidermolysis bullosa simplex (EBS), mutant keratins fail to form IF networks. This results in cell lysis in the basal layer of the epidermis following standard mechanical stress (Coulombe, Hutton et al. 1991). Mutant keratins are also responsible for epidermolytic hyperkeratosis. Keratin aggregations result in abnormal filament networks that weaken the suprabasal skin layer (Cheng, Syder et al. 1992). Emery-Dreifuss muscular dystrophy is caused by mutations in lamin A that result in a weakened muscle fibre (Bonne, Di Barletta et al.

1999). Charcot-Marie-Tooth disease type 2E (CMT2E) is the result of abnormal mitochondrial distribution caused by mutations in the neurofilament light chain (Perez-Olle, Lopez-Toledano et al. 2005).

IFs are important for extracellular as well as intracellular structure. For example, vimentin and keratins bind α6β4 integrins which are connected to the ECM (van der Neut, Krimpenfort et al. 1996, Homan, Mercurio et al. 1998). The importance of vimentin is shown in vimentin-null fibroblasts that are unable to reorganise collagen in the ECM (Eckes, Dogic et al. 1998) and in vimentin siRNA knock-down cells that have reduced cell adherence under fluid shear stress (Tsuruta, Jones 2003).

1.3.5 Intermediate filaments and intracellular signalling

In addition to their structural function, IFs are known to bind several signalling proteins. It is hypothesised that IFs use the filament network to guide signalling proteins to their proper subcellular localisation (Perlson, Hanz et al. 2005, Dinsdale, Lee et al. 2004). IFs also play an important mechanical role in the cell. Recent studies suggest that IFs are able to initiate signalling cascades following mechanical stress that result in protein synthesis, cell growth or survival response (Kim, Wong et al. 2006, Galarneau, Loranger et al. 2007).

Two examples of IFs in signalling are keratins 8 and 17 (K8 and K17). K8 and K17 interact with adaptor protein 14-3-3, a modulator of the Akt/mTOR (mammalian target of rapamycin) signalling pathway. Akt/mTOR regulates protein synthesis and cell growth (van Heusden 2005). K8-null hepatocytes have changes in Akt activation and reductions in protein synthesis and cell size (Galarneau, Loranger et al. 2007). In response to injury, K17-null keratinocytes have reductions in Akt/mTOR signalling,

resulting in smaller cells and decreased protein translation. This suggests that K17 is necessary for normal Akt/mTOR-mediated signalling in response to damage (Kim, Wong et al. 2006).

In addition to cell growth and regeneration, the keratins are also involved in apoptosis. K8 and K18 bind death effector domain-containing DNA-binding protein (DEDD) and assist DEDD in activating the caspases, an important family of proteins in the apoptotic pathway (Dinsdale, Lee et al. 2004). In fact, IF proteins vimentin and desmin are cleaved by caspases during apoptosis and disrupt IF networks (Marceau, Schutte et al. 2007). Vimentin plays an important signalling role following axonal injury by preventing the dephosphorylation of ERK1/2. Phosphorylated ERK1/2 activates transcription factors that contribute to axonal regeneration. Vimentin-null mice have impaired axonal regeneration following damage (Perlson, Hanz et al. 2005).

1.3.6 Intermediate filaments in neurons

As discussed in Section 1.2, syncoilin is expressed in skeletal and cardiac muscle. However, Chapter 6 in this thesis will show that syncoilin is also expressed in neurons. IF expression in neurons is limited to six other proteins: peripherin, neurofilaments NF-M, NF-H and NF-L, α-internexin and synemin. Many IF proteins are associated with diseases of the peripheral nervous system. Some of these neuropathies are associated with abnormal accumulations of IF proteins that are hypothesized to interfere with axonal transport (Lariviere, Julien 2004).

1.3.6.1 Peripherin

Peripherin is a type III IF primarily expressed in the peripheral nervous system (PNS) (Troy, Brown et al. 1990). Peripherin is upregulated following injury such as sciatic

nerve crush, a response that is associated with neuronal regeneration (Troy, Muma et al. 1990).

Peripherin-null mice display no overt phenotype but have reductions in unmyelinated sensory neurons. Type IV IF protein α-internexin is upregulated in the peripherin-null mouse, suggesting compensation by another IF protein (Lariviere, Nguyen et al. 2002). Transgenic mice overexpressing peripherin have a more substantial phenotype with late-onset motor neuron loss. This could be due to the presence of peripherin inclusions in the axon and cell body (Beaulieu, Nguyen et al. 1999). Peripherin is known to form heteropolymers with neurofilaments, so the peripherin overexpressing mouse was crossed with mice overexpressing and lacking neurofilaments (Lee, Xu et al. 1993). A mouse that overexpresses peripherin but is null for type IV IF protein NF-L had an earlier onset of IF inclusions and motor neuron death than the peripherin overexpressing mouse (Beaulieu, Nguyen et al. 1999). However, the overexpression of NF-H combined with the overexpression of peripherin resulted in a rescue of the disease phenotype. Overexpression of both proteins shifted inclusions from the axon to the cell body, suggesting that the disease was caused by axonal accumulations resulting from abnormal IF protein stoichiometry (Beaulieu, Julien 2003).

Peripherin is associated with the disease amyotrophic lateral sclerosis (ALS). ALS is characterised by progressive degeneration of motor neurons in the spinal cord, motor cortex and brainstem. Peripherin is often found in inclusion bodies in motor neurons of patients with the disease (Xiao, McLean et al. 2006, Mitchell, Borasio 2007). Two peripherin mutations are known to increase ALS susceptibility. An asparagine to tyrosine substitution (D141Y) within the linker 1 region results in improper filament

formation and aggregates (Leung, He et al. 2004). A base pair deletion (222ΔC) in the tail domain disrupts the assembly of neurofilament NF-L (Gros-Louis, Lariviere et al. 2004). Two alternatively spliced isoforms of peripherin are also associated with ALS. Per28 includes introns 3 and 4 and causes peripherin aggregation when upregulated. Per28 expression is upregulated at the mRNA and protein levels in ALS patients and is associated with inclusions in those patients (Xiao, Tjostheim et al. 2008). Per61 includes intron 4 and disrupts the normal assembly of peripherin. Per61 is found in axonal inclusions of familial ALS patients and mouse models for familial ALS but is not present in wild-type mice (Robertson, Doroudchi et al. 2003).

1.3.6.2 Neurofilaments

Neurofilaments (NFs) are type IV IFs and are the most abundant cytoskeletal protein in neurons (Hirokawa 1982). Knockout mice have been made for all three neurofilaments, yet none of the mice had an overt phenotype. NF-H-null mice had little reduction in neurofilament density or axon survival but did display an upregulation in microtubules (Elder, L. et al. 1998, Rao, Houseweart et al. 1998, Zhu, Lindenbaum et al. 1998). NF-L-null mice had a complete loss of neurofilaments and hypertrophied axons, yet the most severe phenotype in NF-L- null mice was only delayed neuronal regeneration following nerve crush injury (Zhu, Couillard-Despres et al. 1997). NF-M-null mice had a reduction in neurofilaments and axon diameter but an increase in microtubules (Elder, L. et al. 1998). These mice suggest that while neurofilaments are important for neuronal regeneration and healthy axons, other cytoskeletal elements, notably microtubules, have compensatory roles in the absence of neurofilaments, resulting in phenotypes that are not severe.

While mouse neurofilament knockouts had no overt phenotype, transgenic mice overexpressing the neurofilaments had neurofilament inclusions in every transgenic line and more severe phenotypes (Lariviere, Julien 2004). Overexpression in mice of human NF-H or mouse NF-L resulted in a phenotype similar to ALS with neuronal degeneration and muscular atrophy (Cote, Collard et al. 1993, Xu, Cork et al. 1993). Mice overexpressing human NF-M had reductions in small myelinated axons in the ventral root and progressive paralysis of the hind limbs (Gama Sosa, L. et al. 2003). The neurofilament transgenic mice all support the hypothesis that neurofilament inclusions are associated with neurological and muscular degeneration indicative of peripheral neuropathies (Lariviere, Julien 2004).

Neurofilaments are associated with several known neurological diseases. In addition to peripherin, neurofilaments have been found in inclusion bodies in motor neurons of patients with ALS. Also, deletions and insertions of phosphorylation sites in NF-H necessary for axonal regulation have been identified in patients with ALS (Al-Chalabi, Andersen et al. 1999, Figlewicz, Krizus et al. 1994).

Charcot-Marie Tooth disease (CMT) encompasses many neurodegenerative diseases of the peripheral nervous system characterised by progressive atrophy of distal limb muscles and sensory defects (Kuhlenbaumer, Young et al. 2002). Several NF-L mutations in the head, rod and tail domains are known to cause CMT (De Jonghe, Mersivanova et al. 2001, Georgiou, Zidar et al. 2002, Mersiyanova, Perepelov et al. 2000). Nerve biopsies of CMT patients reveal neurofilament aggregations and axonal degeneration (Fabrizi, Cavallaro et al. 2007, Jordanova, De Jonghe et al. 2003, Miltenberger-Miltenyi, Janecke et al. 2007).

1.3.6.3 α-internexin

Type IV IF protein α-internexin is the first neuronal IF protein expressed in developing neurons. α-internexin is expressed at its highest during development and regeneration, when it is believed to be involved in neurite outgrowth (McGraw, Mickle et al. 2002, Chien, Liu et al. 2005, Shea, Beermann 1999). In mature neurons, α-internexin expression is restricted to the CNS (Fliegner, Kaplan et al. 1994). Like peripherin, α-internexin can homopolymerise or copolymerise with neurofilaments (Ching, Liem 1998, Yuan, Rao et al. 2006). α-internexin-null mice have no overt phenotype and have no abnormalities in neurofilament structure or axon development, number or size (Levavasseur, Zhu et al. 1999). Transgenic mice overexpressing α-internexin have abnormal swellings of Purkinje cell axons that are commonly seen in neurodegenerative diseases of the cerebellum. The swellings result in loss of motor coordination and loss of neurons (Ching, Chien et al. 1999).

1.3.6.4 Synemin

Type VI IF protein synemin was briefly mentioned in Section 1.1.1 for its interaction with dystrophin in muscle. Synemin is also expressed in neurons, but its function is still largely unknown. Synemin isoforms -H, -M and -L all differ in their C-terminal tail domains (Xue, Cheraud et al. 2004) and developmental expression patterns (Izmiryan, Cheraud et al. 2006). Synemin does not form homofilaments but does form heterofilaments with vimentin and desmin (Bellin, Sernett et al. 1999).

The association of a majority of neuronal IF proteins with neurological diseases suggests that neuronal IFs are an important field in the continuing study of neurodegenerative disease.

1.4 Aims

The aim of this thesis was to better understand the function of syncoilin. This introduction has explained the initial identification of syncoilin and subsequent experiments. Syncoilin has been studied extensively in muscle, but little is still known of its functional role. This thesis will initially attempt to elucidate syncoilin expression in muscle and examine a potential signalling function for syncoilin in muscle. The second half of this thesis will examine syncoilin expression in neurons through syncoilin neuronal binding partners and a neuronal characterisation of the *sync-/-* mouse.

The study of syncoilin is important for a number of reasons described throughout this introduction. As an IF protein and component of the cytoskeleton, syncoilin could have significant structural, mechanical and signalling functions that are still unknown. Syncoilin was identified because of its association with the DAPC, a complex involved in many neuromuscular diseases. Syncoilin is also a neuronal IF protein. Almost all identified neuronal IF proteins are associated with neurological diseases. A better understanding of syncoilin or one of its binding partners could improve the knowledge of neuromuscular and neurological diseases and aid in the development of therapies for these diseases.

Chapter 2: Materials and Methods

2.1 Cell culture

2.1.1 Cell culture conditions

All cells were grown at 37 ºC, 5 % CO_2, in a humidified chamber. Reagents were purchased from Invitrogen.

N2a cells were cultured in MEM + Earle's, 1 % non-essential amino acids (NEAA), 10 % foetal calf serum (FCS), 2 mM glutamine, 100 U/ml penicillin and 0.1 mg/ml streptomycin and were passaged approximately 1:5 two times a week.

NSC-34 cells were cultured in DMEM, 10 % FCS, 2 mM glutamine, 100 U/ml penicillin and 0.1 mg/ml streptomycin and were passaged 1:10 approximately two times a week.

SW-13 cells were cultured in F12:DMEM, 5% FCS, 100 U/ml penicillin and 0.1 mg/ml streptomycin and were passaged 1:2 approximately three times a week.

2.1.2 Cloning Constructs

All constructs of wild-type and variant syncoilin used in cell culture were made in this laboratory by Ben Edwards. cDNA from skeletal muscle was used as a template for the amplification of sync-1, sync-2 and sync-3. Primers are as follows: sync-1/2/3/-F: ATG GCC AGC CCG GAA CCC CT; sync-1R: A AAC AGT CCC TGG GGA TTG TG; sync-2R: GTG ATC CTT TAA TAA ATG TT; sync-3R: CTA CAG GTC CGA CCA TAT AT. These constructs all contain a HA tag and are in the pcDNA3 vector (Invitrogen).

All peripherin constructs used in this thesis were made in this laboratory by Ben Edwards. Per58 and per45 were amplified from the appropriate mouse cDNA and inserted into pCDNA3.0 (5'*Eco*RI, 3' *Not*I) using standard cloning techniques and the following primers: per58F: TTT GAA TTC ATG CCA TCT TCC GCC AGC AT; per58R: TTT AAG CTT ATC AGT AGC TGT GGA TAG AAG; per45F: TTT GAA TTC ATG GCC GAG GCC CTC AAC CA; per45R: TTT AAG CTT ATC AGT AGC TGT GGA TAG AAG. The perΔ58 construct that expresses only per58 due to a mutated per45 start site was created using an A→C mutation as underlined: CCT CGG AGC GCC TCG ATT TCT CCC TGG CCG AGG CCC TCA ACC. Constructs were transformed into chemically competent JM109 *E.coli* using standard techinques. Construct fidelity was verified by bidirectional sequencing prior to plasmid stock production using minipreps or maxipreps in accordance with the manufacturer's instructions (Qiagen).

2.1.3 Transfection of cultured cells

For transfection of N2a cells for co-immunoprecipitation, cells were seeded at approximately 70% confluence on a 175 cm^2 flask. After 24 hours, flasks were transfected with 18.7 μg DNA per well, using the FuGENE transfection reagent (Roche) at a ratio of 1:3 μg DNA:μl FuGENE. DNA-FuGENE complexes were formed by following the manufacturer's protocol. 1 ml of DNA-FuGENE complexes in OptiMEM (Invitrogen) were added to the existing media. Cells were cultured at 37ºC, 5 % CO_2 for 48 hours before harvesting.

For transfection of SW-13 cells for immunostaining, cells were seeded on 12 well plates at 1 x 10^5 on uncoated coverslips. After 24 hours, they were transfected with 0. 5 μg DNA per well, using FuGENE at a ratio of 1:3 μg DNA:μl FuGENE. DNA-

FuGNE complexes were formed by following the manufacturer's protocol. Cells were cultured for 48 hours before analysis by immunostaining.

2.1.4 Primary muscle cell lines

2.1.4.1 Generation of mouse primary muscle cell lines

Three-day-old mice were sacrificed with a rising concentration of CO_2. Hind limbs and fore limbs were removed and cleaned of all skin and as much non-muscle tissue as possible, including the foot. Limbs were washed in filter-sterilized PBS with antibiotic antimycotic (Sigma Aldrich) and then placed in 10ml filter-sterilized collagenase solution (0.1% collagenase and 0.1% bovine serum albumin in PBS [all from Sigma Aldrich]). The tissue was shaken and incubated at 37ºC for 10 minutes. The supernatant was removed and added to 25ml media (F10 Ham's, 15% horse serum, 6ng/ml human recombinant basic fibroblast growth factor [Sigma Aldrich], 1mM L-glutamine, 1mM $CaCl_2$ [Sigma Aldrich], 100 U/ml penicillin and 0.1 mg/ml streptomycin [all from Invitrogen unless noted]) that was stored at 37 ºC, 5 % CO_2, in a humidified chamber through the course of the collagenase exposure. Three more rounds of 5ml of collagenase were added to the limbs for 10 minutes each with all supernatants added to the original media.

The supernatant and media mixture was shaken to mix and filtered through a 40µm filter (Falcon). The filtered mixture was centrifuged at 250 x g for 10 minutes and then resuspended in 20 ml of media. Five plates were coated with gelatine, and the resuspended cells were added to plates at varying concentrations.

2.1.4.2 Maintenance of primary muscle cell lines

Cells were harvested by trypsinisation, centrifuged at 250 x g for 5 minutes, resuspended in media and added to gelatine-coated plates. Cells were grown at 37 ºC,

5 % CO_2, in a humidified chamber. Cells were passaged daily and typically remained viable for one week. All experiments using these cells were started within 72 hours of the initial plating.

2.1.4.3 Cell growth rate analysis

Cells were passaged as standard but plated at a density of 5 x 10^4 cells per gelatine-coated plate. Three plates were used for each cell line at each of five time points: 12, 18, 24, 36 and 48 hours. For counting, cells were washed once with PBS, harvested by trypsanization and centrifuged at 250 x g for 10 minutes. The pellet was resuspended in 1ml of media and counted using trypan blue and a neubauer haemocytometer. Each plate was counted sixteen times and averaged.

2.1.4.4 Primary cell line drug resistance assay

Cells were passaged as standard but plated at a density of 10^6 cells per gelatine-coated plate. Two plates were used for each cell line under each of five different drug conditions: no drug, 1ng/ml TNFα, 10ng/ml TNFα, 1ng/ml CHX + 1ng/ml TNFα and 10ng/ml CHX + 10ng/ml TNFα (TNFα and CHX from Sigma Aldrich). Drugs were added 24 hours after plating and cell counts were taken 24 hours after administration as described in Section 1.1.3.3.

2.1.4.5 Primary cell line pulse chase assay

Cells were passaged as standard but plated at a density of 10^6 cells per gelatine-coated plate and allowed to grow for 24 hours. The pulse media of 3ml methionine and cysteine-free DMEM (Invitrogen) with 13.5ul S35 (1.85MBq/ml) (PerkinElmer) was added to each plate and incubated with the cells for 1 hour at 37°C and 5% CO_2. The pulse media was washed three times with 5ml DMEM and then the chase media of 3ml methionine and cysteine-free DMEM supplemented with 500ug cysteine and 100ug methionine was added to each plate and incubated with the cells for 30 minutes

at 37°C and 5% CO_2. Cells were washed once again three times with 5ml DMEM, trypsinized and centrifuged at 250 x g for 5 minutes. Pellets were added to 2ml scintillation buffer (Amersham) and read on a scintillation counter according to manufacturer's instructions.

2.2 Immunocytochemistry and immunohistochemistry

2.2.1 Immunocytochemistry

For immunostaining of SW13 cells, media was removed and cells fixed and permeabilised for 10 min in ice cold methanol at -20°C. Cells were washed 3x10 minutes in PBS and blocked in 5 % FCS and 0.1% Triton X-100 (Sigma Aldrich) in PBS for 1 hour at room temperature. Primary antibodies (see Table 2.1) in blocking solution were added for at least 1 hour at room temperature in a humidified chamber. Coverslips were washed in 3x10 minutes in PBS and fluorescent secondary antibodies (Molecular Probes) were added at 1:2000 in blocking solution for 1 hour. Coverslips were washed 3x10 minutes in PBS and were mounted on slides with Vectashield plus DAPI (Vector Laboratories). Samples were viewed on a Zeiss Axioplan 2 fluorescent photomicroscope, and digital images were extracted using Axiovision LE 4.3 software.

Table 2.1 Antibodies used in this thesis

Antibody	Species and type	Source	Antigen	Applications	Dilution
Anti-syncoilin N-term 2991	Rabbit polyclonal	In house	N-term syncoilin	WB, IHC, ICC, IP	WB, IHC and ICC 1:500
Anti-syncoilin Skg001	Goat polyclonal	In house	Full-length syncoilin	IP	
Anti-α tubulin DM1A	Mouse monoclonal	Sigma	All α-tubulin isoforms	WB, IHC, IP	WB and IHC 1:500
Anti-α tubulin B512	Mouse monoclonal	Sigma	All α-tubulin isoforms	WB, IP	WB 1:1000
Anti-β tubulin ab6046	Rabbit polyclonal	Abcam	Residues 1-100	WB, IP	WB 1:500
Anti-peripherin AB1530	Rabbit polyclonal	Chemicon	Full-length peripherin	WB, IP	WB 1:500
Anti-peripherin MAB5380	Mouse monoclonal	Chemicon	Full-length peripherin	IP	

Anti-peripherin AB9282	Chicken polyclonal	Chemicon	Full-length peripherin	IHC, ICC	IHC and ICC 1:500
Anti-HA ab4C12	Mouse monoclonal	Abcam	HA tag	IP	
Anti-HA H6908	Rabbit polyclonal	Sigma	HA tag	IP	
Anti-β-actin ab8226	Rabbit polyclonal	Abcam	N-term β-actin	WB	1:1000
Anti-α-actinin SC7453	Goat polyclonal	Santa Cruz	α-actinin C-20	WB	1:1000
Anti-Neurofilament MAB1615	Mouse monoclonal	Chemicon	Full-length Neufilament 70kDa	WB	1:500

Abbreviations: ICC, immunocytochemistry; IHC, immunohistochemistry; WB, Western blotting; IP, immunoprecipitation.

2.2.2 Immunohistochemistry

2.2.2.1 Preparation of sciatic nerve single neurons

All animal work was carried out in accordance with Home Office regulations. Mice were sacrificed by cervical dislocation. The sciatic nerve was dissected and stored in 4 % paraformaldehyde (PFA) for at least 24 hours. A small 1.0cm long segment of sciatic nerve was desheathed and subdivided into nerve fasicles using a fine #5 forceps and #30 gauge needle in PBS on a Petri dish. Fasicles of approximately 10-20 neurons are transferred to a Frost Plus slide and further separated and straightened. The neurons are allowed to dry briefly to improve attachment to the slide. Slides can be used immediately or stored at -80°C.

2.2.2.2 Cardiotoxin-induced damage of hind limb muscle

Adult mice were induced and maintained under isofluorane inhalation anesthetic. A small incision was made to expose the tibialis anterior (TA) muscle. Using a 100µl insulin syringe, A 10µM solution of Cardiotoxin 1 (Sigma Aldrich) in sterile PBS was introduced into the muscle, and the overlying skin was sutured to close the wound. The contralateral limb was treated with an identical volume of PBS to serve as a control. Following treatment, mice were monitored for 1, 3, 5 and 7 days before being

sacrificed. TA muscle for histologic analysis was dissected, embedded in OCT and snap-frozen in liquid nitrogen-cooled isopentane. TA muscle for protein analysis was dissected and snap-frozen in liquid nitrogen.

2.2.2.3 Denervation of hind limb

Adult mice were induced and maintained under isofluorothane inhalation anesthetic. A small incision was made in the posterior part of the hind limb to expose the sciatic nerve at the level of the femoral trochanter. The nerve was severed and a section of nerve (~0.5cm) excised, and the overlaying skin was sutured to close the wound. The contralateral limb was incised but left innervated to serve as a control. Post-operative pain was managed via intraperitoneal administration of Buprenorphine. Animals were monitored for 1, 5 or 7 days, before being sacrificed. TA muscle for histologic analysis was dissected, embedded in OCT and snap-frozen in liquid nitrogen-cooled isopentane. TA muscle for protein analysis was dissected and snap-frozen in liquid nitrogen.

2.2.2.4 Immunostaining of spinal cord and sciatic nerve

Spinal cord sections, muscle sections and sciatic nerve single neuron preparations were incubated for 1 hour in blocking solution of 10% foetal calf serum and 1% Triton-X100 in PBS. Primary antibodies (see Table 2.1) in blocking solution or blocking solution alone were added for 1 hour at room temperature or overnight at 4ºC, in a humidified chamber. Slides were washed 3x10 minutes in PBS. Fluorescent secondary antibodies were added at 1:2000 in blocking solution for 1 hour at room temperature. Slides were washed 3x10 minutes in PBS and dried. Slides were then mounted with Vectashield containing DAPI. Samples were viewed on a Zeiss 510 confocal laser-scanning microscope, and digital images were extracted using Zeiss LSM Image Browser 4.2.

2.3 Western blotting

2.3.1 Preparation of tissue and cell homogenates

Tissue was crushed in liquid nitrogen with a pestle and mortar and then homogenised in Newcastle buffer (75 mM Tris-HCl pH6.8, 3.8 % sodium dodecyl sulphate (SDS), 4 M urea, 20 % glycerol, 1 % v/v protease inhibitor cocktail [Sigma Aldrich]) with a Radley Pro homogeniser and 5 mm probe. Homogenates were rotated at 4ºC for two hours and then centrifuged at 18 000 x g and 4ºC for 30 min.

Cells were washed with PBS, re-suspended with trypsin and centrifuged at 200 x g for 5 minutes. Pellets were re-suspended in Newcastle buffer and then rotated at 4ºC for two hours followed by centrifuged at 18 000 x g and 4ºC for 30 minutes. Protein concentrations of all lysates were assayed using the Bio-Rad DC protein assay.

2.3.2 SDS-PAGE

Proteins were separated using an 8 % SDS-acrylamide gel (stacking gel: 5 % acrylamide (at a ratio of 37.5:1 acrylamide:bisacrylamide), 130 mM Tris-HCl pH6.8, 0.1 % SDS, 0.1 % ammonium persulphate (APS), 1 x 10^{-3} % tetramethylethylenediamine (TEMED); resolving gel: 8 % acrylamide (as above), 375 mM Tris-HCl pH8.8, 0.1 % SDS, 0.1 % APS, 1 x 10^{-4} % TEMED).

The lysates were combined with NuPAGE LDS Sample Buffer with β-mercaptoethanol (Invitrogen) and boiled for one minute before loading onto SDS-polyacrylamide gels. Electrophoresis was done for approximately three hours at 80 V.

2.3.3 Transfer and Western blotting

Proteins were transferred to nitrocellulose (Schneider & Schneider) overnight at 30 V at 4ºC cooling with an ice pack.

Membranes were blocked (5 % skimmed milk powder / TBST (10 mM Tris-HCl pH8, 150 mM NaCl, 0.05 % TWEEN 20)) for one 1 hour at room temperature. Primary antibodies (see Table 2.1) diluted in blocking solution were added for 3 hours or overnight rocking at room temperature. Blots were washed in 3 x 10 minutes in TBST. Horseradish peroxidase (HRP)-conjugated secondary antibodies (Amersham; used at 1:3000) were added in blocking solution for 1 hour and followed by 3 x 10 minute washes in TBST. ECL reagents (GE) were added and X-ray film (Kodak) exposed. Films were developed using a Compact X4 developer (X-o-graph Imaging Systems).

2.3.4 Blot stripping for re-probing

Membranes were incubated in stripping solution (100 mM β-mercaptoethanol, 2 % SDS, 62.5 mM Tris-HCl pH 6.8) at 50 ˚C for 30 minutes, agitating every 10 minutes. They were then washed 3 x 10 minutes with TBST.

2.4 Co-immunoprecipitation

Cells and tissue were prepared using IP lysis buffer with CHAPS (50 mM Tris-HCl pH7.5, 150 mM NaCl, 1 % w/v 3-[(3-Cholamidopropyl)dimethylammonio]-1-propanesulfonate (CHAPS), 1 % v/v protease inhibitor cocktail [Sigma Aldrich]) as described in Section 2.3.1. Lysates were pre-cleared by adding 20 µl Protein G sepharose beads and rotating for 2 hours at 4ºC. Samples were centrifuged at 4 000 x g and 4 ˚C for 1 minute, and supernatants were transferred to fresh tubes. Approximately 5 µg antibody was added to samples and incubated overnight at 4 ºC. Protein G sepharose beads were pre-equilibrated in CHAPS buffer. Approximately 30 µl of beads were added to each sample and rotated at 4 ºC for two hours. Samples were centrifuged for at 4 000 x g at 4 ˚C for 1 minute, and supernatants kept for possible running of voids. Beads were washed three times with 1 ml IP lysis buffer

(50 mM Tris-HCl pH7.5, 150 mM NaCl) and proteins were eluted by boiling in 1x diluted NuPAGE LDS Sample Buffer with β-mercaptoethanol for 2 minutes. Samples were centrifuged for 1 min at 1 000 x g and supernatants were used for SDS-PAGE and Western blotting.

2.5 RT-PCR

2.5.1 Preparation of RNA from N2a cells

RNA was prepared from spinal cord using TRIzol Reagent (Invitrogen) following the manufacturer's instructions. RNA was quantified by absorbance at 260 nm using a ND-1000 spectrometer (Nanodrop Technologies).

2.5.2 Reverse transcription

Total RNA was reverse transcribed into cDNA using random decameric primers and superscript II reverse transcriptase (Invitrogen) following the manufacturer's instructions.

2.5.3 Real-Time PCR

Real-Time PCR analysis was performed using SYBR Green PCR Master Mix (Applied Biosystems) on a Step One Plus Real-Time PCR System (Applied Biosystems) following the manufacturer's instructions. α-tubulin primers used were: Forward: AT TCC ATC CAT GTT GGC CA; Reverse: TCC AGG TCT ACG AAC ACT GC. Data was analysed using StepOne Software v2.0 (Applied Biosystems) according to the manufacturer's instructions. All reactions were performed in triplicate. Reaction efficiency was calculated for each primer pair using averaged kinetic data obtained from at least 50 individual reactions (Tichopad, Pfaffl et al. 2003). Data was pooled and then processed using a method described by Funke-Kaiser and co-workers (Schefe, Lehmann et al. 2006).

2.6 Neuronal analysis of sync-/- mouse

2.6.1 Behavioural Testing

2.6.1.1 Rotarod

All animal work was carried out in accordance with Home Office regulations. The rotarod device consists of a mechanically-controlled grooved plastic beam 5 cm in diameter (Ugo Basile, Italy). Mice were placed on the beam rotating initially at a speed of 5 rotations per minute (rpm). The rod speed was gradually accelerated to a maximum of 40 rpm over 5 minutes. Mice were tested for their ability to stay on the rod. Mice were tested four times each on separate days.

2.6.1.2 Hot plate

Mice were placed on a hot plate heated to a constant temperature of 55^{o}C surrounded by a clear acrylic cage. Mice were timed from the moment they were put on the hot plate until the observation of a physical response. The response to the mild thermal stimulus was identified by hindpaw lick, hindpaw flick or jump. Mice were allowed to stay on the hot plate for a maximum of thirty seconds and were tested only once.

2.6.1.3 Accelerating treadmill

Mice were placed on a motorized treadmill (Exer6-M, Columbus Instruments) initially at a speed of 5 metres per minute (mpm). The treadmill speed was gradually accelerated to a maximum of 30 mpm over 5 minutes, and mice were tested for their ability to stay on the treadmill. Mice were tested only once.

2.6.1.4 Grip strength

Mice were tested using a commercial grip strength monitor (Chatillon). Each mouse was held by the base of the tail and lowered down to allow its forepaws to grip a protruding metal bar attached to the apparatus. Each mouse was pulled gently until the

grip was released. The maximum force exerted was recorded and controlled for animal weight.

2.6.1.5 Static Beam

A wooden dowel 28 mm diameter and 60 cm in length was clamped to bench 60 cm above a padded surface. Mice were placed on the protruding end of the rod, facing away from the bench. The time taken to reach the end of the beam attached to the bench or fall from the rod was recorded up to a maximum of three minutes. Mice were measured only once.

2.6.2 Perfusion

Mice were given a lethal overdose (~140 mg/kg) of pentobarbitone. Once all reflexes had been lost and heart rate had slowed and become irregular, the thoracic cavity was opened to expose the heart. The right atrium was cut and an 18G needle was inserted into the left ventricle and clamped in place. Animals were perfused with ~50 ml PBS containing 10 units/ml heparin to prevent blood clotting, using a perfusion pump, until the perfusate ran clear. The perfusate was then switched to 2 % paraformaldehyde (PFA) in 0.1 M phosphate buffer and animals were perfused with ~50 ml until viscera engorged and tissue stiffened.

2.6.3 Preparation of spinal cord sections

Spinal cords were dissected at the L4 region and post-fixed overnight in 4% PFA at 4°C. Cords were then transferred to 30 % sucrose and left overnight at 4°C. Cords were embedded in optimum cooling temperature (OCT) medium (Bright Instrument Co.) by freezing on dry ice. Embedded cords were sectioned immediately at a thickness of 10 μm or stored at -80°C.

2.6.4 Motor neuron counts of spinal cord anterior horn

Sections of spinal cords were stained with 0.5% cresyl violet (Sigma Aldrich), washed in dH_2O and an alcohol series, cleaned with Histochoice Clearing Agent (Sigma Aldrich) and mounted with Histomount (RA Lamb). Pictures were taken with a Leica DMRE microscope and counted blindly by two different people for dark, large and irregularly shaped staining in the anterior horn region of the spinal cord. The spinal cords of three mice of each strain were used. Ten slides of six sections were taken from the L4 region of the spinal cord. Two sections from each slide were counted to prevent the repeated counting of the same motor neurons.

2.6.5 Preparation of ventral roots

Ventral roots were dissected from the L5 region of the spinal cord in perfused mice. Ventral roots were post-fixed overnight in 4% PFA at 4°C and then stored in 70% ethanol for one week. Embedding, sectioning and staining were done by Mohan Masih (DPAG, University of Oxford).Ventral roots were embedded in Araldite resin and sectioned at a thickness of 1 micron. Staining was done with a solution of 1% Toluidine Blue and 1% Borax.

Pictures were taken with a Leica DMRE microscope. Axons were outlined using Axiovision Release 4.7 (Carl Zeiss Imaging). Two sections from different parts of the ventral root were counted from each of three different mice per genotype.

Chapter 3: Syncoilin expression in muscle

3.1 Introduction

Despite significant progress in syncoilin research, little is still known about the function of syncoilin in muscle. The work in this chapter characterizes further the expression of syncoilin in striated muscle with the aim that any new insight will build upon a foundation of knowledge that will lead to a better understanding of the function of syncoilin. Immunoblot analysis of protein samples from striated muscle previously led to the identification of a syncoilin species that is significantly smaller than the normal size for syncoilin (Newey, Howman et al. 2001). This chapter describes two newly identified syncoilin isoforms.

Recent investigations have shown that syncoilin expression is altered in response to a variety of stimuli. Syncoilin has been shown to be up-regulated and aggregated in two patients with desmin-related myopathies (Howman, Sullivan et al. 2003). Syncoilin expression has also been investigated in patients afflicted with a range of neuromuscular disorders. Syncoilin immunolabeling was broadly altered in muscle fibres with alterations in the DAPC, the extracellular matrix and calcium channel receptors (Brown, Torelli et al. 2005).

Intermediate filament (IF) proteins are increasingly being identified in a new range of processes. It is possible that syncoilin could play a role in one of these non-structural functions. Several IF proteins including the laminins, keratin 8, keratin18 and vimentin have been shown to be involved in apoptotic processes (Ndozangue-Touriguine, Hamelin et al. 2008). Vimentin has also been shown to play a role in the

nuclear translocation of phosphorylated MAP kinases in injured sciatic nerve (Perlson, Hanz et al. 2005).

The expression of syncoilin has been well documented under standard conditions. Previous unpublished work done in this lab by Dr. Karl McCullagh studied the effect of syncoilin on muscle undergoing atrophy following denervation of the sciatic nerve at the hind limb. One experiment showed that the muscle fibre area in denervated *sync-/-* mice was approximately 10% smaller than the area in denervated *sync+/+* mice. Studying syncoilin in striated muscle during regeneration and further examining syncoilin during atrophy will provide insight into the reaction of syncoilin to physiological changes and could provide insight into the functional role of syncoilin.

It is important to have a base understanding that includes what syncoilin isoforms exist, where those isoforms are expressed, and under what conditions syncoilin and its isoforms are upregulated or downregulated. One or more of these insights could provide a valuable clue to understanding the functional role of syncoilin in striated muscle.

3.2 Syncoilin isoforms

The projected intermediate filament domain organisations and the sequences of the three syncoilin isoforms expressed in striated muscle are outlined in Figure 3.1. These isoforms have been named sync-1, sync-2 and sync-3. Sync-1 is the originally discovered isoform whose sequence yielded a 470 residue and approximately 64 kDa protein. Sync-1 is comprised of a 157 residue N-terminal head domain, a 296 residue rod domain and a short 18 residue C-terminal tail domain.

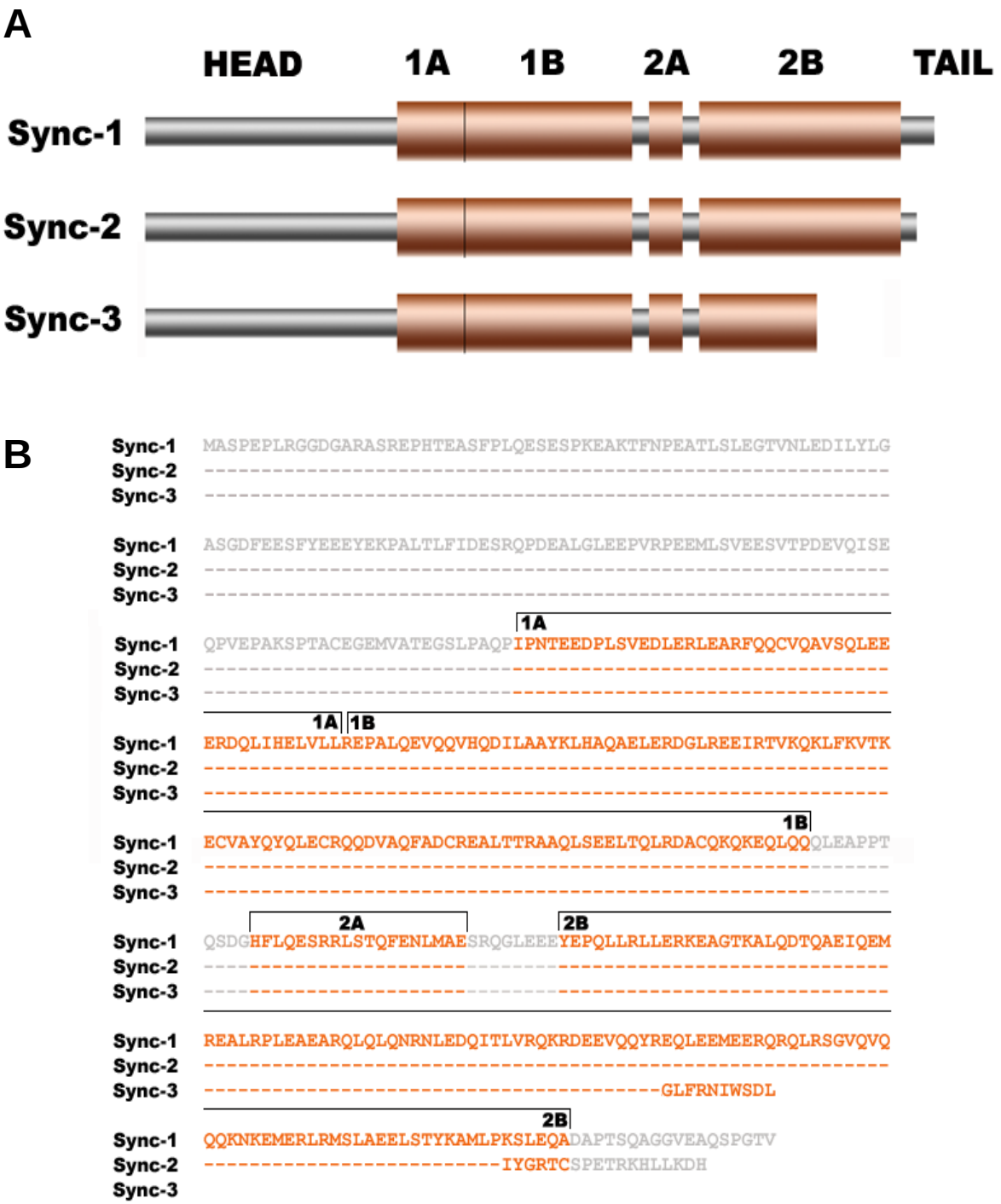

Figure 3.1. Syncoilin isoforms.

A. Intermediate filament domain organisation for sync-1, sync-2 and sync-3. Sync-2 has a shortened tail region and sync-3 has a shortened 2B region and no tail region.

B. Sequence alignment for sync-1, sync-2 and sync-3. Alpha helical regions are shown in orange.

Sync-2 is derived from an excision in the fourth of syncoilin's five exons. This excision results in a change to the last 10 residues of rod domain segment 2B and the tail domain, creating a 464 residue protein that is nearly identical in size to sync-1. Sync-2 maintains much of sync-1's coiled-coil character and interchain ionic interactions at the end of the rod domain. However, the C-terminal domain in sync-2 is shorter and more highly charged than the C-terminal domain in sync-1.

The sync-3 isoform is derived from the skipping of exons three and four, resulting in a shorter 410 residue protein that is approximately 55 kDa in size. The change in sequence occurs in rod domain segment 2B, resulting in a shortened rod domain and no C-terminal tail domain.

Immunoblots in Figure 3.2 show syncoilin expression in skeletal and cardiac muscle. An N-term antibody to syncoilin which recognizes all isoforms was used. Due to their near identical sizes, sync-1 and sync-2 are indistinguishable by immunoblot and migrate to approximately 64kDa. Sync-3 is distinguishable from sync-1 and sync-2 and runs to approximately 55kDa. Expression of sync-3 was far lower than the combined expression of sync-1 and sync-2, as seen by the less intense band on the immunoblot. Sync-3 expression was highest in cardiac muscle, and in skeletal muscle, sync-3 was most highly expressed in the soleus. Soleus consists almost entirely of oxidative fibres expressing Type I and IIa myosin (Li, Larsson 1997, Allen, Harrison et al. 2001, Burkholder, Fingado et al. 1994). In quadriceps, EDL and TA, sync-3 expression is barely detectable. EDL and TA are both rich in fast-twitch glycolytic fibres that express primarily Type IIb or IIx myosin.

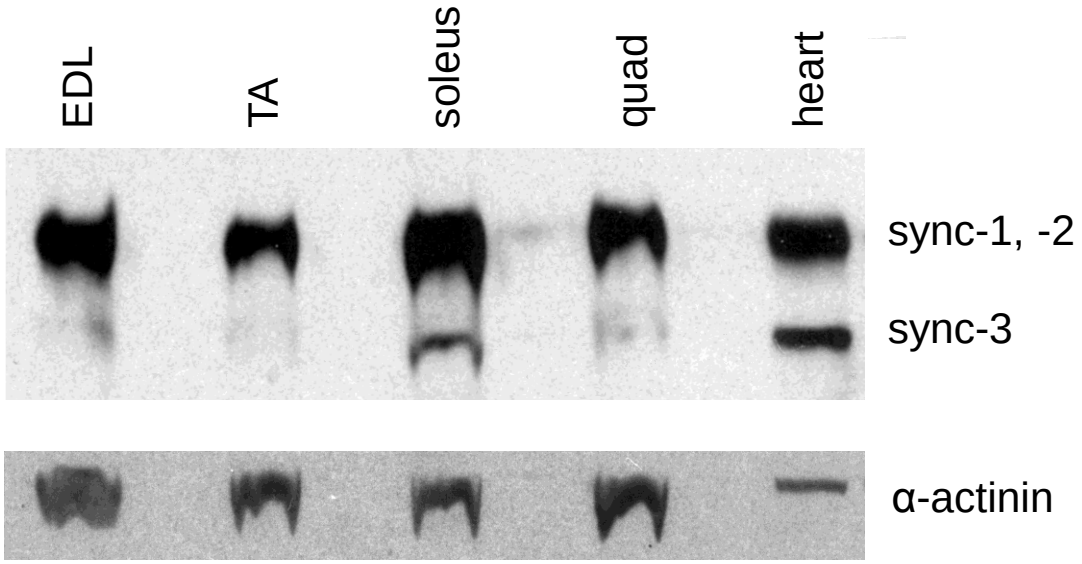

Figure 3.2. Syncoilin isoforms in muscle.

Immunoblot probed with syncoilin N-term 2991 showing syncoilin protein expression in adult mouse striated and cardiac muscle. It is not possible to distinguish between sync-1 and sync-2 due to their near identical molecular weight. Sync-3 is only evident in tissue from heart, soleus and quad. 50 µg of protein were resolved on an 8% gel under denaturing conditions and probed with an antibody against syncoilin N-term which recognizes all three syncoilin isoforms. Probing for α-actinin confirmed equal loading.

3.3 Analysis of syncoilin levels during muscle regeneration

Despite continued effort, little is known about the structural role of syncoilin in striated muscle. Given the importance of muscle regeneration in neuromuscular diseases such as Duchenne muscular dystrophy, it was examined if syncoilin levels were changed during cardiotoxin-induced muscle regeneration.

The administration of necrosis-inducing cardiotoxin resulted in an increase in syncoilin protein levels. Immunohistological analysis of transverse TA sections in Figure 3.3A showed both an increase and a spatial reorganization in syncoilin expression. At the one day time point, significant tissue destruction is seen by the absence of organized cells in the immunohistological analysis as well as by the absence of syncoilin and actinin protein from TA muscle in the immunoblot in Figure 3.3B. At day three, there is a dramatic increase in sync-1 and sync-2 protein expression in the immunoblot while at the same time small regenerating cells begin to appear in the immunohistology. Sync-3 was not detectable by immunoblot. Sync-1 and sync-2 protein levels continue to remain high at the five- and seven-day time points as muscle regeneration continues. During these early stages of regeneration, syncoilin is diffusely expressed throughout the entire cytoplasm, in contrast to the organized distribution of syncoilin to the Z-lines and sarcolemma seen in control sections.

3.4 Analysis of syncoilin levels during muscle atrophy

While it is now clear that syncoilin expression is increased during muscle regeneration, a related experiment was performed to determine whether muscle atrophy affects syncoilin expression in skeletal muscle. A small section of sciatic nerve was excised from the hind limb, thereby preventing signalling and inducing atrophy in muscles such as the TA and EDL.

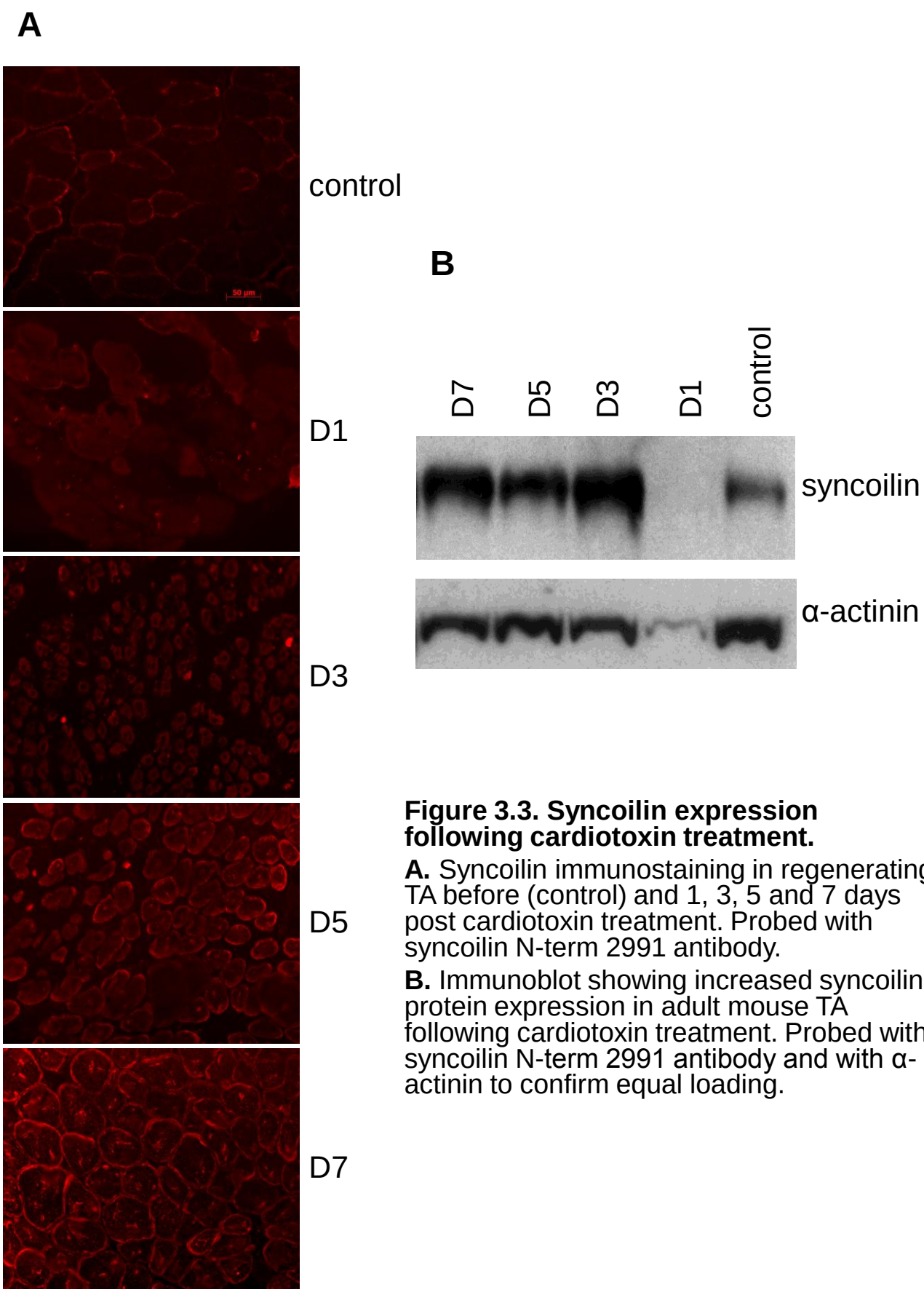

Figure 3.3. Syncoilin expression following cardiotoxin treatment.

A. Syncoilin immunostaining in regenerating TA before (control) and 1, 3, 5 and 7 days post cardiotoxin treatment. Probed with syncoilin N-term 2991 antibody.

B. Immunoblot showing increased syncoilin protein expression in adult mouse TA following cardiotoxin treatment. Probed with syncoilin N-term 2991 antibody and with α-actinin to confirm equal loading.

As seen in Figure 3.4A, immunohistological analysis of syncoilin expression in an atrophying TA indicates that syncoilin expression progressively increases over the 7 days following denervation, reaching its peak intensity at day 7, the last day of the trial. However, unlike during regeneration, there is no significant spatial redistribution of syncoilin during this process.

Immunoblot analysis in Figure 3.4B of syncoilin protein expression in atrophying EDL supports the immunohistological evidence that sync-1 and sync-2 expression is increasingly upregulated following denervation. Once again, sync-3 was not detectable by immunoblot.

3.5 Discussion

In this chapter, the characteristics of syncoilin in muscle have been further elucidated with the analysis of two syncoilin isoforms and the discovery that syncoilin expression is increased both during regeneration and atrophy.

Three syncoilin isoforms have been identified and are now known as sync-1, sync-2 and sync-3. Interestingly, only one other IF gene, synemin, is known to encode isoforms in the cytoplasm of non-neuronal cells (Xue, Cheraud et al. 2004, Sun, Critchley et al. 2008, Timmusk, Fossum et al. 2006). Significant work has subsequently been performed by Dr. Matthew Kemp, Ben Edwards and Matthew Burgess in this laboratory on the syncoilin isoforms. Sync-1 has been identified by RT-PCR as the primary isoform in muscle with approximately 40–50% as much sync-2 and very low levels of sync-3. Blot overlays were also performed to identify binding affinities between syncoilin isoforms and previously identified syncoilin binding

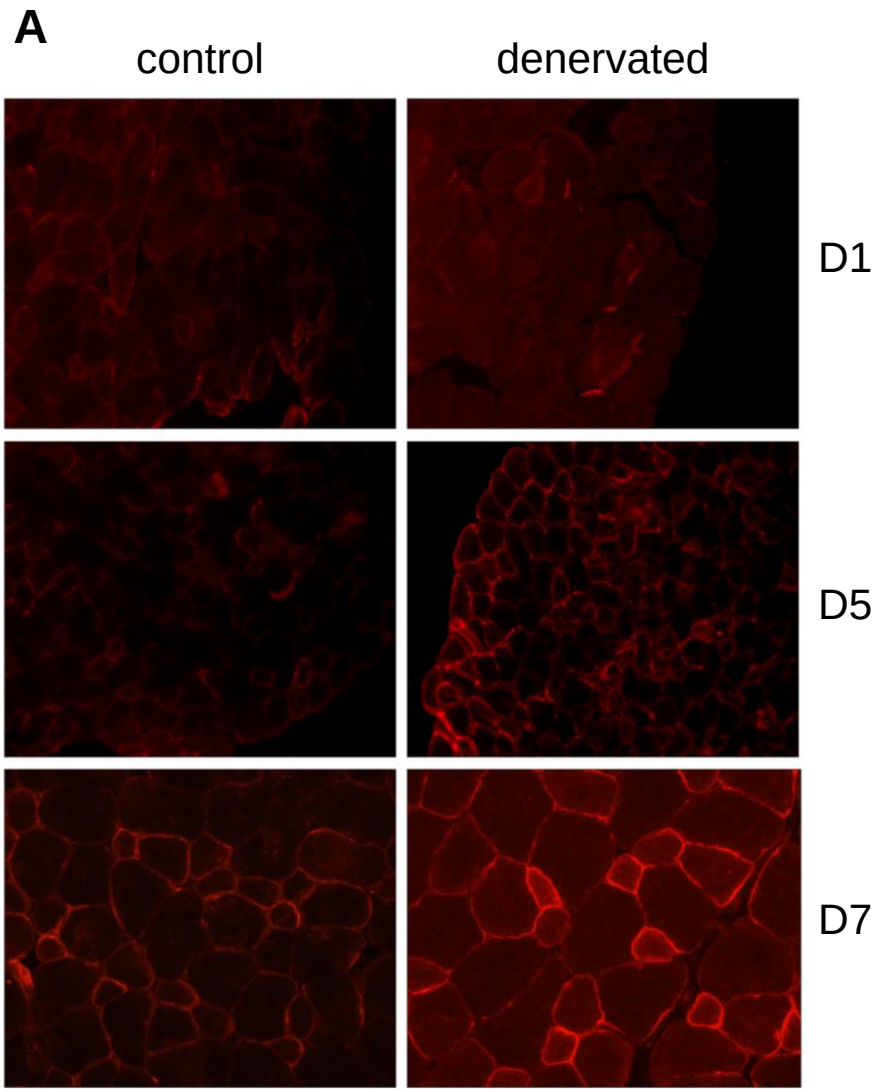

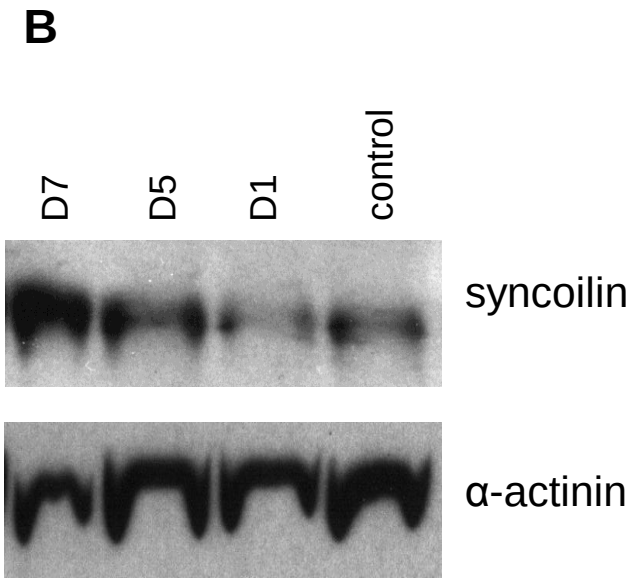

Figure 3.4. Syncoilin expression following denervation.

A. Syncoilin immunostaining in denervated and mock-denervated TA 1, 5 and 7 days following procedure. Probed with syncoilin N-term 2991 antibody.

B. Immunoblot showing increased syncoilin protein expression in adult mouse EDL following denervation. Probed with syncoilin N-term 2991 antibody and with α-actinin to confirm equal loading.

partners. For example, in the case of the type III intermediate filament desmin, sync-1 and sync-2 have similar binding affinities while sync-3 has a large reduction in binding affinity (Kemp, Edwards et al. 2008). This is not surprising given the sequence and domain similarities between sync-1 and sync-2 and the divergence of sync-3.

Also of interest is the difference in sync-3 expression between oxidative and glycolytic skeletal muscle. Syncoilin has been shown by immunoblot to be expressed 2-fold greater in soleus compared to EDL (McCullagh, Edwards et al. 2007). The immunoblot in this thesis confirms that overall syncoilin as well as sync-3 expression is highest in oxidative soleus muscle. Sync-3 is barely distinguishable in TA, EDL and quadriceps. It is unclear if the observation of sync-3 in soleus is due to overall higher syncoilin expression or an unknown property of oxidative muscle that results in higher levels of sync-3. Sync-3 expression is also detected by immunoblot in heart. Cardiac muscle also happens to be rich in highly oxidative fibres (Kassiotis, Rajabi et al. 2008). Any future studies into the functional role of sync-3 should focus on oxidative muscle and should also attempt to explain the disparity of sync-3 expression between oxidative and skeletal muscle.

Whether immediately relevant or not, the information relating to syncoilin isoforms and the expression of those isoforms in different types of muscle provides important knowledge for the future study of syncoilin. Our laboratory has recently received antibodies specific to the C-terminus regions of sync-1 and sync-2. These tools will allow for further characterisation of the syncoilin isoforms by immunoblot and immunohistochemistry in the future.

Cardiotoxin and denervation treatments induce regeneration and atrophy, respectively, both of which offer insight into muscle development. While the function of syncoilin in muscle is still not clear, the accelerating up-regulation of sync-1 and sync-2 during regeneration and the rapid and significant up-regulation of sync-1 and sync-2 during atrophy suggest that syncoilin might play a role in both of these processes. Immunohistological analysis demonstrates that syncoilin is redistributed throughout the cytoplasm of regenerating cells but remained localized to the sarcolemma in atrophying cells. This difference in localisation in these two processes indicates that syncoilin plays multiple developmentally regulated roles in myofibres.

The standard distribution of syncoilin in mature muscle is along the sarcolemma and z-line. One hypothesis is that syncoilin has a structural role given that syncoilin is an intermediate filament protein and has connections to the dystrophin-associated protein complex at the sarcolemma. However, the presence of syncoilin throughout the cytoplasm in regenerating cells suggests that syncoilin could be playing a structural role away from the sarcolemma and z-line or that syncoilin is playing an unknown signalling function. In either case, syncoilin could play a part in muscle cell growth, an important function throughout life and especially in neuromuscular diseases.

The hypothesis that syncoilin has a structural role at the sarcolemma is consistent with the possibility that syncoilin is upregulated at the sarcolemma in atrophying muscle. Muscle that is in atrophy would likely attempt to increase structural stability in a final effort to avoid apoptosis. More information is needed to clarify the function of

syncoilin in regenerating and atrophying tissue and to determine whether syncoilin plays an indispensable structural or signalling role in muscle tissue.

Chapter 4: Examination of sync-/- primary muscle cell culture

4.1 Introduction

In the previous chapter, the upregulation of syncoilin during regeneration and atrophy suggested that syncoilin might play a role in development. To further examine the function of syncoilin in development, possibly through cell signalling, it was necessary to examine syncoilin at the cellular level. Using the *sync-/-* mouse, it was possible to generate primary muscle cells deficient in syncoilin. Although the *sync-/-* mouse has yet to demonstrate a significant phenotype, primary cell culture allowed for a new and specific set of experiments. Measuring cell growth, drug resistance and protein translation enables an analysis of signalling pathways regulating growth, maintenance and apoptosis. The aim of the work described in this chapter was to identify whether the absence of syncoilin affects primary muscle cells, thereby suggesting an important role for syncoilin in signalling.

4.2 Cell growth assay

Primary cell lines were generated from three day old *sync+/+* and *sync-/-* mice. The presence or absence of syncoilin was verified by immunoblot in Figure 4.1.

A standard tissue culture cell growth assay is a simple measure of the number of living cells. *Sync+/+* and *sync-/-* cell lines were seeded at equal density from established primary cell lines. A cell growth curve was established from a series of five time points. The cell count at each time point was calculated from multiple counts of each of three different plates.

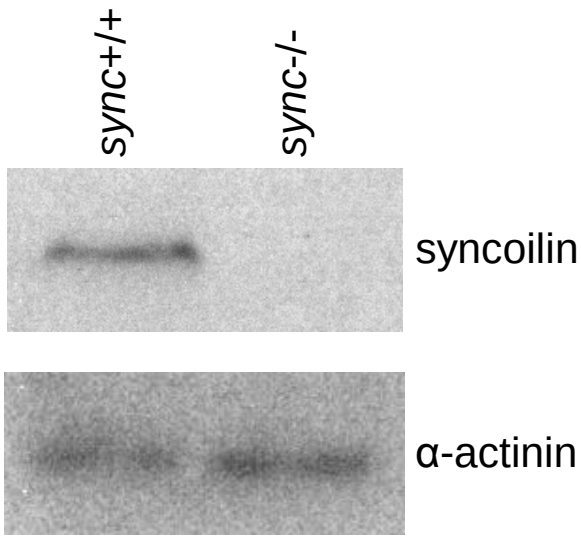

Figure 4.1. Syncoilin expression in primary cell lines. Immunoblot showing syncoilin protein expression in *sync*+/+ and *sync*-/- primary muscle cells. Probed with syncoilin N-term 2991 antibody and with α-actinin to confirm equal loading.

Figure 4.2 reveals a nearly identical growth curve for the *sync+/+* and *sync-/-* cell lines. Growth was stagnant for the first 18 hours but had nearly doubled from the original seeding of $5x10^4$ by 24 hours. At 36 hours, the number of cells had tripled from the original seeding, and at 48 hours, the cells numbered nearly five times the original seeding. Cell counts at all time points with the exception of 24 hours showed a slightly higher number of *sync-/-* cells than *sync+/+* cells. However, in all cases, the difference was well within the standard deviation.

4.3 Pulse-chase analysis

Another common experiment for use with cell culture and primary cell lines is the pulse-chase analysis. Pulse-chase experiments allow for the study of proteins after synthesis. This can include quantification, processing, intracellular transport and degradation (Takahashi, Ono 2003). The pulse-chase performed in this chapter measured the amount of protein synthesis in *sync+/+* and *sync-/-* cells using the amino acid methionine with a radioactive 35S sulphur atom. Cells were exposed to the labeled compound for a limited time during the pulse part of the experiment. Excess labelled compound was then washed away and cells were exposed to unlabelled methionine during the chase part of the experiment. The amount of radioactive methionine taken up by the cells and incorporated into proteins during the pulse period was calculated by measuring the cells' radioactivity. This amount of radioactivity is indicative of the amount of proteins produced and the rate of translation during the pulse period.

In the case of the *sync+/+* and *sync-/-* primary muscle cell lines, there was a slight increase in 35S counts in the *sync-/-* cell line, as seen in Figure 4.3. However, this

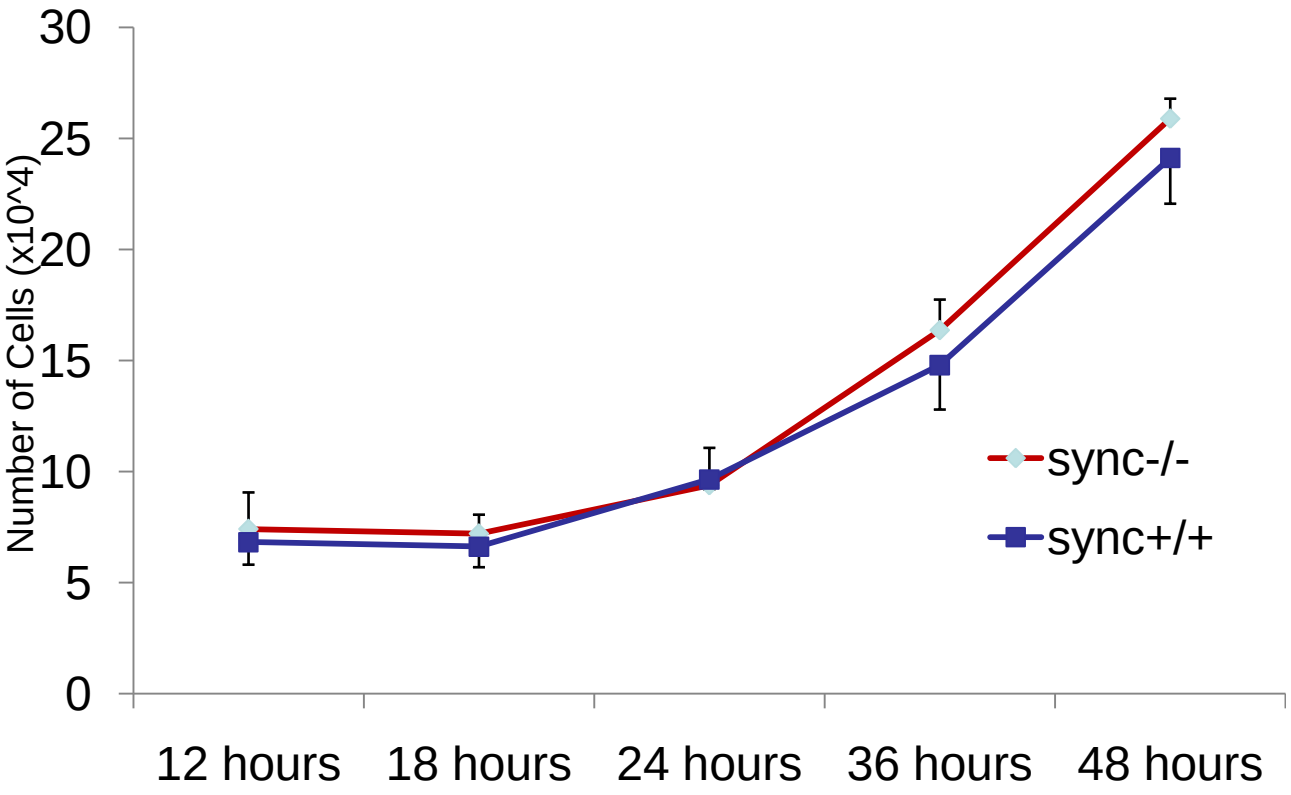

Figure 4.2. Primary cell line growth assay.
Graph showing the number of cells counted for *sync*+/+ and *sync*-/- primary muscle cell lines at five time points after seeding. 5x10^4 cells were initially seeded per plate. N=3 for each cell line at each time point.

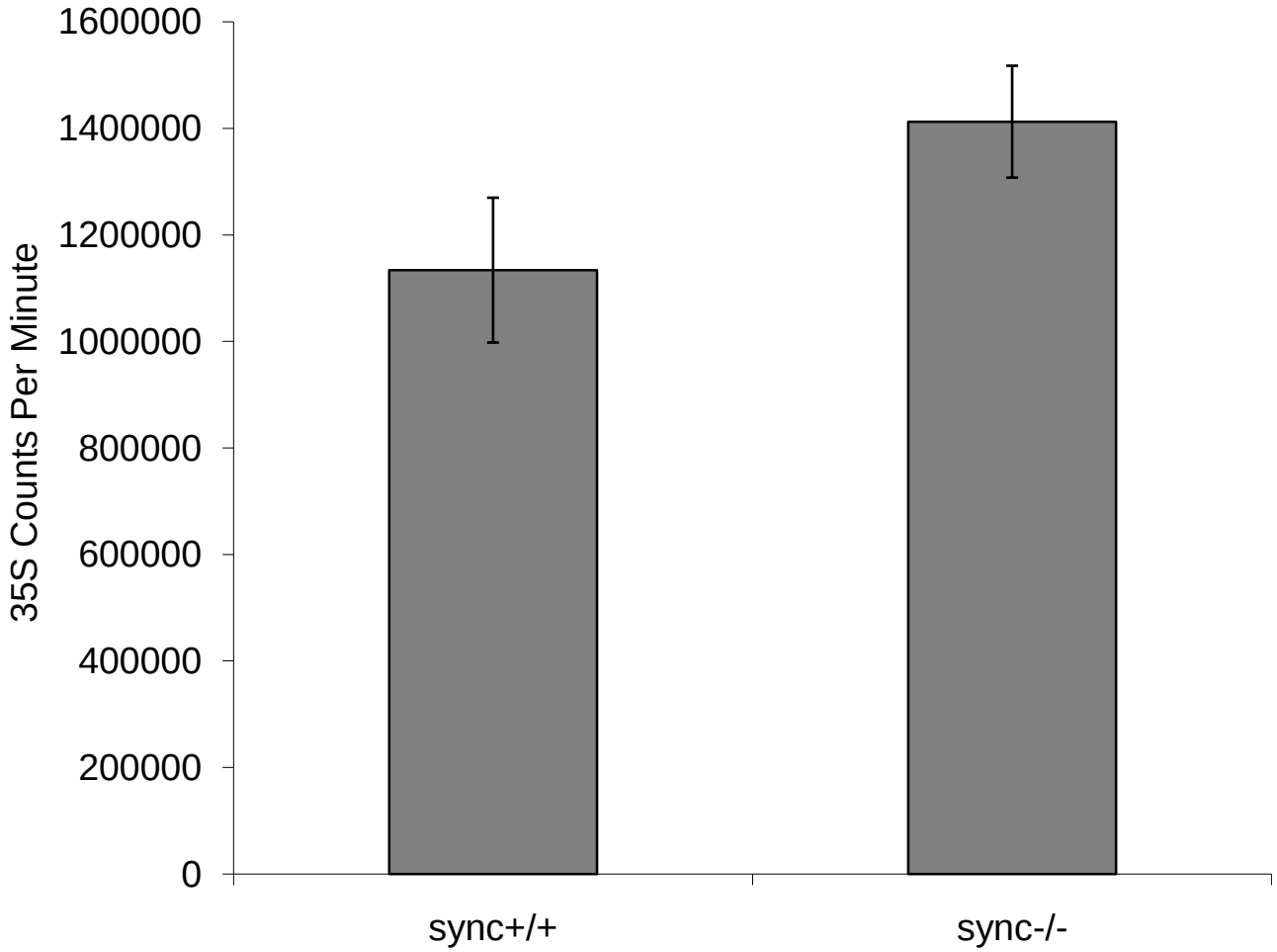

Figure 4.3. Primary cell line pulse chase analysis.
Graph showing the counts per minute of 35S after the incubation of *sync*+/+ and *sync-/-* primary muscle cell lines with 35S-labeled amino acids. 1x10^6 cells were initially plated 24 hours prior to 35S exposure. N=5 for each cell line.

difference was within the standard deviation of the two samples and was not considered significant.

4.4 Drug sensitivity assay

Tumor necrosis factor (TNF) is a pleiotropic cytokine that can induce differentiation, proliferation and apoptosis in many cell types. Specifically, TNF contains two receptors. TNFR1 activates downstream apoptotic signals and TNFR2 is associated with two factors that inhibit apoptosis (Andreani, Payne et al. 1991). In drug resistance assays, TNFα is commonly used with the protein synthesis inhibitor cyclohexamine (CHX) (Xiao, Yan et al. 2003). Together, these two drugs are capable of initiating the apoptotic pathway.

Keratin 8 (K8) and keratin 18 (K18) are intermediate filament proteins found in single cell layered internal epithelia. K8 and K18 both bind the cytoplasmic domain of TNFR2, activating signalling pathways that work to resist the apoptotic effects of TNF. Primary cultured epithelial cells deficient in keratin 8 and keratin 18 have been shown to be approximately 100 times more sensitive to TNFα-induced death (Caulin, Ware et al. 2000). This TNFα/CHX drug sensitivity assay will determine whether the presence or absence of syncoilin influences the TNF apoptotic or anti-apoptotic pathways.

The *sync+/+* and *sync-/-* primary muscle cell lines were exposed to varying combinations and concentrations of TNFα and CHX for 24 hours. Counts of live cells were taken to analyze the affects of TNFα and CHX, as seen in Figure 4.4. TNFα alone was incapable of inducing considerable cell death, but together with CHX, the two drugs significantly increased the number of apoptotic cells. The most cell death

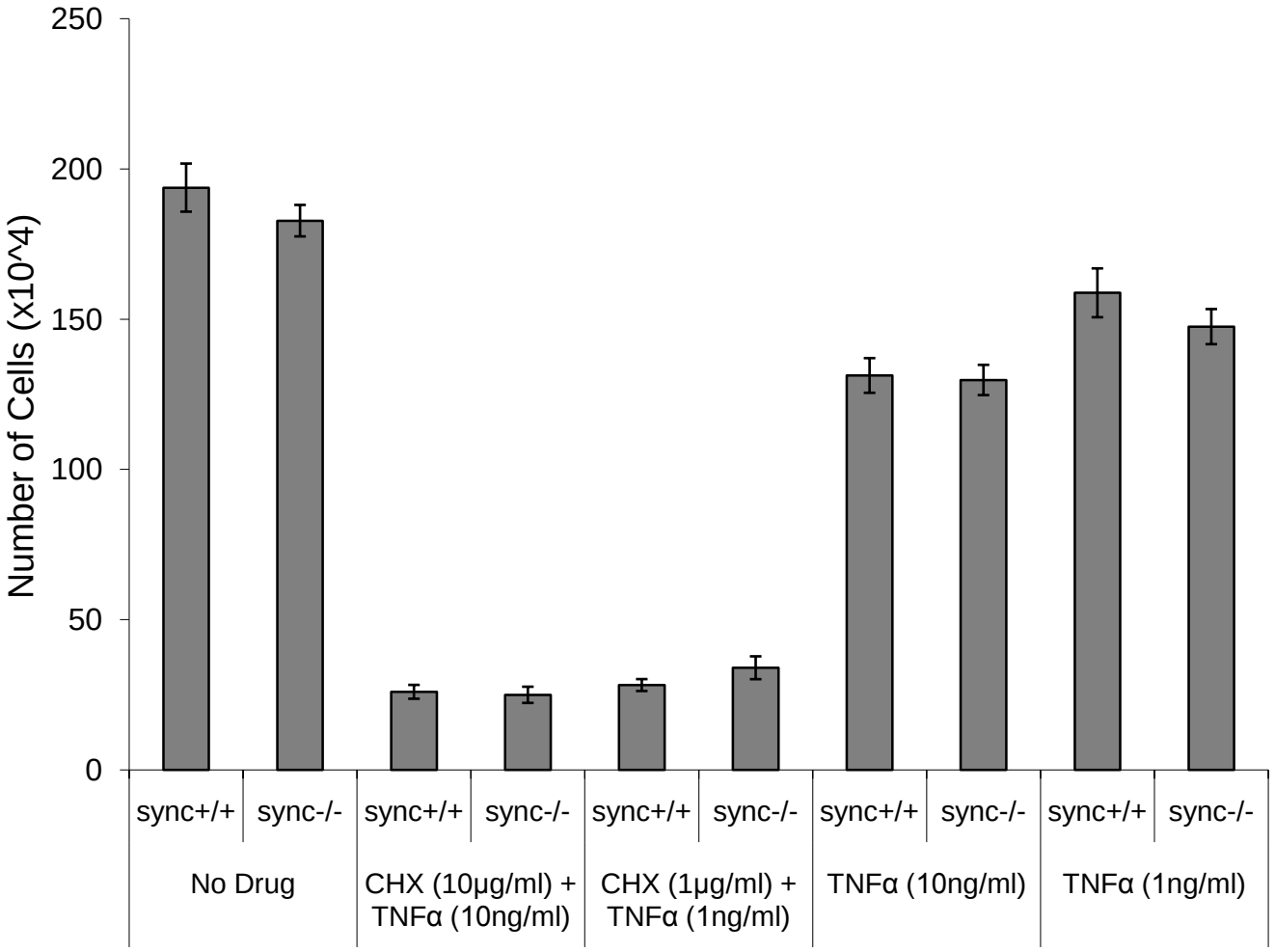

Figure 4.4. Primary cell line drug resistance assay.
Graph showing the number of cells counted for *sync*+/+ and *sync*-/- primary muscle cell lines 24 hours after drug administration. 1x10^6 cells were initially plated 24 hours prior to drug administration. N=2 for each cell line under each drug condition.

occurred at the highest concentration of TNFα and CHX, while the least cell death occurred at the lowest concentration of TNFα alone. In none of the five counts was there a statistically significant difference in cell survival between *sync*+/+ and *sync*-/- cell lines.

4.5 Discussion

In this chapter, primary muscle cell culture lines were generated from *sync*+/+ and *sync*-/- mice. Isolating single cells allowed for experiments that could potentially identify a role for syncoilin in muscle cell development, signalling, growth or apoptosis but could not be performed on whole animals or tissue. Given that syncoilin is upregulated in muscle undergoing regeneration or apoptosis, it was hypothesized that perhaps syncoilin could be involved in signalling that could be best examined at the cellular level.

Prior to these experiments, analysis of the *sync*-/- mouse had yet to reveal any significant phenotype. The results from all three primary cell line experiments produce similar findings. In the cell growth assay, *sync*+/+ and *sync*-/- cells grew at an almost identical rate. While cell growth is a very simple assay, it is also one of the most comprehensive. In tissue culture, one of the most basic analyses of a cell line's health is the rate at which the cells divide. A cell line with any structural or signalling impairments resulting from the absence of a protein is unlikely to divide at the same rate as a wild-type cell line.

A pulse-chase analysis using radioactive methionine to calculate the rate of protein translation revealed no difference between *sync*+/+ and *sync*-/- cells. This result is largely expected after the cell growth assay because cells that divide at the same rates

would be expected to have similar rates of protein production. However, this experiment provided further evidence that syncoilin is dispensable in signalling needed for protein translation and normal cellular funciton.

Finally, a drug survival assay using two drugs that promote apoptosis had similar effects in *sync+/+* and *sync-/-* cells. This study is much more focused, as it is largely based on whether syncoilin is involved in a limited subset of apoptotic signalling pathways. More experiments can be performed using *sync-/-* cells and different signalling pathways, but these experiments should not be a top priority without additional evidence of the involvement of syncoilin in signalling.

Combined, these results suggest that syncoilin might not play a role in certain signalling pathways regulating cell growth and apoptosis or that any role syncoilin has in these pathways is largely redundant. The conclusions drawn from these experiments mirror the conclusions drawn from the muscle analysis of the *sync-/-* mouse. The function of syncoilin remains unclear, and any function is likely redundant given the absence of any significant overt or muscle phenotype in the *sync-/-* mouse.

Chapter 5: Confirmation of syncoilin expression in neurons and further investigation of the interaction between syncoilin and α-tubulin

5.1 Introduction

The previous two chapters described experiments designed to gain a better understanding of the function of syncoilin in muscle. While these experiments and many others have revealed new insights into the structure, expression and binding partners of syncoilin, little has been learned about a functional role for syncoilin in muscle. Given the likelihood that syncoilin is functionally redundant in muscle, another field was chosen for the further study of syncoilin.

Previous work done in this laboratory had begun to explore the role of syncoilin outside of muscle, particularly in neurons. The work performed in this chapter and the remainder of this thesis will be a continuation and advancement of the study of syncoilin in neurons.

Some background work and experimental optimization was necessary before experimental work in neurons could commence. The expression of syncoilin in neurons was confirmed by immunoblot and immunohistochemistry, and a neuronal tissue source for many experiments was chosen.

In an attempt to discover novel binding partners for syncoilin in neurons, Catherine Moorwood from this laboratory performed mass spectrometry and identified α-tubulin as the top hit. One of the aims of this chapter will be to examine α-tubulin as a potential binding partner of syncoilin in neurons.

5.2 Syncoilin expression in neurons as seen by immunoblot

While syncoilin expression in neurons had previously been shown in this laboratory, the immunoblot in Figure 5.1 probed with syncoilin N-term 2991 gives confirmation and offers new insight into the expression of syncoilin in brain, sciatic nerve and spinal cord relative to the skeletal muscle TA. Equal amounts of protein lysate were loaded for the brain, sciatic nerve and spinal cord. One-fourth of the amount of protein lysate loaded for neuronal tissues was loaded for the TA. Since the sync-1 and sync-2 band for TA has the strongest signal despite being loaded four times less than the neuronal samples, it is clear that the relative expression of syncoilin is significantly higher in muscle than in neurons. Within neurons, spinal cord has the highest relative expression of sync-1 and sync-2. Previous unpublished immunohistochemsitry work in this laboratory has shown that syncoilin is specifically expressed in the spinal cord in motor neurons and interneurons.

The immunoblot showed sciatic nerve to contain relatively less sync-1 and sync-2 than spinal cord but more sync-1 and sync-2 than the brain. Since syncoilin is most highly expressed within motor neurons of the spinal cord and the sciatic nerve has a higher concentration of neuronal material than the spinal cord, it is unclear why the relative expression of sync-1 and sync-2 is higher in spinal cord than sciatic nerve. It is possible that neuronal material within the spinal cord contains more syncoilin, or it is possible that syncoilin is expressed in another unknown cell type within the spinal cord.

Sync-1 and sync-2 expression in the brain was the lowest of the three neuronal tissue sources. The brain consists of a large number of cell types, few of which are the motor neurons that are believed to express syncoilin in the spinal cord and sciatic nerve. In

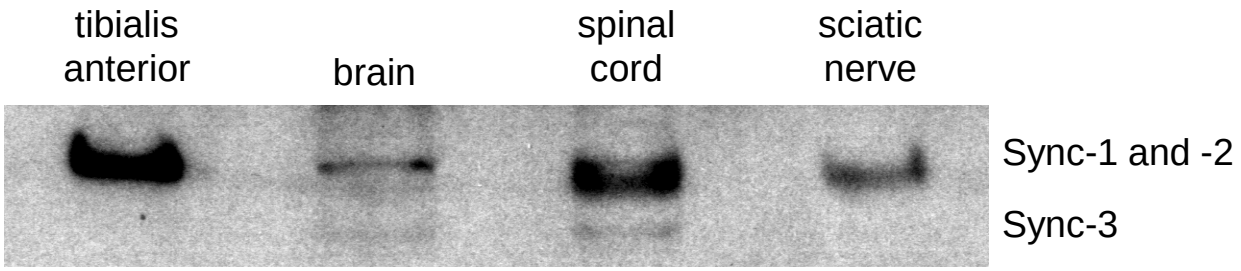

Figure 5.1. Immunoblots of syncoilin protein expression in nerve. Western blot probed with syncoilin N-term 2991 antibody. Samples from mouse include 50µg of tibialis anterior muscle and 200µg of brain, spinal cord and sciatic nerve.

fact, previous studies in our laboratory have been inconclusive about the presence of syncoilin in the brain. Interestingly, detection by immunoblot of sync-3 is seen only in the spinal cord and brain, both components of the central nervous system. The detection of sync-3 exclusively in the central nervous system could suggest that sync-3 is expressed at a high level in a cell type seen only in the central nervous system. This hypothesis would also help to explain the high concentration of syncoilin in spinal cord relative to sciatic nerve.

5.3 Immunohistochemistry of syncoilin in sciatic nerve

Sciatic nerve was chosen as a tissue source for the neuronal study of syncoilin using immunohistochemistry. Sciatic nerve contains a high proportion of neuronal material, is large and easily accessible in mice and has the potential to be separated into single neurons. Single neuron preparations allow for long sections of axons to be isolated on a slide, resulting in unobstructed views and staining of axons, nuclei and nodes of Ranvier. Figure 5.2 provides a panel of confocal images of syncoilin expression in sciatic nerve using the syncoilin N-term 2991 antibody. Panels A and B in Figure 5.2 are single neuron preparations. Punctate and diffuse syncoilin immunostaining is visible along the length of the axons. Panels C and D are longitudinal and transverse images of bundles of sciatic nerve, all displaying high levels of syncoilin immunostaining. These images serve both to confirm the presence of syncoilin in the sciatic nerve and to confirm the use of sciatic nerve as an ideal tissue source for syncoilin immunostaining in neurons.

5.4 α-tubulin is a potential neuronal binding partner of syncoilin

Blot overlay and mass spectrometry experiments using the neuronal N2a cell line were previously performed in this laboratory in an attempt to find novel binding

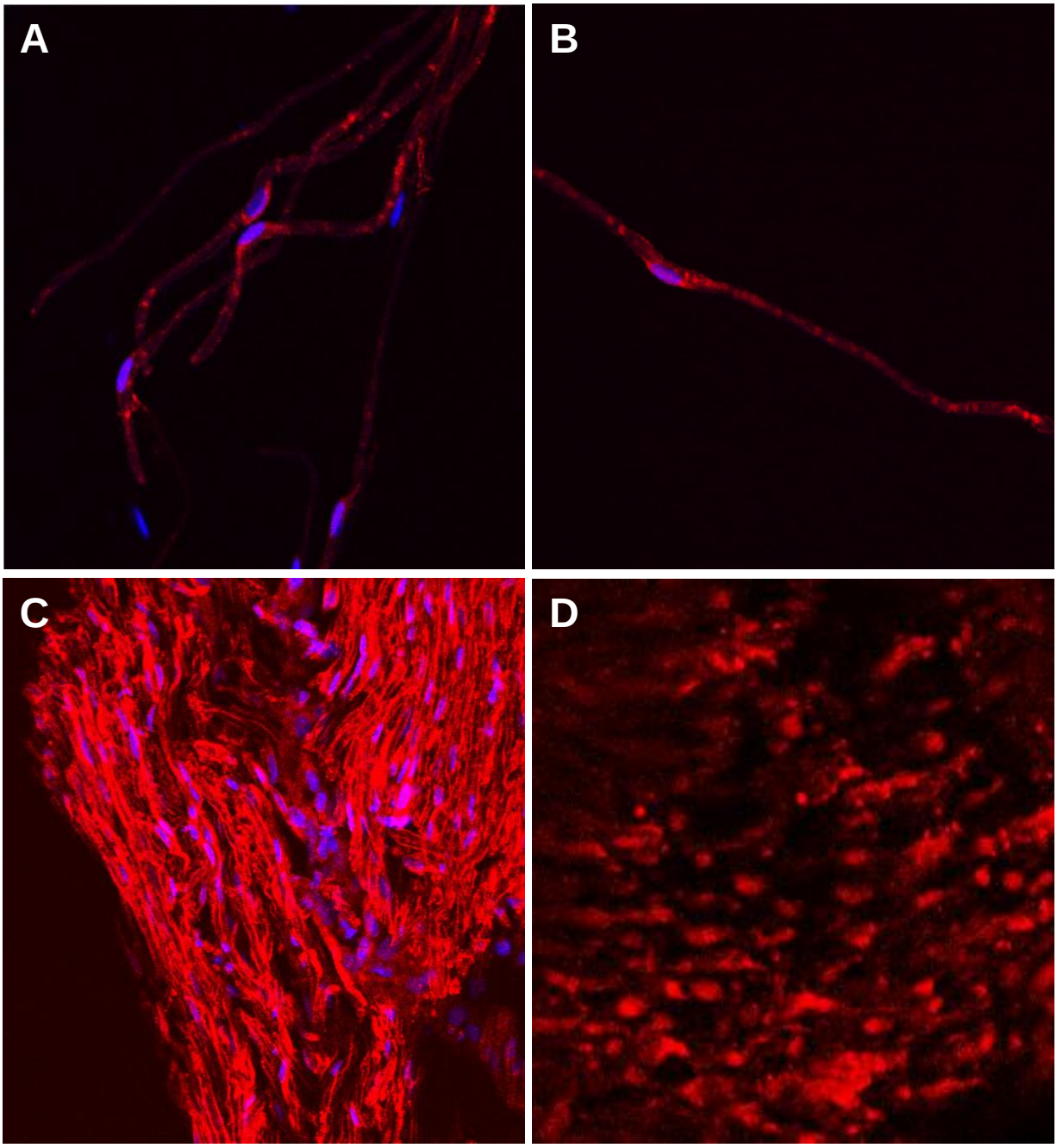

Figure 5.2. Syncoilin expression in sciatic nerve.

Syncoilin immunostaining in mouse sciatic nerve. Stained with syncoilin N-term 2991 antibody (red). Panels A, B and C are co-stained with DAPI (blue). Panels **A** and **B** are from a single fibre preparation. Panel **C** is a longitudinal view of a cluster of neurons in the sciatic nerve and panel **D** is a transverse view of a cluster of neurons in the sciatic nerve.

partners for syncoilin. α-tubulin is a highly expressed cytoskeletal protein that is often identified non-specifically in blot overlays and mass spectrometry. However, α-tubulin emerged as a top candidate when it was identified separately both in a blot overlay and as a top hit in the syncoilin neuronal mass spectrometry experiment. Syncoilin is an intermediate filament cytoskeletal protein that is known to bind the dystrophin associated protein complex (DAPC) component α-dystrobrevin and the intermediate filament protein desmin. An interaction between syncoilin and α-tubulin would be very important because it would provide a link between the DAPC, tubulin cytoskeleton and intermediate filament network. The exciting possibility of syncoilin serving as a connection between three different structural complexes led to the investigation as to whether syncoilin and α-tubulin interact.

Co-immunoprecipitation is a standard tool used to test for *in vivo* protein-protein interactions. Co-IPs were performed between syncoilin and α-tubulin using protein lysates from N2a cells. N2a cells were chosen because the large amounts of protein needed made using mouse neuronal tissue unrealistic. Early attempts at co-IPs showed no interaction between syncoilin and α-tubulin. One hypothesis for the unsuccessful results was that the ratio of α-tubulin to syncoilin in the cells was overwhelming. Low levels of syncoilin would have difficulty pulling down enough α-tubulin for its visualisation. Also, low levels of syncoilin would not provide enough protein to be bound by α-tubulin, pulled down and visualised by immunoblot. It was attempted to correct for the significant difference in syncoilin and α-tubulin protein levels by transfecting the N2a cells with HA-tagged syncoilin prior to the co-IP.

Protein lysates were immunoprecipitated with a variety of antibodies from different species to avoid the heavy chain IgG in the immunoprecipitating antibody from reacting with the immunoblotting secondary antibody and blocking relevant bands. Syncoilin antibodies used were from rabbit and goat while the α-tubulin antibodies were mouse monoclonals. Positive controls included HA antibodies that target the tag on transfected syncoilin and β-tubulin that is known to bind α-tubulin.

Figure 5.3A reveals that α-tubulin binds to syncoilin. A band for α-tubulin was present in the lysate, and bands of α-tubulin are seen in the positive control lanes of α-tubulin and β-tubulin, confirming that the tubulin antibodies are successfully binding α-tubulin. The co-IP immunoblot also suggests that α-tubulin was also pulled down by goat and rabbit antibodies to syncoilin and an antibody to the HA tag. This signifies that α-tubulin was bound to syncoilin when syncoilin was being pulled down by its own antibodies. Also very important, the no antibody lane is blank, meaning there was no non-specific pull down of α-tubulin by the protein G sepharose beads. The peripherin negative control is difficult to interpret due to overlap from the lysate lane and due to the large IgG band that exists at 55 kDa since peripherin is a mouse monoclonal and the band was probed with a mouse secondary antibody. It is important to note that tubulin is a 50 kDa protein and the heavy chain IgG is a 55 kDa protein. However, the experience in this laboratory has always been that tubulin runs higher than the heavy chain IgG. It is unclear why this occurs, but one theory is that post translational modifications such as phosphorylation add weight to α- and β-tubulin, resulting in their slower migration through the SDS-PAGE gel.

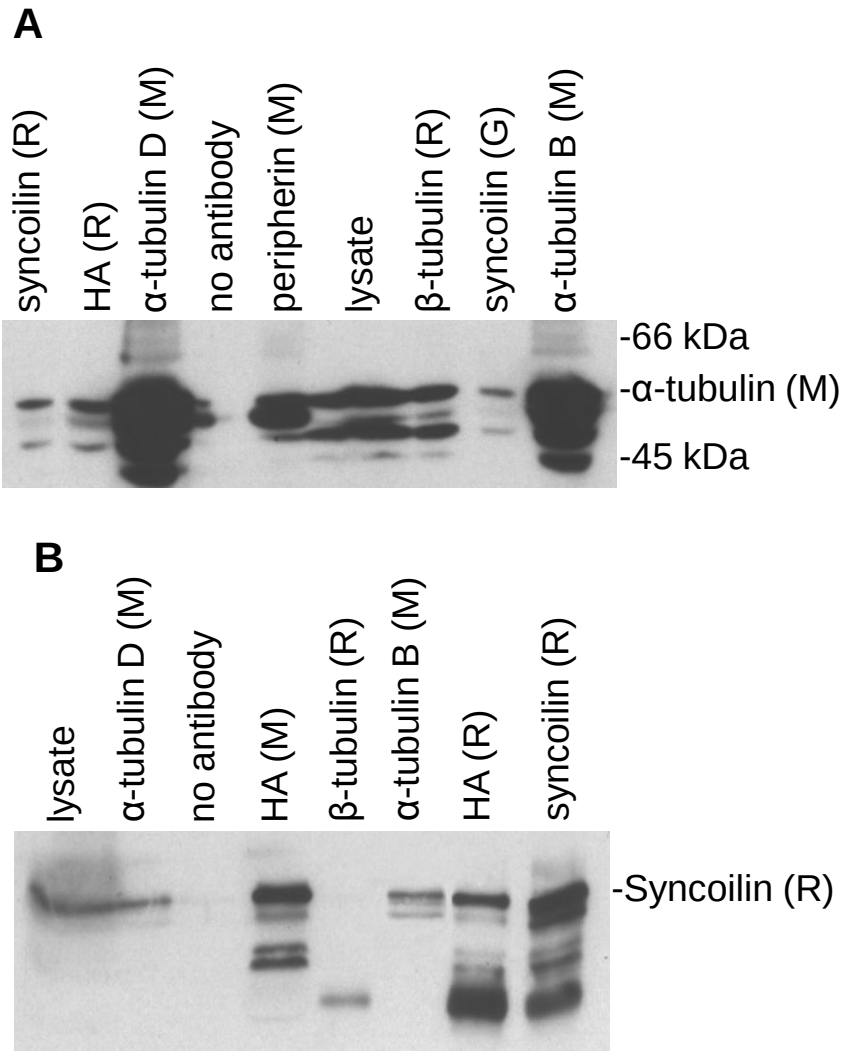

Figure 5.3. Co-immunoprecipitation of syncoilin and α-tubulin from N2A cells.

N2A cells were transfected with syncoilin-HA to increase syncoilin expression. Immunoprecipitating antibodies are listed above the immunoblots with the host species of each antibody in parentheses (M=mouse, R=rabbit, G=goat). α-tubulin mouse monoclonal antibodies used are B512 and DM1A. The rabbit syncoilin antibody used was N-term 2991.

A. Probed for α-tubulin DM1A. α-tubulin is pulled down by α-tubulin, β-tubulin, syncoilin and HA. α-tubulin is also present in the lysate but not in the no antibody control lane. Tubulin is a 50 kDa protein, but in our experience, tubulin runs higher than the IgG heavy chain which is predicted to run at 55kDa.

B. Probed for syncoilin rabbit N-term 2991. Syncoilin is pulled down by α-tubulin, syncoilin and anti-HA but not β-tubulin. Syncoilin is also present in the lysate but not in the no antibody control lane.

Figure 5.3B demonstrates that syncoilin binds to α-tubulin. Bands of syncoilin are seen in the lysate and positive control lanes of syncoilin, HA rabbit and HA mouse. These bands confirm the presence of syncoilin and confirm that the syncoilin antibodies were successfully pulling down syncoilin. The no antibody lane was clean, signifying that there was no non-specific reaction between syncoilin and the protein G sepharose beads. There were bands in the two lanes of α-tubulin monoclonal antibodies, suggesting that syncoilin and α-tubulin were bound during the co-IP process. Interestingly, the lane for β-tubulin is clean, signifying that the interaction between α-tubulin and syncoilin is specific only to α-tubulin.

5.5 No colocalisation of α-tubulin and syncoilin in sciatic nerve

In the previous section, syncoilin and α-tubulin were shown to co-immunoprecipitate in N2a cells. However, a potential problem with co-immunoprecipitations is that they use whole cell protein lysates. These lysates do not reflect physiological conditions because they combine proteins expressed in different subcellular compartments, meaning there is a potential for interactions between proteins that would not contact each other in a cell. Immunohistochemistry was performed to determine whether syncoilin and α-tubulin co-localise *in vivo*. A sciatic nerve single neuron preparation was co-stained with antibodies against syncoilin and α-tubulin.

Figure 5.4 shows two different series of images of sciatic nerve single neurons. Panels A and B stain for syncoilin using the rabbit N-term 2991 antibody. Panels C and D stain for the α-tubulin DM1A mouse monoclonal antibody. Panels E and F are merges of the syncoilin and α-tubulin staining and also include DAPI staining of the nucleus. The two axons in panels A, C and E and the one axon in panels B, D and F all show diffuse syncoilin staining down the length of the axon and more specific α-tubulin

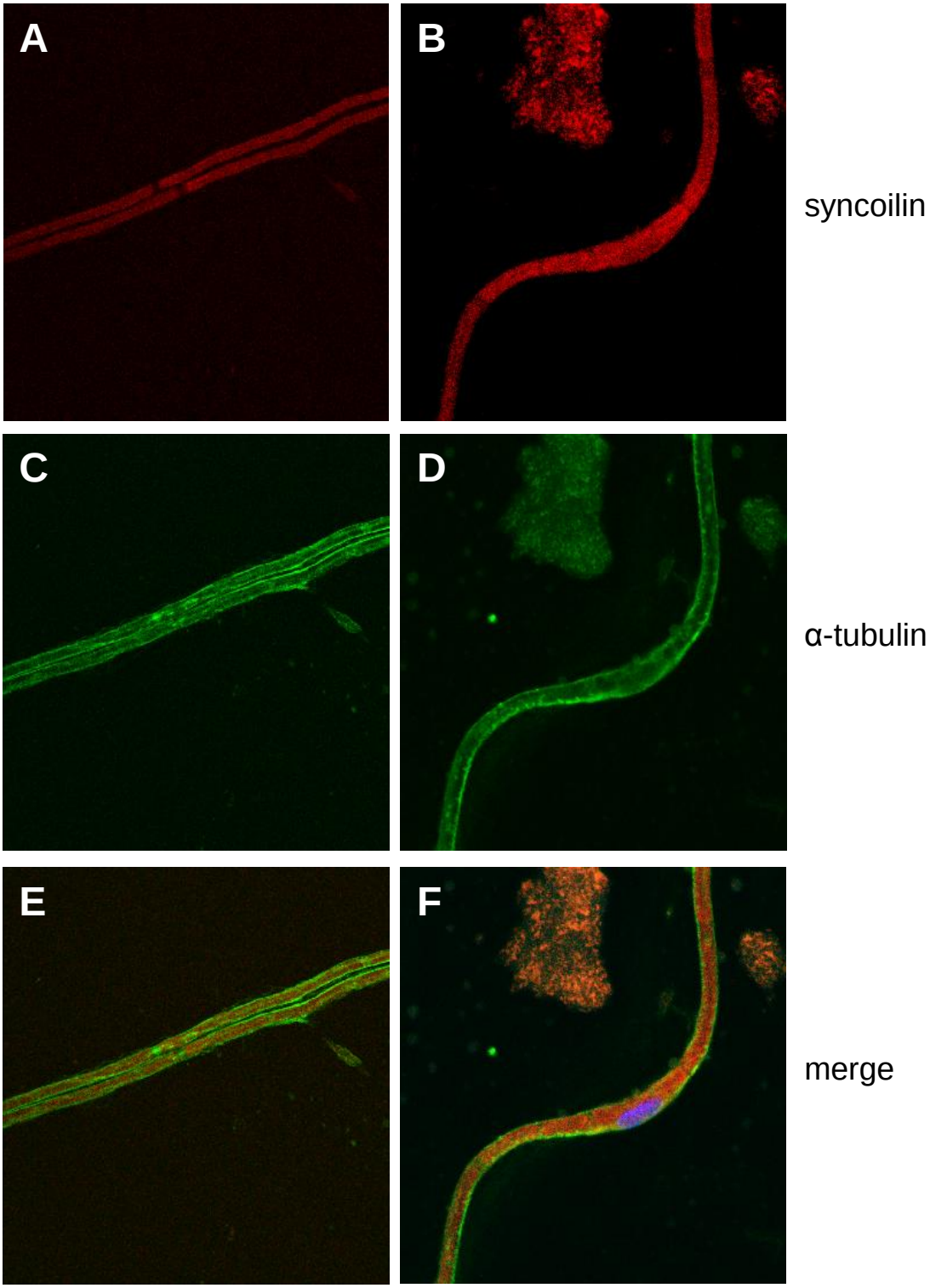

Figure 5.4. Syncoilin and α-tubulin do not co-localise in sciatic nerve. Syncoilin and α-tubulin immunostaining in single neuron preparation mouse sciatic nerve. Stained with syncoilin N-term 2991 antibody (red), α-tubulin monoclonal DM1A antibody (green) and DAPI (blue).

staining along the outer edges of the axon. Since these are confocal images that scan one very thin cross section of the nerve, these images can be interpreted to show that syncoilin localises down the middle of the axon and α-tubulin localises along the outside of the axon. The apparent lack of co-localisation calls into question whether the physical interaction between syncoilin and α-tubulin could ever happen in a cell and whether this potential interaction is physiologically relevant

5.6 α-tubulin in the syncoilin-null mouse

Previous experiments with syncoilin in muscle including those from Chapter 4 in this thesis led to a hypothesis that syncoilin is a potentially functional yet redundant intermediate filament protein. In an effort to identify a potential functional role for syncoilin in neurons, a number of experiments were performed using the *sync-/-* mouse. These experiments aimed to examine whether α-tubulin expression in neurons was altered by the absence of syncoilin.

5.6.1 α-tubulin localisation is unchanged in the syncoilin-null mouse

The first step in examining α-tubulin expression in the *sync-/-* mouse was to determine if α-tubulin localisation is altered in the *sync-/-* mouse. A difference in α-tubulin localisation in the *sync-/-* mice could signify that syncoilin is necessary for the proper distribution or function of α-tubulin within the cell. Figure 5.5 contains confocal images of sciatic nerve single neuron preparations from *sync+/+* and *sync-/-* mice immunostained for α-tubulin with a mouse monoclonal antibody.

In both the *sync+/+* and *sync-/-* mice, there is strong immunostaining for α-tubulin that localises along the outside of the axon. There is no apparent difference in immunostaining localisation between the neurons, suggesting that the absence of syncoilin along the axon does not alter subcellular α-tubulin localisation. Any

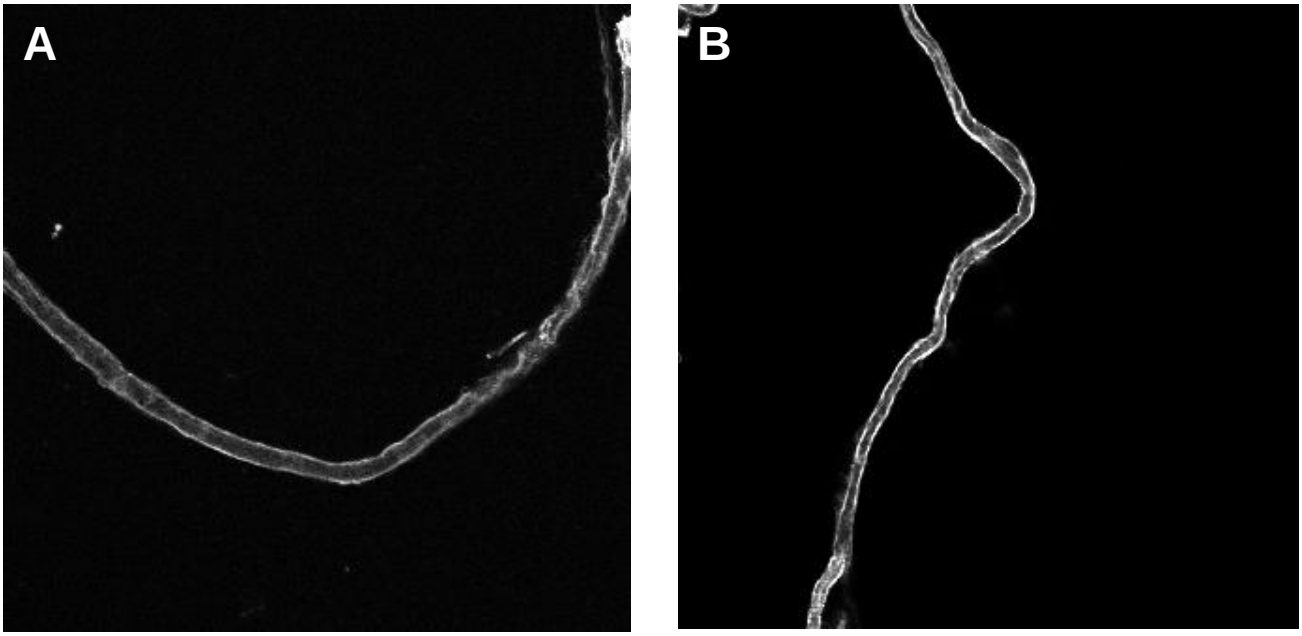

Figure 5.5. α-tubulin expression in sciatic nerve.
α-tubulin immunostaining in mouse sciatic nerve from a single neuron preparation. Stained with α-tubulin monoclonal DM1A. Panel A is from a *sync+/+* mouse and panel B is from a *sync-/-* mouse. Both images show α-tubulin to have the same localisation along the axon of the sciatic nerve.

difference in staining intensity is possibly a result of different microscope exposure times. Instead, more precise measures of α-tubulin expression are made in the following sections.

5.6.2 α-tubulin RNA levels unchanged in the syncoilin-null mouse

Measuring expression of α-tubulin can be done on an mRNA level and on a protein level. First, α-tubulin mRNA was compared between the *sync*+/+ and *sync*-/- mice using quantitative RT-PCR. Ideally, sciatic nerve would have been used given its high proportion of neuronal material. However, the large amounts of mRNA needed for RT-PCR made the use of sciatic nerves unrealistic. Instead, spinal cords were used as a substitute in order to reduce the number of mice needed for this experiment. Given the high expression of syncoilin in spinal cord, any change in neuronal α-tubulin mRNA due to the loss of syncoilin should be evident in spinal cord.

Figure 5.6 shows relative α-tubulin mRNA levels in *sync*+/+ and *sync*-/- mice. This data is taken from six mice per genotype, normalised to GAPDH levels and adjusted for primer reaction efficiency. The 15% increase in α-tubulin mRNA is well within the standard deviation and represents a small increase given the high variability of mRNA levels in tissues from different mice. Based on this data, a conclusion can be drawn that there is no difference in α-tubulin mRNA levels between *sync*+/+ and *sync*-/- mice.

5.6.3 α-tubulin protein levels are unchanged in the syncoilin-null mouse

Differences in protein levels can be examined by the relative strengths of bands in an immunoblot. Both spinal cord and sciatic nerve protein lysates were used from *sync*+/+ and *sync*-/- mice. Lysates were loaded at equal protein concentrations and equal volumes. Four identical blots were probed for α-tubulin, β-tubulin, the neuronal

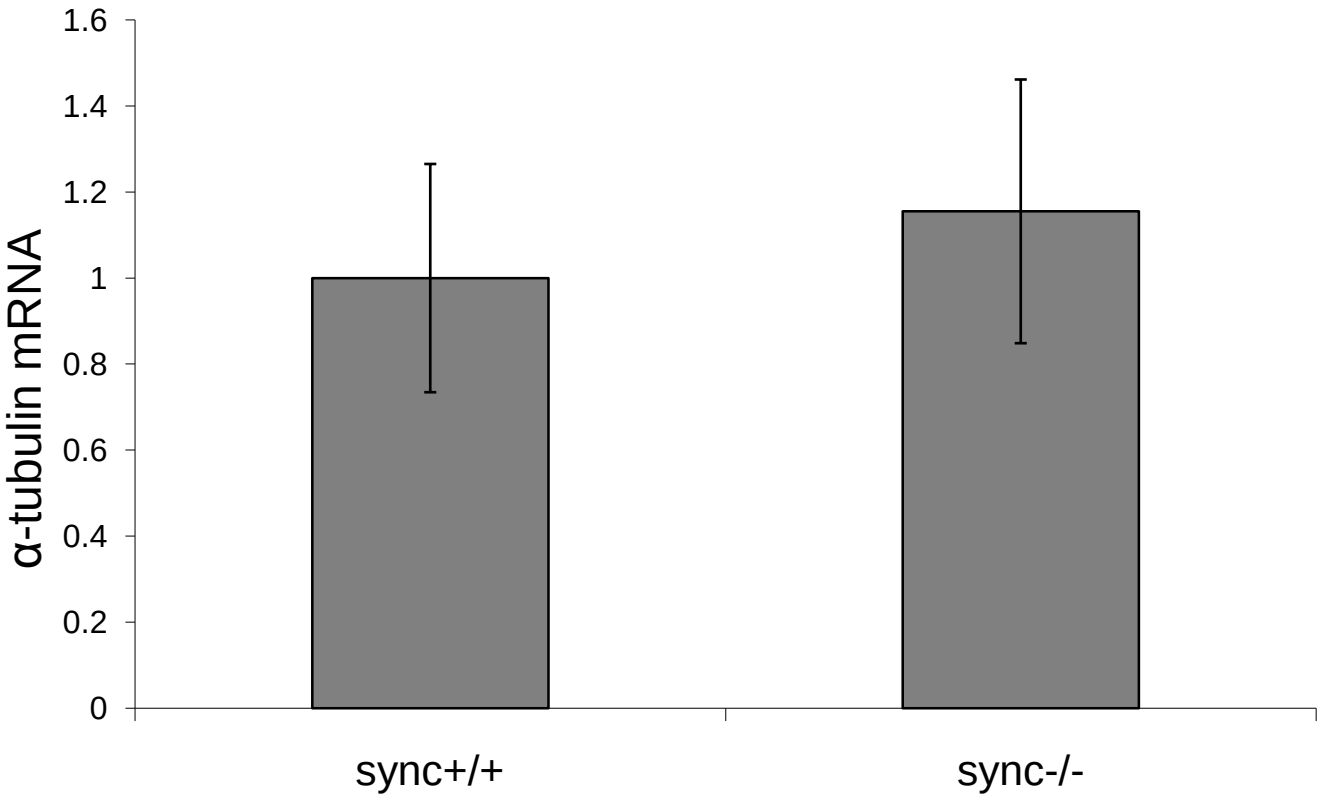

Figure 5.6. RT-PCR of α-tubulin mRNA in *sync*+/+ and *sync*-/- spinal cord.
Quantitative RT-PCR analysis was used to determine the amount of α-tubulin mRNA in *sync*+/+ and *sync*-/- in spinal cord. Data are normalized to GAPDH controls and mRNA levels are represented relative to *sync*+/+.

intermediate filament protein neurofilament and the cytoskeletal protein β-actin. The use of multiple proteins allowed for redundant loading controls in the event of differences in band intensity.

These immunoblots in Figure 5.7 and other repeats consistently revealed no significant difference in α-tubulin protein levels either in spinal cord or sciatic nerve between *sync*+/+ and *sync*-/- mice. The intensity of the α-tubulin bands relative to the β-actin bands was analysed using Image J software, and differences between *sync*+/+ and *sync*-/- samples were well within the standard deviation (Abramoff, Magelhaes et al. 2004). The immunoblots, combined with RT-PCR data, provide evidence that α-tubulin levels are unchanged on the protein and mRNA levels in the *sync*-/- mouse.

5.7 Discussion

The experiments in this chapter provide new and important data for the study of syncoilin in neurons. Syncoilin expression in neurons was confirmed by immunoblot and immunohistocheimstry. An interaction between syncoilin and α-tubulin was verified using co-immunoprecipitation, but further experiments revealed no co-localisation between the two proteins and no change in α-tubulin localisation or expression in the syncoilin-null mouse.

Syncoilin was initially discovered in muscle due to its link to the DAPC and potential connection to neuromuscular disease. Previous work in this laboratory identified the expression of syncoilin in neurons and initiated the study of this field. Groundwork for the remainder of this thesis was presented in this chapter. Immunoblots of syncoilin expression in sciatic nerve and spinal cord show that both tissues are good

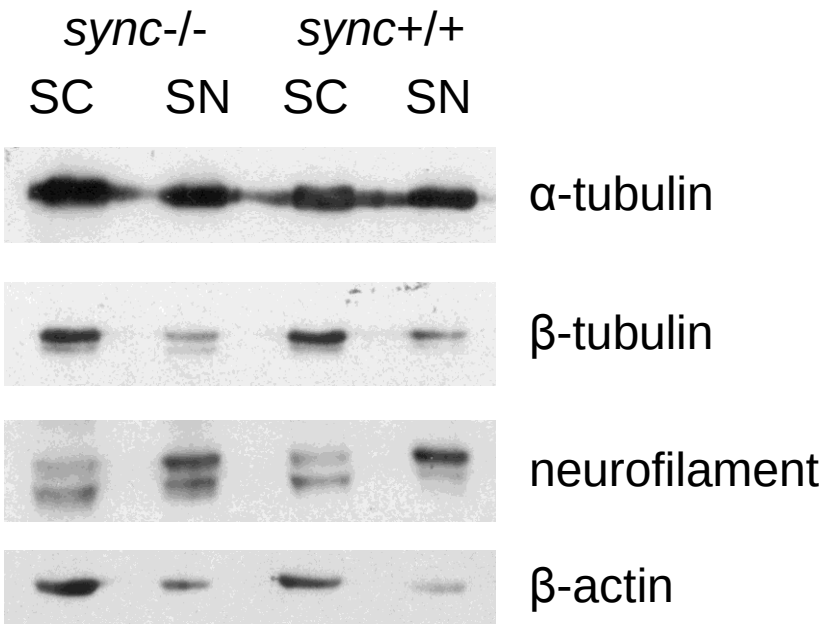

Figure 5.7. Immunoblots of tubulin levels in *sync-/-* spinal cord and sciatic nerve.
100µg of spinal cord (SC) and sciatic nerve (SN) from *sync-/-* and *sync*+/+ mice was loaded at equal concentrations and equal volume. Western blots were probed with α-tubulin monoclonal DM1A, pan β-tubulin rabbit polyclonal, neurofilament monoclonal and rabbit polyclonal β-actin. There appears to be no difference in expression of these proteins between the *sync-/-* and *sync*+/+ mice.

protein sources for future experiments. Spinal cord has high levels of syncoilin while sciatic nerve has a high proportion of neuronal material.

This chapter also marks the introduction of a new protocol in this laboratory, the single neuron preparation of sciatic nerve. This single neuron preparation allows for the examination of single axons and is especially useful because it provides superior clarity in immunohistochemistry. Without this protocol, experiments in this chapter such as the co-localisation of syncoilin and α-tubulin would have been significantly more difficult to interpret because it would be impossible to decipher one axon from another.

Previous experiments on the neuronal expression of syncoilin included blot overlays and mass spectrometry that identified α-tubulin as a potential binding partner of syncoilin. The work done in this chapter on α-tubulin set out to confirm these preliminary experiments. First, a reciprocal co-immunoprecipitation confirmed in both directions that syncoilin pulled down α-tubulin and that α-tubulin pulled down syncoilin. Co-immunoprecipitation is the gold standard for showing interactions between insoluble proteins from tissue lysates. Co-IP requires proteins to bind each other in a gentle lysis buffer and be pelleted by a bead connected to the proteins by an antibody. This stringent protocol requires strong protein-protein interactions to be successful. Proper controls, as used in the experiments in this chapter, can ensure the absence of non-specific or false positive results. The inability to immunoprecipitate syncoilin and α-tubulin without the addition of transfected syncoilin is unfortunate because it makes the experiment more artificial. However, repeated attempts to immunoprecipitate untransfected neuronal cells were unsuccessful.

Interestingly, repeated attempts to co-immunoprecipitate syncoilin and α-tubulin in muscle cells, muscle cells transfected with syncoilin and muscle tissue have been unsuccessful. This information suggests that any interaction between syncoilin and α-tubulin might be specific to neuronal cells. Further evidence of a specific interaction is the fact that α-tubulin but not β-tubulin pulled down syncoilin in the co-immunoprecipitations. This selective binding shows a high level of specificity and suggests that the binding of syncoilin to α-tubulin is more than an experimental artefact.

A co-immunoprecipitation demonstrates protein-protein interactions, but these interactions need to be verified by co-localisation as well. During the co-IP protocol, protein lysates are extensively mixed. This process combines subcellular compartments that would never interact in a cell. It is possible that two proteins which interact and bind in a lysate would never have the opportunity to interact in a cell. For this reason, co-localisation allows verification that proteins which are thought to bind *in vivo* are actually within the same subcellular region. In sciatic nerve, syncoilin and α-tubulin did not co-localise. Syncoilin appears to localise along the length of the axon within the middle while α-tubulin appears to localise along the length of the axon but on the outer edge. While this does not mean that syncoilin and α-tubulin never meet or interact in the neuron, it does suggest that any interaction or binding would be limited.

With these mixed results, it was decided to look directly at whether syncoilin affects the function, localisation or expression of α-tubulin. This decision was made for three

reasons. First, given the lack of co-localisation, further investigation of the relationship between syncoilin and α-tubulin would require evidence of a meaningful interaction. Second, any clinical or physiological relevance that syncoilin might have is brought into question by the theory that other similar proteins have the same function and are able to compensate for syncoilin in the event of the loss of syncoilin. Syncoilin's interaction with α-tubulin is most interesting if there are not additional compensatory proteins that can easily replace syncoilin. Third, there exist hundreds of proteins that are known to bind α-tubulin, many with unknown function (Chuong, Good et al. 2004). Without further evidence of syncoilin's functional relevance to α-tubulin, other avenues of research would likely be a better use of time and resources.

Three experiments were performed to examine the effect that the absence of syncoilin has on the localisation and expression of α-tubulin. The localisation of α-tubulin along the axon of the sciatic nerve had no apparent change in the *sync-/-* mouse. Dimers of α-tubulin and β-tubulin assemble into microtubules, so identical α-tubulin localisation suggests that microtubules are forming as normal. Combined, this information leads to the conclusion that syncoilin is not necessary for the proper localisation of α-tubulin or for the proper formation of microtubules.

Additionally, α-tubulin mRNA and protein levels were unchanged in the *sync-/-* mouse, signifying that syncoilin is not involved in any processes that regulates α-tubulin expression. The information gained from these experiments does not attempt to portray a complete account of the relationship between syncoilin and α-tubulin in neurons. It is possible that syncoilin and α-tubulin meaningfully interact in ways not measured in these assays or that the role of syncoilin is largely redundant and covered

by another protein in its absence. It is also highly possible that syncoilin and α-tubulin do not interact within neurons, as suggested by the lack of subcellular co-localisation. Considering all of this information, further work on α-tubulin was suspended so other potential syncoilin binding partners in neurons could be investigated.

Chapter 6: Syncoilin and peripherin

6.1 Introduction

The preceding chapter described the investigation of α-tubulin as a potential binding partner of syncoilin in neurons. Previous work done in this laboratory by Dr. Karl McCullagh identified the IF protein peripherin as another potential syncoilin neuronal binding partner. As described in Section 1.2, syncoilin binds the intermediate filament desmin in skeletal muscle. Desmin is a type III IF protein and is expressed exclusively in muscle (Costa, Escaleira et al. 2004). The only type III IF protein expressed in neurons is peripherin. It was hypothesized that since desmin and peripherin share features as type III IF proteins, syncoilin and peripherin might interact in neurons.

Previous unpublished experiments performed by Dr. Karl McCullagh showed syncoilin and peripherin to co-immunoprecipitate in spinal cord tissue and NSC-34 neuronal cells. These experiments also showed syncoilin and peripherin to co-localise in cell bodies of the dorsal root ganglia (DRG). Dr. Matthew Kemp in this laboratory has further unpublished evidence of the interaction in the form of blot overlays that use purified proteins including the three syncoilin isoforms. These blot overlays show equal binding of peripherin in sync-1 and sync-2 and lesser binding in sync-3.

A series of experiments were used to further characterise the interaction between syncoilin and peripherin in neurons. Co-localisation was performed using the new sciatic nerve single neuron preparation to allow the visualisation of syncoilin and peripherin staining along the length of the axon. Syncoilin and peripherin were transfected into cells to study the formation of filament networks. Finally, in an unexpected result, peripherin and α-tubulin were found to co-immunoprecipitate.

6.2 Syncoilin and peripherin co-localise in sciatic nerve

In unpublished work, Dr. Karl McCullagh demonstrated co-localisation of syncoilin and peripherin in the DRG. While co-localisation was apparent in these cross-section images, it was difficult to determine the exact subcellular expression of syncoilin and peripherin because of the overwhelming number of neurons. As previously described in Section 5.3, single neuron preparation of the sciatic nerve allows for immunostaining along the length of a single axon.

Figure 6.1 shows two examples of single neuron immunostaining. Panels A and B are stained with syncoilin N-term 2991 antibody while panels C and D are stained with peripherin chicken antibody. Panels E and F are merges of these two immunostains and include a DAPI stain of the nucleus in blue. Both of the nerves pictured reveal significant co-localisaiton of syncoilin and peripherin. This co-localisation appears to be within the centre of the axon, consistent with previous images of syncoilin immunostaining in sciatic nerve presented in Figures 5.2 and 5.4 in this thesis. In fact, peripherin immunostaining appears to be more specific to the centre of the axon than syncoilin. This can be especially seen in the left column of panels. In the inverted U-shaped bend of the neuron near the nuclei on the left side of the picture, there appears to be faint syncoilin staining but no peripherin staining outside of the centre of the axon.

This data confirms the previous evidence of co-localisaiton of syncoilin and peripherin in DRG. By viewing the immunostaining of syncoilin and peripherin down the length of the axon, it is possible to more confidently assert that syncoilin and peripherin share the same subcellular localisaiton in sciatic nerve. Combined with the knowledge that syncoilin and peripherin co-immunoprecipitate and interact in blot

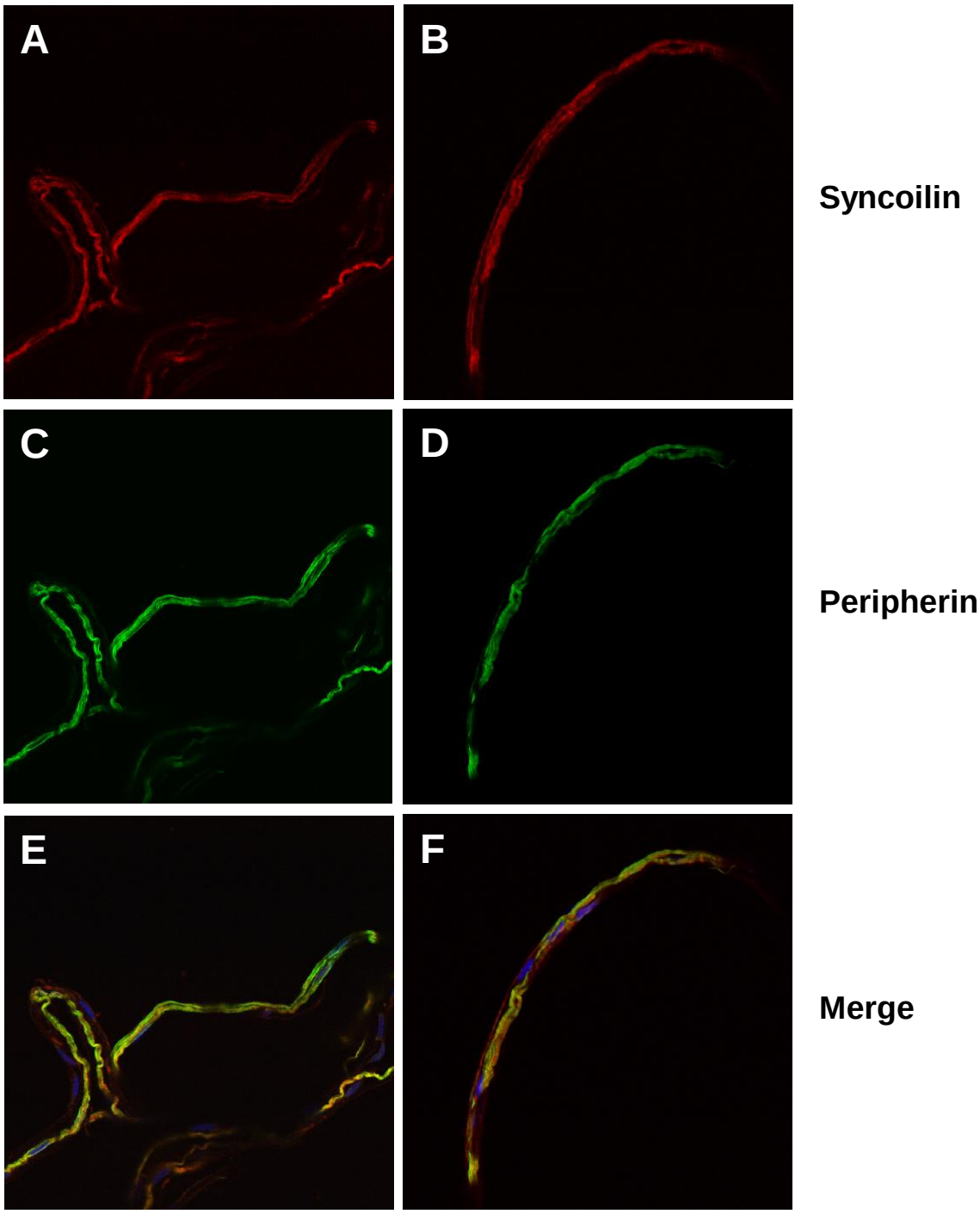

Figure 6.1. Syncoilin and peripherin co-localise in sciatic nerve.
Syncoilin and peripherin immunostaining in single fibre preparation mouse sciatic nerve. Stained with peripherin chicken antibody (green), syncoilin N-term 2991 antibody (red) and DAPI (blue).

overlay, the current evidence suggests that there is a high likelihood syncoilin and peripherin interact *in vivo*. The next sets of experiments in this chapter will aim to assess whether syncoilin and peripherin have a functional relationship in neurons.

6.3 Peripherin and syncoilin filament formation

A subclone of the SW13 human adrenal cortex carcinoma-derived cell line known as SW13vim(-) lacks all five known classes of IF proteins including vimentin and the keratins (Hedberg, Chen 1986). These SW13 cells allow for the transfection of an IF gene and the study of how that IF protein assembles in the absence of any other IF protein.

Recent studies have revealed a novel peripherin isoform generated through the use of an in-frame downstream initiation codon. This isoform is approximately 45 kDa in size and is known as Per45. The previously known peripherin isoform generated by all nine exons of the human and mouse gene is approximately 58 kDa and is known as Per58. For a review of peripherin isoforms, see Figure 6.2. Both isoforms are constitutively expressed in mice, and Per45 is required for normal network formation. The absence of Per45 or disruption of Per45 to Per58 ratios has been shown to disrupt the normal peripherin filamentous structures (McLean, Xiao et al. 2008).

Figure 6.3 confirms pervious reports of peripherin filament formation in transfected SW13 cells (McLean, Xiao et al. 2008). Transfection was performed with three peripherin constructs, and immunostaining was performed with the peripherin chicken antibody. As seen in panel A, transfection of peripherin, the gene encoding both Per45 and Per58, results in a fully formed filament network. Individual Per45 and Per58 cDNA constructs were created to allow expression of only one isoform at a time.

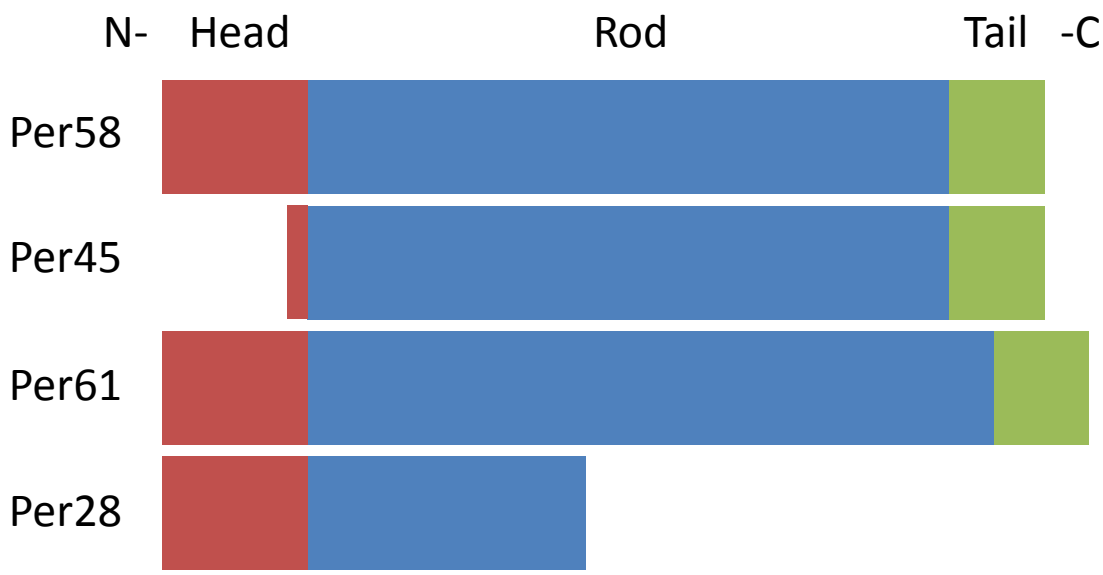

Figure 6.2. Peripherin isoforms.
Per58 (58 kDa) is the originally characterised peripherin isoform consisting of all nine exons of the human and mouse gene. Per45 is generated from an in-frame downstream initiation codon. In this thesis, cDNA identified as "peripherin" results in the production of Per58 and Per45. As discussed in section 1.3.6.1, Per61 and Per28 are associated with ALS. Per61 includes 32 amino acids from intron 4 in the rod domain. Per28 retains introns 3 and introduces a premature stop codon 30 bp downstream of the intron.

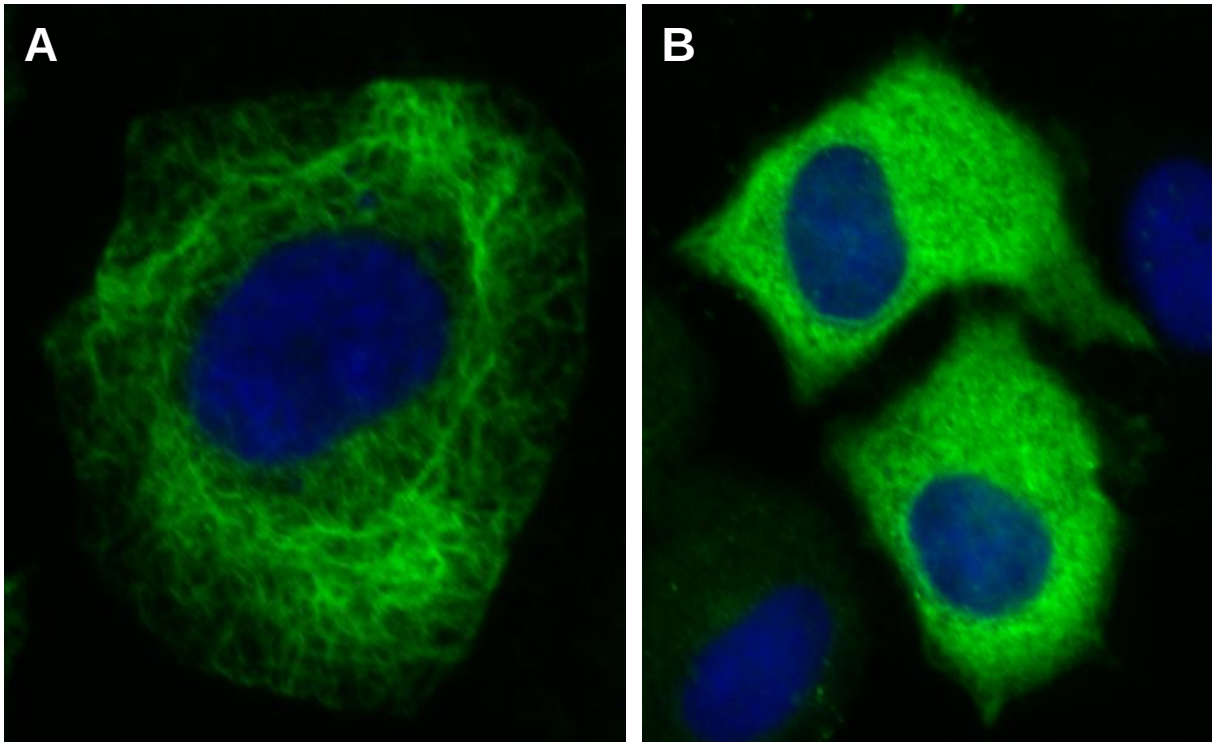

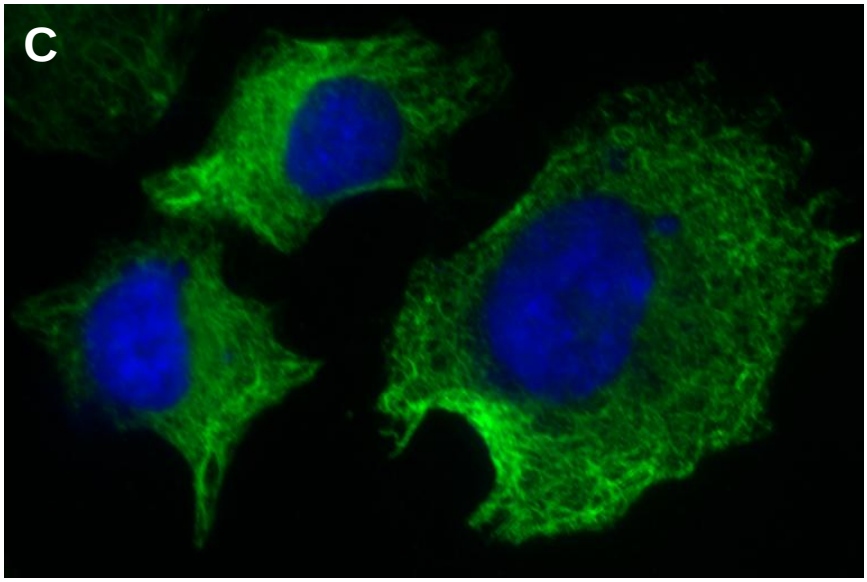

Figure 6.3. Peripherin filament formation in SW13 transfected cells.
SW13 cells were transfected with three peripherin constructs: peripherin, Per45 and Per58. The peripherin construct codes for both the Per45 and Per58 transcripts. Immunostaining with peripherin chicken antibody (green) plus DAPI (blue).

Per45 transfected alone in Panel B formed no filament network, instead resulting in dense and diffuse immunostaining in the cytoplasm. Per58 transfected alone in Panel C formed a filament network, but this network appeared to contain shorter and less organised filaments than the network in peripherin transfected cells.

Figure 6.4 shows syncoilin expression in SW13 transfected cells. Three syncoilin isoforms were transfected alone and immunostained using the N-term 2991 antibody. In all three cases, syncoilin expression is punctate and diffuse throughout the cytoplasm. Although not shown, the staining pattern of the full length syncoilin gene was the same as the staining pattern in the individual isoforms (Newey, Howman et al. 2001, Poon, Howman et al. 2002).

Given that syncoilin is an IF protein but does not form filaments, it is hypothesized that syncoilin has an alternative function. Syncoilin is known to interact and co-localise with peripherin, and peripherin appears to have a regulated IF network. The next section will aim to examine whether syncoilin is involved in peripherin IF network formation or regulation.

6.4 Syncoilin and peripherin co-transfections

To determine if syncoilin has a potential involvement in peripherin network formation, a series of co-transfections were performed in SW13vim(-) cells. All three syncoilin constructs were transfected with the three peripherin constructs discussed in the previous section. Sync-1 and sync-2 exhibited similar staining and had a similar effect on peripherin. Recent unpublished data from an RT-PCR performed by Dr. Matthew Kemp in this laboratory suggests that sync-2 is the dominant syncoilin isoform in neurons. For this reason, the sync-2 isoform is presented in the figures in

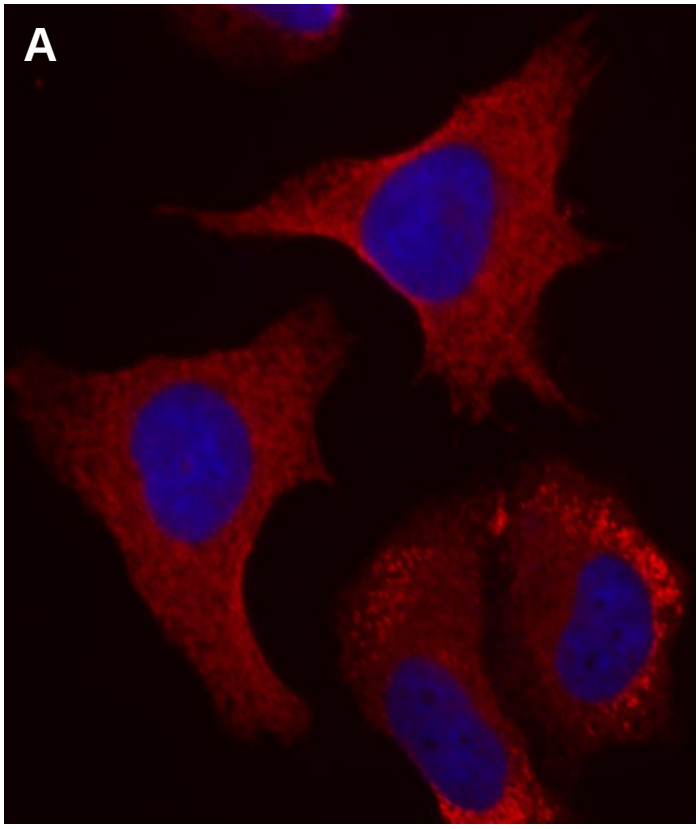

Sync-1

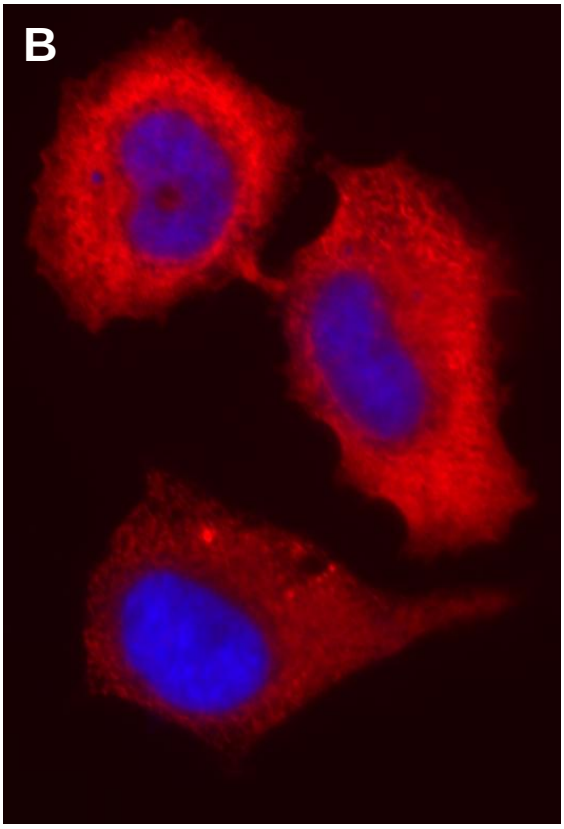

Sync-2

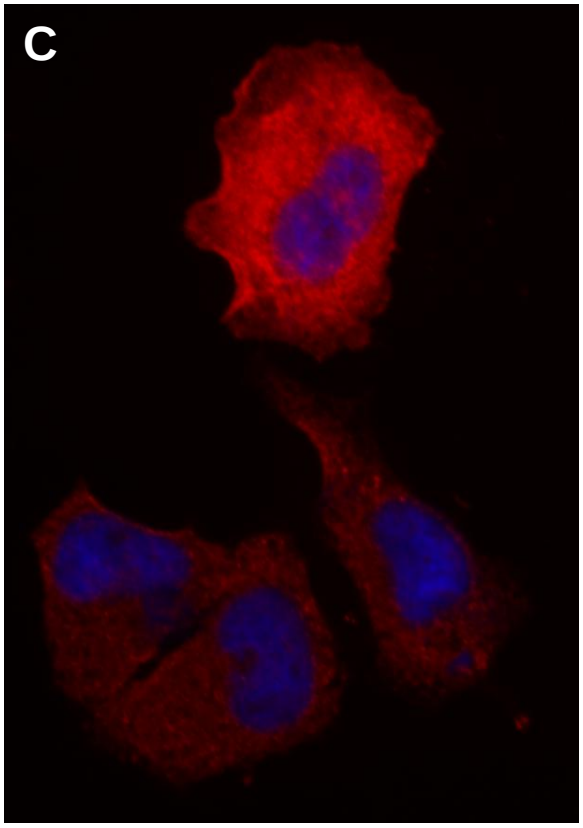

Sync-3

Figure 6.4. Syncoilin expression in SW13 transfected cells.

SW13 cells were transfected with three syncoilin constructs: sync-1, sync-2 and sync-3. Immunostaining with syncoilin N-term 2991 antibody (red) plus DAPI (blue).

this section. The same RT-PCR showed sync-3 expression to be very low in neurons. Given that sync-3 is likely of much less physiological importance than sync-1 and sync-2 and had no novel function in the following experiments, sync-3 was also omitted from this section.

6.4.1 Sync-2 co-transfected with peripherin

SW13 cells were co-transfected with the same constructs used in Section 6.4 for sync-2 and peripherin. Syncoilin was immunostained red using the N-term 2991 antibody and peripherin was stained green using its chicken antibody. Figure 6.5 panels A and C show merges of the two antibody immunostainings plus DAPI while panels B and D show peripherin staining alone. The cell in the top row and the cell in the bottom row are both co-transfected, as seen in the merged image. Sync-2 staining is punctate and diffuse throughout the cytoplasm, similar to what is seen in the singly transfected sync-2.

Peripherin staining in the two co-transfected cells is noticeably different from singly transfected peripherin, and these two cells are highly representative of the two dominant cell populations observed in these co-transfections. Peripherin staining in panels A and B appears to show a filamentous network that is less organised and more fractured than peripherin transfected alone. Furthermore, this image appears to strongly resemble the image of Per58 transfected alone from Section 6.4. The cell in panels C and D most notably forms a number of very thick aggregates. Surrounding these thick aggregates is a diffuse and punctate pattern of peripherin localisation. Both the thick filaments and unconnected punctate spots are representative of a collapsed and non-functional IF system. Futhermore, this subset of sync-2 and peripherin co-transfected cells shows similar peripherin expression to a singly transfected peripherin

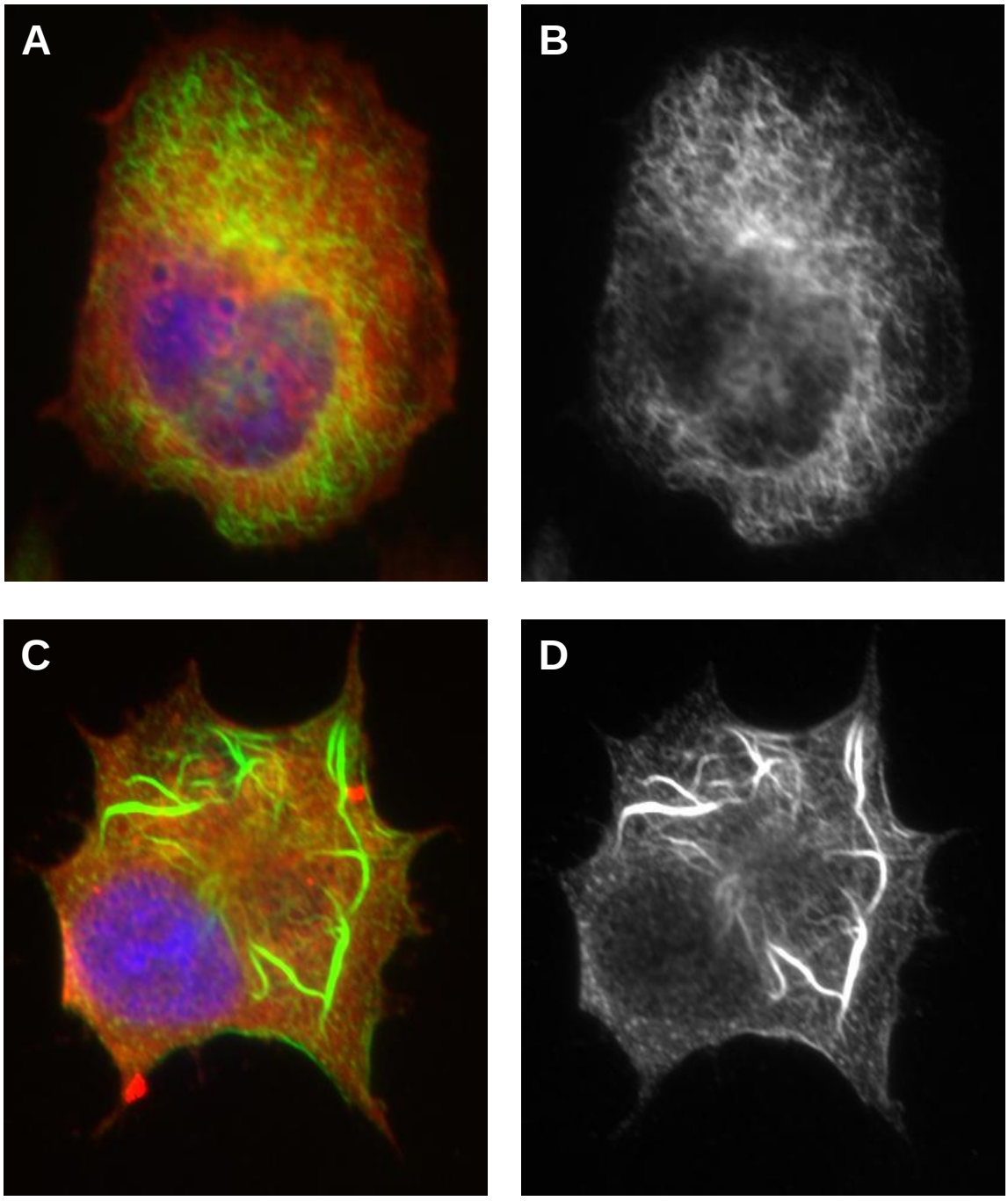

Figure 6.5. Syncoilin expression alters peripherin filament formation in SW13 transfected cells.

SW13 cells were co-transfected with sync-2 and peripherin. Immunostaining with syncoilin N-term 2991 antibody (red) and peripherin chicken (green) plus DAPI (blue). Panels **A** and **C** are merged images while panels **B** and **D** show only peripherin staining.

construct with an aspartate to tyrosine substitution at amino acid 141 (D141Y). The D141Y mutation was discovered in a patient with amyotrophic lateral sclerosis (ALS) and results in a disrupted peripherin filament assembly (Leung, He et al. 2004).

The two cells represented in Figure 6.5 demonstrate that the addition of sync-2 to peripherin in SW13 cells results in the disruption of the peripherin filament network. The cause of this disruption is unclear, so more co-transfections were performed with the aim of gaining further insight.

6.4.2 Sync-2 co-transfected with Per45 and Per58

Sync-2 was co-transfected with Per45 or Per58 in SW13 cells immunostained with syncoilin N-term 2991 antibody and peripherin chicken antibody. One representative image of sync-2 co-transfected with Per45 is in Figure 6.6A and B. Panel A shows a merge image confirming co-transfection and co-localisation with sync-2 in red, Per45 in green and DAPI nuclear staining in blue. As seen in Panel B, the Per45 pattern of staining is unchanged in the co-transfection from its pattern when transfected alone. Both stainings are diffuse throughout the cytoplasm and punctate. Based on this and other images, it appears that sync-2 does not alter the Per45 expression pattern in SW13 cells.

Figure 6.6C and D are images of sync-2 co-transfected with Per58. Co-transfection and limited co-localisation is confirmed in the merge image in Panel C. The single channel image of peripherin in Figure 6.6D shows a peripherin network that resembles the incomplete networks of Per58 transfected alone in Figure 6.3 and of peripherin co-transfected with sync-2 in Figure 6.5B. The absence of any change in

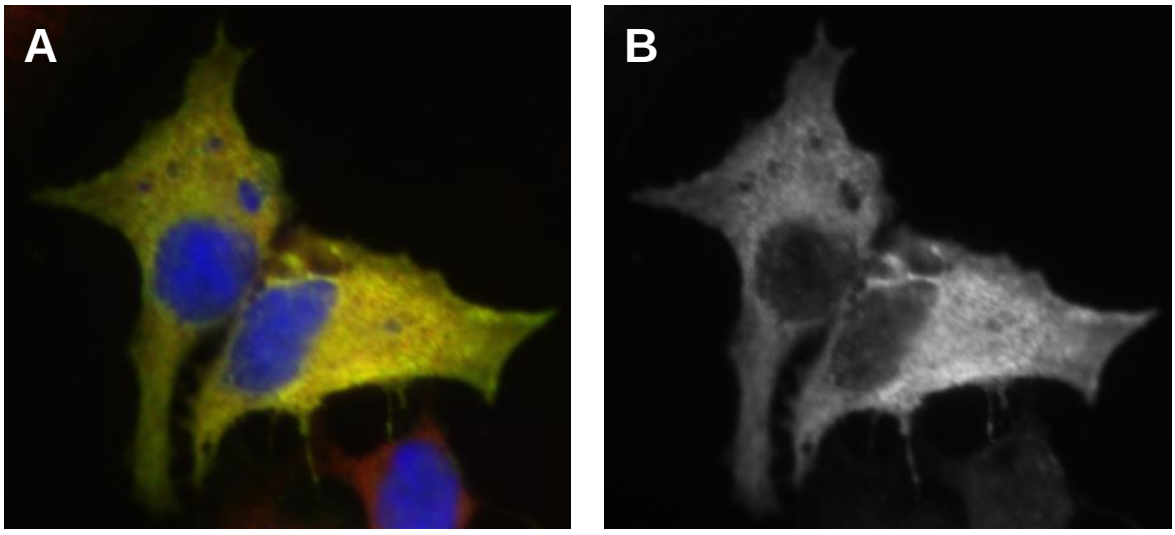

Sync-2 and per45

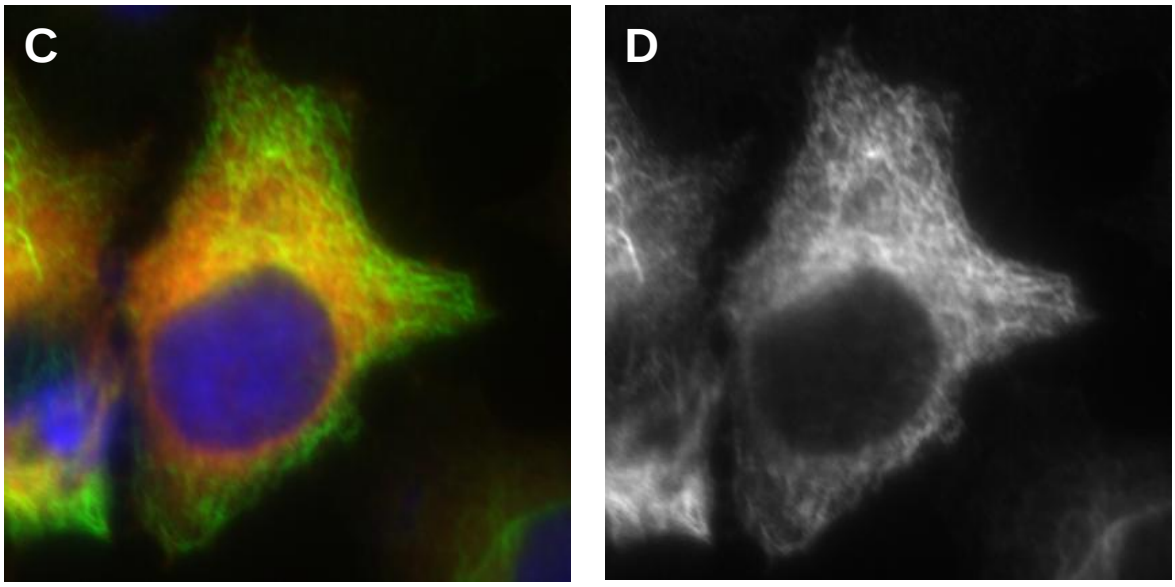

Sync-2 and per58

Figure 6.6. Syncoilin and peripherin constructs co-transfected in SW13 cells.

SW13 cells were co-transfected with sync-2 and per45 (**A**, **B**) or per58 **(C**, **D**)**.** Immunostaining with syncoilin N-term 2991 antibody (red) and peripherin chicken (green) plus DAPI (blue). Panels **A** and **C** are merged images while panels **B** and **D** show only peripherin staining.

Per58 filament network formation suggests that sync-2 plays no significant role in Per58 filament formation or localisation.

6.4.3 Peripherin transfected with syncoilin patient variants

Ben Edwards in this laboratory previously performed a large unpublished screen of patient samples for syncoilin variations. This screen included 120 patients with ALS, 200 patients with unidentified neuropathies and 200 control samples with no identified neuropathy. From this screen, three variants were identified. Variants at amino acids E191G (glutamate to glycine) and R349Q (arginine to glutamine) were discovered in patients with unidentified myopathies and a variant at amino acid R263C (arginine to cysteine) was discovered in a control male of unknown age. It is unknown whether or not this control male ever developed a neuropathy.

Constructs containing the full length syncoilin gene and the patient variants were co-transfected with the full length peripherin gene. While there is no direct evidence to suggest that the syncoilin variants affect peripherin filament formation, it was considered that if the syncoilin variants do contribute to a neuropathy and if syncoilin is involved in peripherin filament formation, it is possible that a change in peripherin filament formation would be seen in these co-transfections.

In Figure 6.7, merge images of syncoilin immunostained in red with N-term 2991 antibody, peripherin immunostained in green with chicken antibody and nuclei stained in blue with DAPI are seen on the left side in panels A, C and E. Single channel images of peripherin alone are on the right side in panels B, D and F. Co-transfections of peripherin with syncoilin E191G (panels A and B), syncoilin R263Q (panels C and D) and syncoilin R349C (panels E and F) all had similar results. Thick peripherin

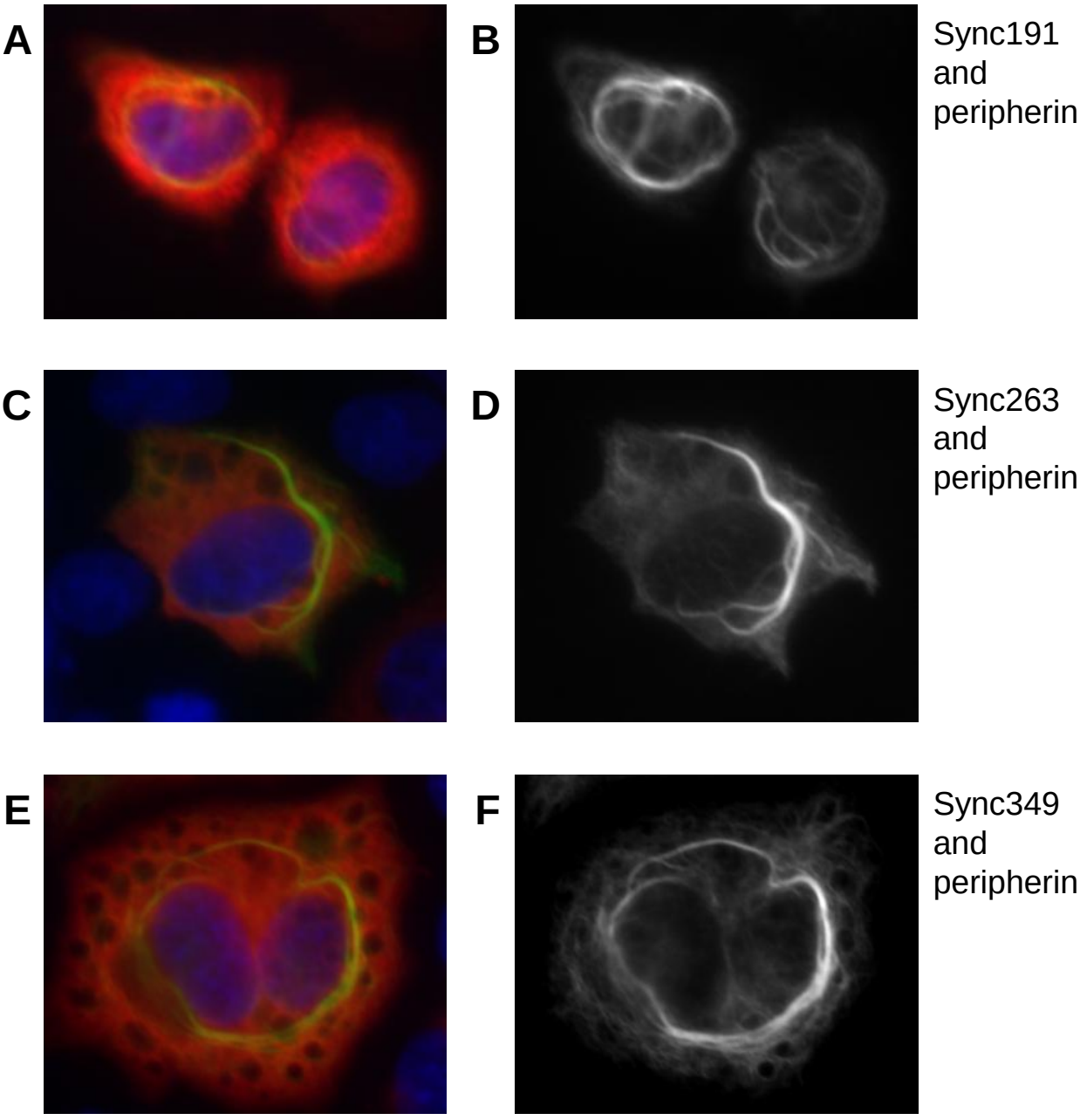

Figure 6.7. Peripherin and syncoilin variants co-transfected in SW13 cells.

SW13 cells were co-transfected with peripherin and syncoilin patient variants 191 (**A**, **B**), 263 (**C**, **D**) and 349 (**C**, **D**). Immunostaining with syncoilin N-term 2991 antibody (red) and peripherin chicken (green) plus DAPI (blue). Panels **A**, **C** and **E** are merged images while panels **B**, **D** and **F** show only peripherin staining.

filament networks formed in all four cells shown, and these thick filaments were surrounded by diffuse and unorganized peripherin. These cells closely resemble the peripherin and syncoilin transfected cell seen in Figure 6.5D. Other peripherin and syncoilin variant transfected cells not shown lack thick filaments but have a more fractured and less structured filament structure similar to the peripherin and syncoilin transfected cell shown in Figure 6.5B.

The three identified syncoilin patient variants appear to have no difference from wild type syncoilin in their effect on peripherin filament formation. Neither the localisation nor organisation of syncoilin or peripherin was affected by the introduction of the syncoilin patient variants.

6.5 Peripherin and α-tubulin co-immunoprecitate in neurons

During attempts to co-immunoprecipiate syncoilin and α-tubulin in neurons, peripherin was often used as a positive control for syncoilin binding. A band of the correct size for α-tubulin regularly appeared in the peripherin IP lane in the blot probed for α-tubulin. Initially, this was discounted as non-specific binding. After multiple repetitions, it was decided to test the reverse IP and see if α-tubulin could pull down peripherin.

Figure 6.8 shows two blots with identical lanes of immunoprecipitations from N2A cells. Five antibodies were used for the pull-downs: peripherin mouse, peripherin rabbit, α-tubulin mouse, β-tubulin rabbit and syncoilin rabbit. A no antibody lane serves as a negative control and the lysate lane serves as a positive control. The top blot was probed for α-tubulin using monoclonal antibody B512. The first lane on the left is pulled down with peripherin mouse. There is a faint band for α-tubulin just

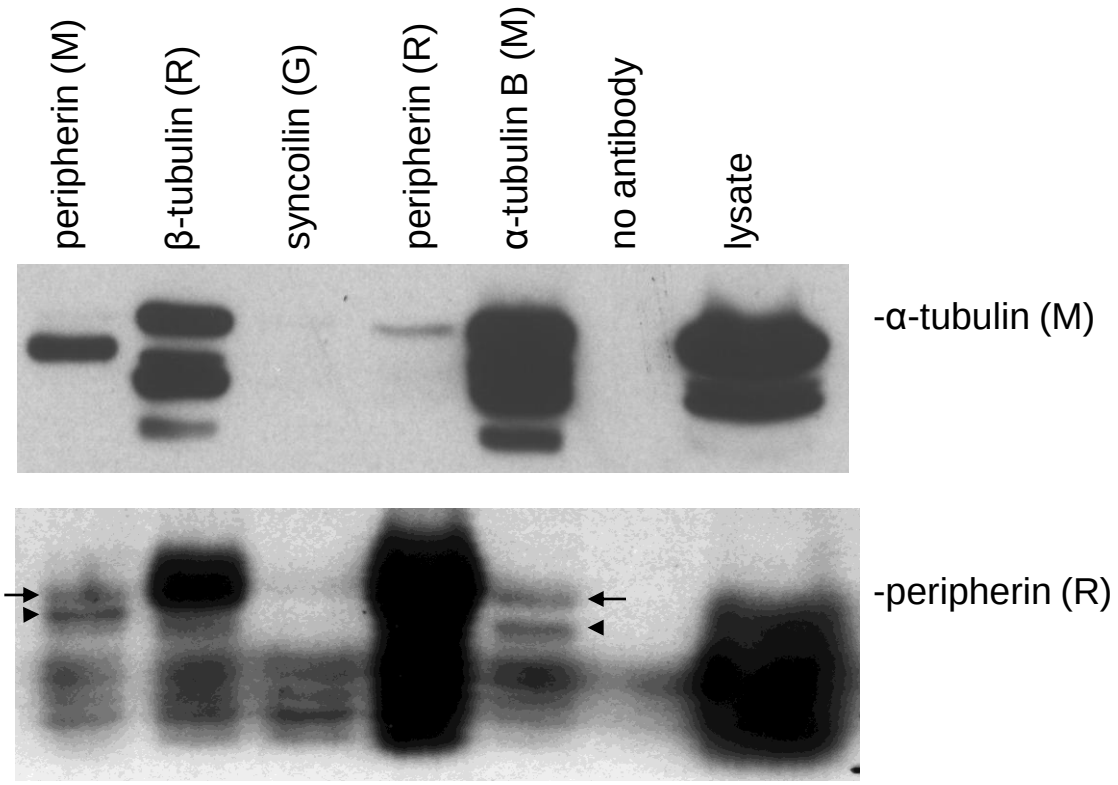

Figure 6.8. Co-immunoprecipitation of peripherin and α-tubulin from N2A cells.
Immunoprecipitating antibodies are listed above the immunoblots with the host species of each antibody in parentheses (M=mouse, R=rabbit, G=goat). α-tubulin mouse monoclonal antibody used is B512.
A. Probed for α-tubulin B512. α-tubulin is pulled down by α-tubulin, β-tubulin, peripherin rabbit and very slightly by peripherin mouse. Tubulin is a 50 kDa protein, but in our experience, tubulin runs higher than the IgG heavy chain which is predicted to run at 55kDa.
B. Probed for peripherin rabbit. Peripherin isoforms 58 (arrow) and 45 (arrowhead) are pulled down by both mouse peripherin and α-tubulin. Rabbit peripherin and β-tubulin are difficult to interpret due to the presence of the IgG heavy chain.

above the IgG band. As seen previously in Section 5.4, despite the fact α-tubulin is expected to be 5 kDa smaller, α-tubulin runs just above the IgG. There is a strong α-tubulin band in the β-tubulin lane and another faint band in the syncoilin lane. There is a strong band of α-tubulin in the peripherin rabbit lane, showing that peripherin indeed pulled down α-tubulin. The presence of α-tubulin in the α-tubulin IP and lysate lanes and the absence of α-tubulin in the no antibody lane confirm the experiment worked.

The bottom blot in Figure 6.8 was probed for peripherin using a rabbit antibody. The first lane on the left is pulled down with peripherin mouse and confirms that both Per58 (arrow) and Per45 (arrowhead) are pulled down by peripherin. The β-tubulin lane is obscured by the IgG heavy chain because the β-tubulin antibody and peripherin antibody used to probe the blot are both rabbit antibodies. The syncoilin lane has a faint band for Per58, but a band is not expected because syncoilin was not transfected in these cells. The peripherin rabbit lane is overexposed. The α-tubulin lane clearly shows two bands for Per58 and Per45, confirming that α-tubulin indeed pulled down peripherin. The no antibody lane is blank, confirming there was no non-specific pull down of peripherin.

Single neuron preparations of sciatic nerve were immunostained for peripherin and α-tubulin. This work is not shown because no new information was gained. As seen previously in Figures 6.1 and 5.4, peripherin localised to the centre of the axon and α-tubulin localised outside of the axon centre with both immunostainings continuing along the entire length of the sciatic nerve axon. This work was not pursued further because syncoilin remains the primary aim of this thesis. However, the interaction

between peripherin and α-tubulin in neurons is noteworthy and could possibly be pursued at another time.

6.6 Discussion

The work performed in this chapter is largely a continuation of research done previously in this laboratory. It was initially speculated that peripherin could be a binding partner of syncoilin given that peripherin and desmin, a known syncoilin binding partner in muscle, are both type III intermediate filaments. Co-immunoprecipiations and blot overlays confirmed this interaction while immunohistochemistry of DRG showed that syncoilin and peripherin are expressed in the same subcellular region.

In this thesis, syncoilin and peripherin were shown to co-localise along the length of the axon in a single neuron preparation of sciatic nerve, confirming further the likelihood of an interaction between the two intermediate filament proteins. The disparity in localisation between α-tubulin outside of the axon centre and peripherin within the centre of the axon emphasises the differences in subcellular expression and suggests that peripherin is more likely than α-tubulin to interact with syncoilin *in vivo*.

Upon transfection in SW13 cells lacking an intermediate filament network, peripherin forms a full IF network. A fully assembled peripherin IF network requires isoforms Per45 and Per58. Alone, Per58 is capable of forming a partially assembled network, but Per45 alone forms no network. Syncoilin transfected in SW13 cells is incapable of forming a network. The addition of sync-2 to peripherin results in a disruption of the peripherin network that resembles the Per58 alone network. However, the addition of

sync-2 to Per58 appears to have no impact on the Per58 disrupted peripherin network. The addition of sync-2 appears to have the same effect as the removal of Per45 in a cell transfected with peripherin. It is hypothesized that sync-2 achieves this effect by sequestering and regulating Per45. It should not be overlooked that sync-2 had much greater co-localisation in co-transfected cells with Per45 than with Per58. Since Per45 is necessary for filament formation, this hypothesis suggests that sync-2 acts to regulate peripherin filament formation. Syncoilin could actively sequester and release Per45, thereby controlling the growth and maintenance of the peripherin IF network.

It is important to consider that while SW13 cells have a unique ability to allow for the visualisation of IF network formation under many different conditions, this transfection-based system is artificial. Intermediate filaments are believed to be highly regulated by the ratios of IF proteins expressed (Yuan, Rao et al. 2006). The amounts and ratios of syncoilin and peripherin in transfected cells are not the same as in neurological tissue. The alteration of the natural ratios could explain the degradation of the filament network in cells transfected with syncoilin and peripherin. However, if this were the case, it would also be expected that the addition of syncoilin to Per58 would result in the further degradation of the Per58 filament network. Instead, there appears to be no difference between Per58 alone and Per58 with syncoilin. The selective disruption by syncoilin of peripherin but not Per58 transfected cells is strong evidence that syncoilin specifically disrupts the peripherin filament network by sequestering Per45 rather than altering IF protein ratios.

While the SW13 co-transfections gave evidence of a function for syncoilin in neurons, three syncoilin variants discovered in patients were co-transfected with peripherin

with the aim of discovering if any of the three amino acid substitutions changed the expression pattern of syncoilin or peripherin. None of the three variants had any overt affect on the expression of syncoilin or network formation of peripherin. This does not rule out the possibility of a role for the syncoilin variants in disease. The continued use of these syncoilin patient variant constructs is an important tool for the continued study of the role of syncoilin in disease.

Finally, in a largely unrelated experiment, it was shown that peripherin and α-tubulin co-immunoprecipitate in neuronal N2A cells. Much like syncoilin and α-tubulin, there is very little co-localisaiton of peripherin and α-tubulin in sciatic nerve. It is difficult to predict the importance of a potential interaction between peripherin and α-tubulin because the two proteins are not localised in the same subcellular compartment. It is also interesting that both peripherin and syncoilin co-immunoprecipitate with α-tubulin even though neither protein localises with α-tubulin in the axon. This could suggest that the successful co-immunoprecipitations are the result of any number of artificial circumstances including the use of cell culture as a protein source, the process of creating lysates that combines the entire cell or the nonspecific binding of α-tubulin and IF proteins under the described experimental procedures.

The information in this chapter confirms peripherin as a binding partner of syncoilin in neurons and establishes that syncoilin plays a role in peripherin filament formation, most likely by sequestering and regulating Per45. As with syncoilin research in muscle, the primary aim in syncoilin neuronal research remains achieving a greater understanding of syncoilin's function and connection to disease. To do this, the

research emphasis was shifted from discovering binding partners to performing a neuronal analysis of the *sync-/-* mouse.

tests allowed for examinations of sensory response, motor skills and coordination. The detection of significant differences between *sync*+/+ and *sync*-/- mice in motor skills tests allowed for a targeted histological analysis of the *sync*-/- neurological system and the discovery of a motor neuron phenotype.

7.2 Neurological Testing

7.2.1 Hot Plate

A number of standard neurological tests were performed to determine if *sync*-/- mice have a neurological phenotype. The hot plate test examines a mouse's ability to respond to a thermal stimulus. Forty-five *sync*+/+ and forty-five *sync*-/- mice were placed on a hot plate set to 55°C. The mice were timed from the moment their paws touched the plate until they responded with a hindpaw lick, hindpaw flick or jump. As seen in Figure 7.1A, *sync*+/+ mice averaged 11.38 seconds on the hot plate before responding while *sync*-/- mice averaged 10.87 seconds. The absence of syncoilin appears to have no effect on a mouse's pain reflex in response to a thermal stimulus.

7.2.2 Grip Strength

A standard grip strength instrument records the tension by which a mouse pulls a bar with its forelimbs. Due to variability in mouse size, relative grip strength was normalized by dividing the recorded tension by mouse weight. Fifteen *sync*+/+ and fifteen *sync*-/- mice were tested, and the average normalised force for *sync*+/+ mice was 5.03 and the average normalised force for *sync*-/- mice was 4.25. This 18.4% difference seen in Figure 7.1B was found to be statistically significant ($p < 0.05$) when analysed using Student's t-test.

7.2.3 Accelerating Rotarod

An accelerating rotarod tests both motor coordination and balance. Fifteen *sync*+/+ and fifteen *sync*-/- mice were tested four times each. On average, *sync*+/+ mice were

Chapter 7: Neuronal characterisation of the *sync-/-* mouse

7.1 Introduction

The *sync-/-* mouse was previously characterised using several muscle-specific analyses. The loss of syncoilin had no effect on skeletal or cardiac muscle morphology or differentiation and had no obvious impact on muscle degeneration or regeneration. In assessing muscle strength, the absence of syncoilin reduced the contractile ability of EDL muscle but not soleus muscle. *Sync-/-* mice performed similar to age-matched *sync+/+* mice on a voluntary running wheel, but *sync-/-* mice suffered increased muscle damage from enforced treadmill running. These experiments suggest that syncoilin is largely dispensable for normal muscle function in the C57BL/6 mouse (McCullagh, Edwards et al. 2008).

Recent work has shown that syncoilin is expressed in neurons and potentially plays a functional role in regulating peripherin filament assembly and organisation. One way to possibly determine if syncoilin is important in neurons is to see if the loss of syncoilin in mice has an effect on the nervous system.

While the *sync-/-* mouse has undergone a number of muscle-specific analyses, no behavioural or neuron-specific tests have been performed. In Figure 5.5, no differences were seen in α-tubulin expression or localisation in sciatic nerve single neuron preparations from *sync-/-* and *sync+/+* mice. Figures 5.6 and 5.7 also showed no difference in α-tubulin expression at the mRNA level in spinal cord or at the protein level in sciatic nerve and spinal cord.

This chapter presents a neuronal characterisation of the *sync-/-* mouse. A series of

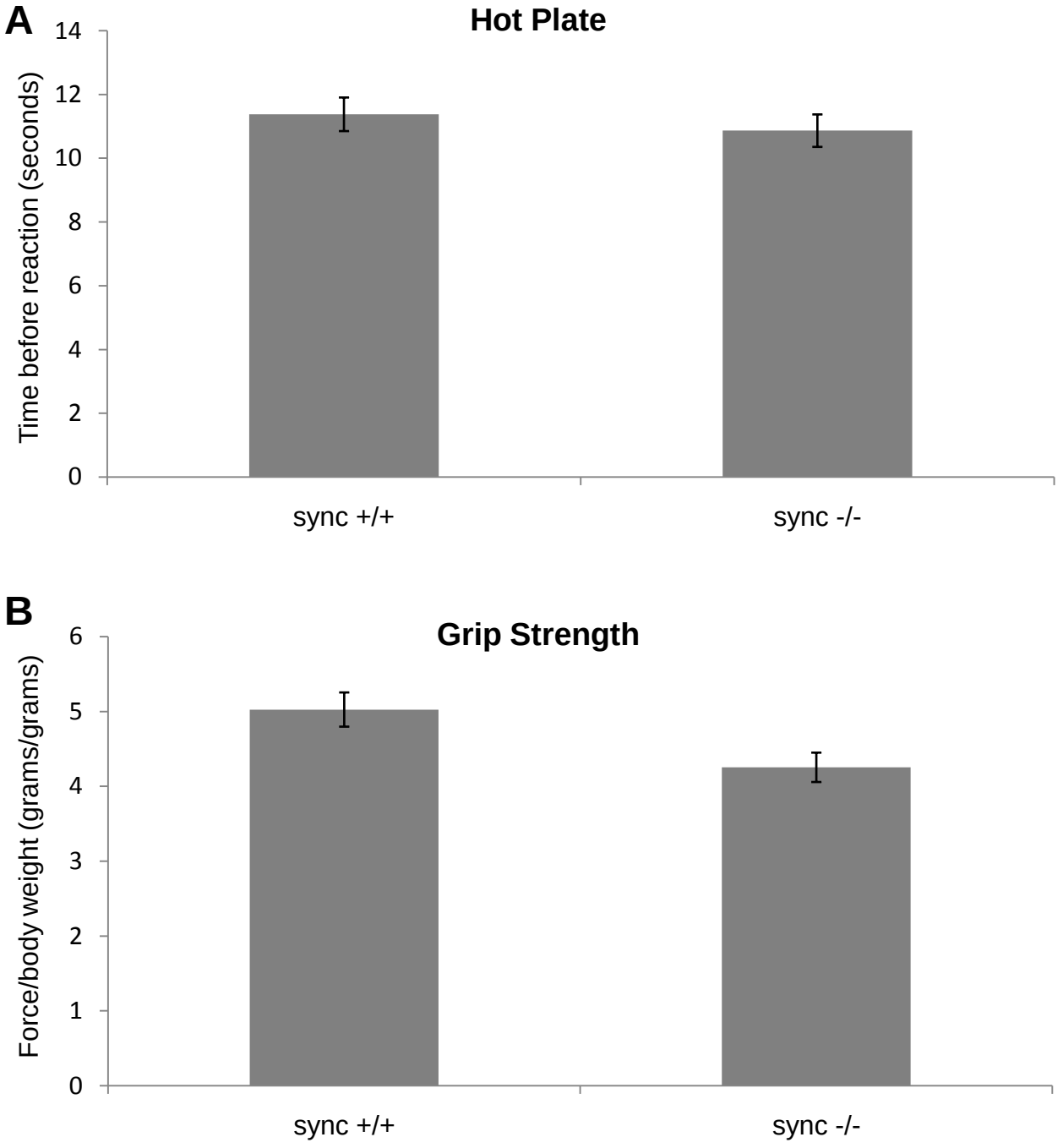

Figure 7.1. Hot Plate and Grip Strength Testing.
A. Mice were tested for their reaction time to a mild thermal stimulus. Forty-five mice of each genotype were tested one time. *Sync*-/- mice had approximately equal response times to age-matched *sync*+/+ mice. **B.** Mice were tested for their forelimb grip strength. Fifteen mice of each genotype were tested once each. Grip strength was calculated relative to body mass. The decrease in relative strength of *sync-/-* mice was found to be statistically significant ($p < 0.05$) when analysed using Student's t-test.

able to stay on the rotarod for 265.90 seconds, and *sync-/-* were able to stay on the rotarod almost a full minute less, averaging only 212.27 seconds. The 20% decline in time spent on the rotarod is illustrated in Figure 7.2A. The reduction in the ability of *sync-/-* mice to stay on the rotarod was found to be statistically significant ($p < 0.001$) when analysed using Student's t-test.

7.2.4 Accelerating Treadmill

Given that the accelerating rotarod tests both motor coordination and balance, two experiments were performed to further explain the accelerating rotarod performance difference. Motor coordination and the ability to respond to acceleration were tested using an accelerating treadmill. Twenty *sync+/+* and twenty *sync-/-* mice were placed on a treadmill that tested the ability of the mice to run at an accelerating pace over a short period of time without significant training. Mice were timed to see how long they could stay on the treadmill. Figure 7.2B shows that *sync+/+* mice averaged 160.25 seconds on the treadmill while *sync-/-* mice averaged 136.45 seconds, a 14.9% decline. The reduction in the ability of *sync-/-* mice to stay on the treadmill was found to be statistically significant ($p < 0.05$) when analysed using Student's t-test.

7.2.5 Static Beam

The second test used to further examine the accelerating rotarod performance difference was the static beam. Balance was assessed as mice were tested for their ability to stay on and walk across a 60 cm round beam raised 60 cm above a padded surface. Twenty-six *sync+/+* and twenty-eight *sync-/-* mice were tested once. None of the mice fell off the beam. Furthermore, fifteen *sync+/+* mice and sixteen *sync-/-* mice completed the task of walking across the beam. The absence of syncoilin appears to have no effect on a mouse's balance on an elevated round beam.

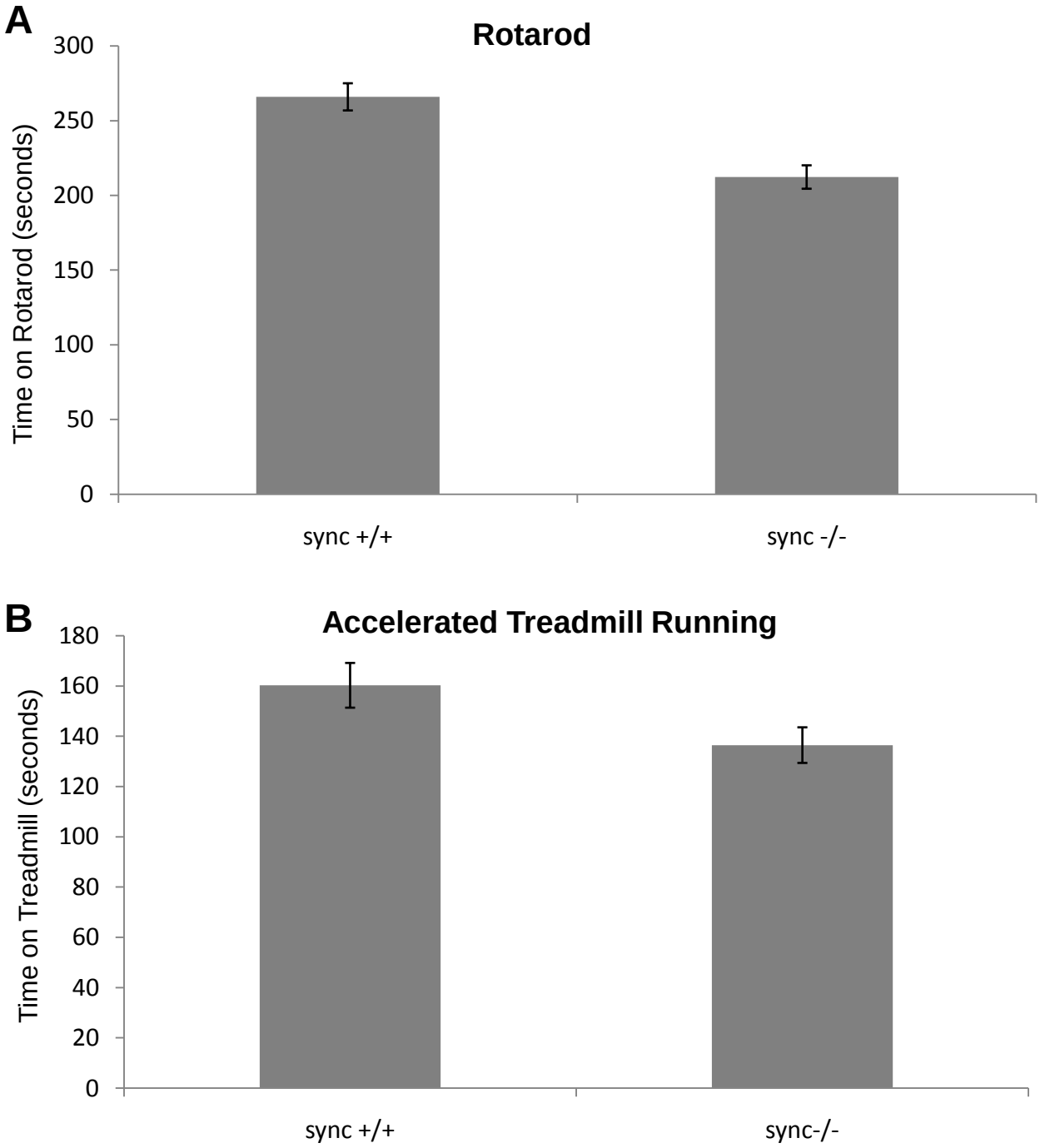

Figure 7.2. Rotarod and Treadmill Testing.
A. Mice were tested for their ability to stay on an accelerating motorized treadmill. Twenty mice of each genotype were tested once each. The decrease in time *sync-/-* mice were able to stay on the treadmill was found to be statistically significant ($p < 0.05$) when analysed using Student's t-test. **B.** Mice were tested for their ability to stay on an accelerating rotating rod. Fifteen mice of each genotype were tested four times each. The decrease in time *sync-/-* mice were able to stay on the rotarod was found to be statistically significant ($p < 0.001$) when analysed using Student's t-test.

7.3 Anterior Horn Motor Neurons

Differences in *sync-/-* mice were observed in motor but not sensory function. Spinal cord sections from the L4 region of the lumbar spinal cord were stained with cresyl violet to identify anterior horn motor neurons. As seen in Figure 7.3B, C and D, motor neurons were identified as dark, large and irregularly shaped. Double-blind counting by two different people of motor neurons from three *sync+/+* and three *sync-/-* mice revealed no difference in the number of anterior horn motor neurons in *sync-/-* mice. As seen in Figure 7.3A, *sync+/+* mice averaged 10.86 motor neurons per anterior horn and *sync-/-* mice averaged 11.27 motor neurons per anterior horn.

7.4 Ventral Root Axons

While there is no difference in the number of motor neurons in the *sync-/-* lumbar spinal cord, it was examined to see if there is any difference in the calibre of motor neuron axons from the ventral roots. Ventral roots, which contain motors neurons, were sectioned at a thickness of 1 micron and stained with Toluidine Blue and Borax, as seen in Figure 7.4B. Motor axons were traced to determine the area of the axon body. Three mice from each genotype and two different sections from each mouse were counted. The average axon body area for the *sync+/+* mouse was found to be 100.2 μm^2 versus 74.2 μm^2 for the *sync-/-* mouse. This difference, as seen in Figure 7.4A, was found to be statistically significant ($p < 0.001$) when analysed using Student's t-test. Individual axon body areas were plotted in Figure 7.4C. This figure illustrates a shift of medium to large axons seen in the *sync+/+* mouse to smaller axons seen more commonly in the *sync-/-* mouse.

7.5 Discussion

This chapter documents the first neuronal analysis of the *sync-/-* mouse. Previous studies of the *sync-/-* mouse focusing on muscle revealed very little difference from

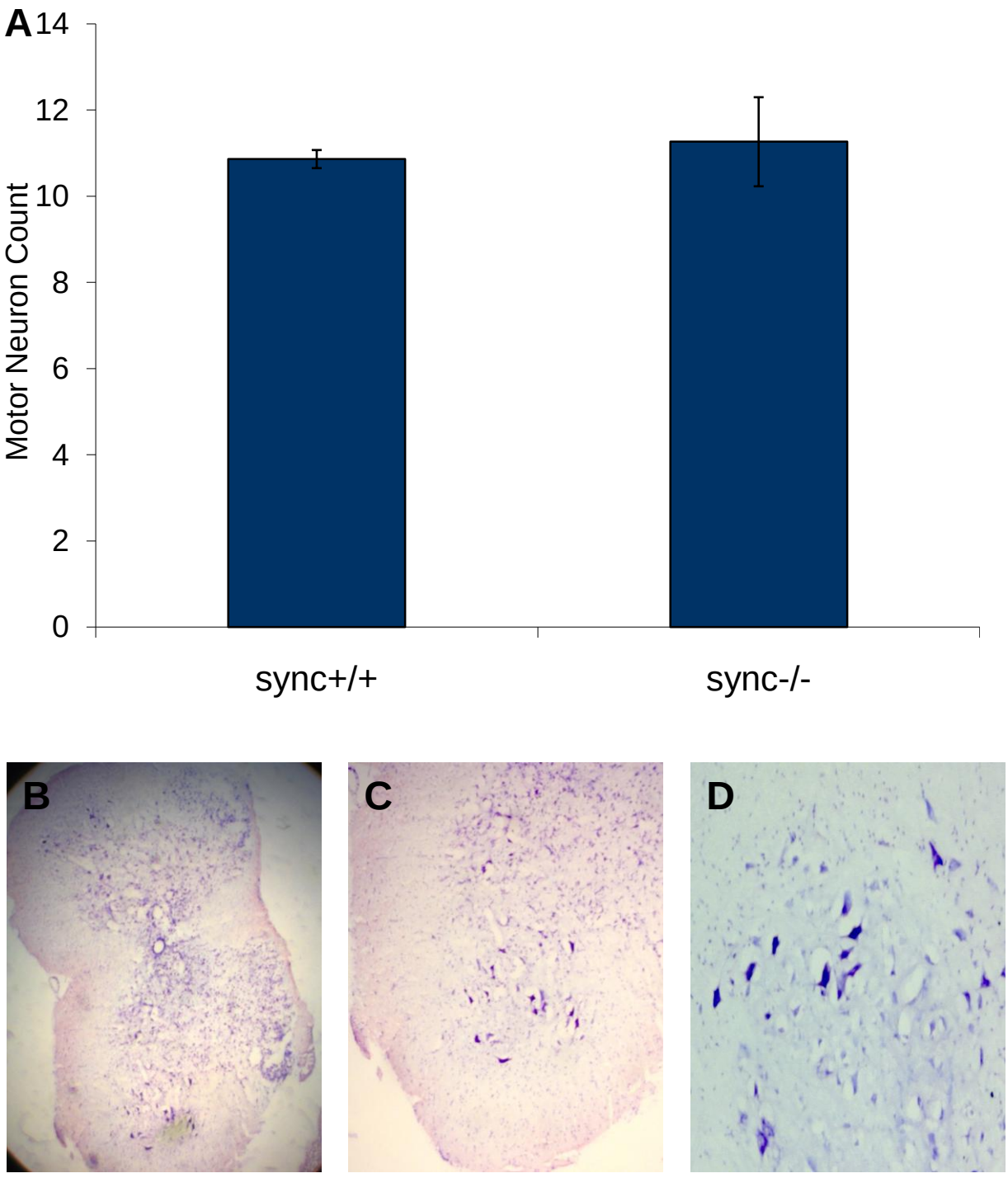

Figure 7.3. Quantification of anterior horn motor neurons.
A. Counts are expressed as the average number of motor neurons in each anterior horn section of *sync+/+* and *sync-/-* mice. Twenty sections from the upper part of the L4 segment from each of three mice of each strain were counted. Sections were cut at 10 mm. Representative images of a Cresyl violet-stained L4 spinal cord segment at 1.6x (**B**), 10x (**C**) and 20x (**D**).

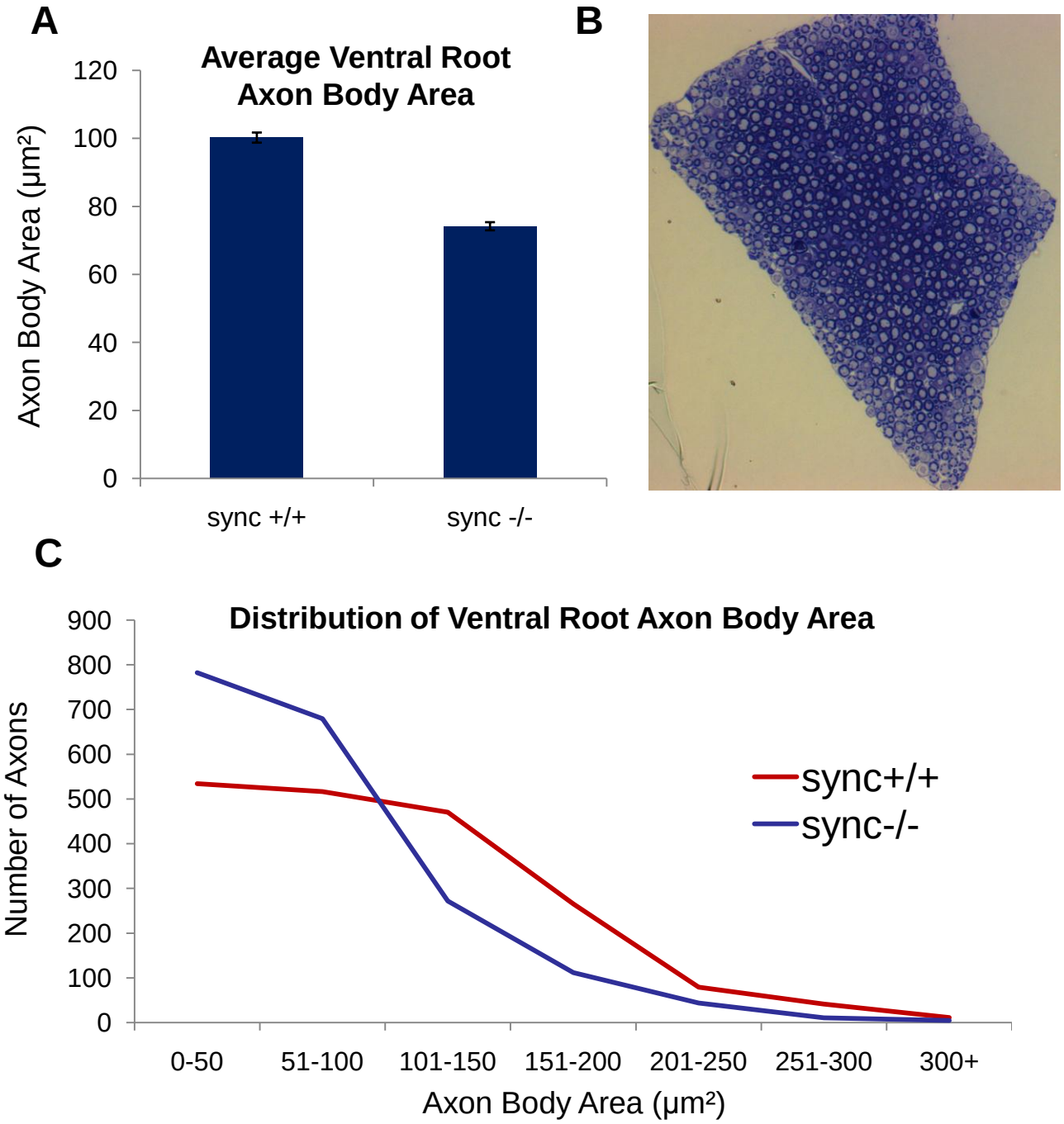

Figure 7.4. Quantification of ventral root axon body area.
A. The average size of axons from the ventral root of *sync*+/+ and *sync-/-* mice. Two distinct sections were counted per mouse. Three mice of each strain were used. The decrease in axon body area in *sync-/-* mice was found to be statistically significant ($p < 0.001$) when analysed using Student's t-test. **B.** Representative image of a Toluidine Blue stained ventral root. **C.** The distribution of ventral root axon body area shows that there are more small calibre axons and fewer large calibre axons in the *sync-/-* mouse.

sync+/+ mice. The experiments in this chapter attempted to find a specific neuronal phenotype using a range of behavioural tests and histological examinations.

The hot plate test is an established method for testing a mouse's response to a thermal stimulus (Gu, McIlwain et al. 2002). The fact that there was no difference in hot plate response time between *sync*+/+ and *sync*-/- mice suggests that syncoilin is not essential for nociception, the neural processing in the central and peripheral nervous system of noxious stimuli.

The absence of a change in response time in the hot plate test suggested that syncoilin is despensible in sensory axons. It was then decided to perform motor neuron-specific tests. Most of these tests could also serve as tests of muscle function. However, voluntary and extended forced running tests and extensive histological analyses revealed minimal muscular difference between *sync*+/+ and *sync*-/- mice (McCullagh, Edwards et al. 2008). Therefore, it is very possible that any motor phenotype discovered in the *sync*-/- mouse is the result of a neuronal change.

The grip strength test is widely used to assess muscle strength of forelimbs and to test for improper neuromuscular functioning in motor neurons and the cerebral brain region (Costa, Walsh et al. 1999). The significant difference in grip strength between *sync*-/- and *sync*+/+ mice suggests that the loss of syncoilin has an adverse effect on forelimb muscles. Whether or not this difference is caused by the loss of syncoilin in nerve or muscle is further investigated with more tests and histology.

An accelerating rotarod requires motor coordination and balance (Dunham, Miya 1957). In the grip strength test, mice are hanging on to the bar for only a few seconds. This requires a quick neurological response. Similarly, the rotarod requires constant neurological responses both to stay on the rod and to keep up with the accelerating speed. The most significant difference between *sync*+/+ and *sync*-/- mice seen in the range of behavioural tests in this chapter came from the accelerating rotarod. This result confirmed the neuromuscular defect seen in the grip strength test but introduced new possible defects including balance and coordination.

The accelerating treadmill test was designed to simulate the rotarod test because both require muscle coordination on an accelerating device. However, the treadmill test does not require the same degree of balance needed to stay on the rotating round rotarod. A previous long-term study of forced treadmill running at lower speeds with an extended training session revealed no difference between *sync*+/+ and *sync*-/- mice (McCullagh, Edwards et al. 2008). This accelerating treadmill test is different from the extended forced running treadmill test in two important ways. First, the lack of an extended training session in the accelerating treadmill test did not give the mice an opportunity to neurologically prepare for their quick run. Second, an accelerating test requires greater motor coordination to adjust to the changing speeds than a slower extended test. These differences could explain why *sync*-/- mice performed significantly worse than *sync*+/+ mice in the accelerating treadmill test but not in the extended forced running treadmill test.

To specifically examine balance, a factor in the accelerating rotarod test, a standard static beam test was used (Le Marec, Caston et al. 1997). Unlike the grip strength,

rotarod or accelerating treadmill, the static beam did not require immediate motor neuron function. Mice were given three minutes to walk to the end or the beam, enough time for the mice to orient and adjust themselves. The ability of *sync-/-* both to stay on the beam and to walk to the end of the beam at the same frequency of *sync+/+* mice suggests that syncoilin is not essential for proper balance.

Taken together, the range of behavioural tests suggests a neuromuscular deficiency in *sync-/-* mice. The absence of a significant histological muscle phenotype in the *sync-/-* mouse leads to the hypothesis that the absence of syncoilin in neurons is responsible for the observed phenotype. Two histological examinations of the quantity and quality of motor neurons were performed in an effort to find a cause for the neuromuscular phenotype.

The anterior horn of the lumbar spinal cord contains motor neurons. An examination of these motor neurons in *sync+/+* and *sync-/-* mice revealed that the loss of syncoilin results in no difference in motor neuron quantity. Ventral roots, which contain motor but not sensory neurons, were used to look at the quality of motor neurons. Motor neuron axon calibre was measured and found to be significantly smaller in the *sync-/-* mouse. This reduction in motor neuron axon calibre could be indicative of reduced neuronal transmission. While *sync-/-* mice have no overt phenotype throughout their lifetimes, moderate neuronal deficiencies caused by the absence of syncoilin may contribute to a reduced ability to perform certain tasks such as the ones discussed in this chapter. In the grip strength, accelerating rotarod and accelerating treadmill tests, *sync-/-* were always able to complete the tasks; instead, the difference between *sync+/+* and *sync-/-* mice was how well the task was completed. This distinction fits

well with the observed histology of motor neurons in *sync-/-* mice. The absence of syncoilin does not result in the loss of motor neurons. Instead, it is hypothesized that the loss of syncoilin results in motor neurons with a reduced ability to transmit neurological signals.

The discovery of a neurological phenotype for the *sync-/-* mouse provides significant opportunities for future experiments. First, dorsal root sensory neurons, the complement to ventral root motor neurons, are being examined for axon calibre. This information is important because it will clarify whether the loss of syncoilin affects all peripheral neurons or only motor neurons. If sensory neuron axon calibre is smaller in *sync-/-* mice, further sensory behavioural tests should be preformed. If sensory neuron axon calibre is unchanged in *sync-/-* mice, the differences seen in motor neuron-specific tests but not sensory neuron-specific tests performed in this chapter will be confirmed.

It is now known that syncoilin affects motor neuron axon calibre, but it is unknown how else that affects motor neuron function. There are plans to examine neuromuscular junctions (NMJs) of *sync-/-* mice. NMJs are where motor neurons meet muscle, and defects in the NMJ would suggest that the loss of syncoilin impairs the ability of motor neurons to reach their destination.

The results of dorsal root axon calibre measurements and NMJ immunohistochemistry will allow for a better understanding of peripheral neurons in the *sync-/-* mouse. However, one area that has not been studied to any extent in the *sync-/-* mouse is the brain. While it is likely that a neurological phenotype in the *sync-/-* mouse is

associated with reduced axon calibre, it is also possible that defects in the central nervous system result from the loss of syncoilin. Any research into brain function in the *sync-/-* mouse would first require a greater understanding of the role of syncoilin in the brain.

This chapter provides evidence of a neurological phenotype in *sync-/-* mice. This phenotype is confirmed both in behavioural tests and in a histological analysis of motor neurons. The conclusions drawn from this chapter provide an exciting result as to the importance of syncoilin and encourage future research into the role of syncoilin in neurons.

Chapter 8: Conclusion

8.1 Summary of Results

Chapters 3 and 4 of this thesis were a continuation of previous work characterising the function of the IF protein syncoilin in muscle. This research included the examination of syncoilin isoforms, syncoilin expression during atrophy and regeneration and syncoilin signalling.

In addition to the commonly referenced syncoilin transcript known as sync-1, two novel syncoilin isoforms now known as sync-2 and sync-3 were discovered. Sync-1 and sync-2 are very similar in size at 64 kDa with a difference only in the IF 2B and tail domains. Sync-3 is 55 kDa and has a shortened 2B domain and no tail domain.

Syncoilin was shown to be upregulated in muscle during atrophy and regeneration both by immunoblot and immunohistochemistry. Interestingly, the pattern of syncoilin localisation during these two processes is different.

Sync+/+ and *sync*-/- primary muscle cell lines were generated in an attempt to elucidate a signalling role for syncoilin in muscle. There was no difference between *sync*+/+ and *sync*-/- cell growth over the course of 48 hours. There was also no difference between the two cell lines in a pulse chase experiment measuring protein synthesis. Finally, combinations of drugs administered to *sync*+/+ and *sync*-/- cell lines showed cell survival was nearly identical under every condition.

Recent discoveries from this laboratory revealed that syncoilin is also expressed in neurons. Chapters 5, 6 and 7 of this thesis attempted to characterise the function of

syncoilin in neurons. First, two potential syncoilin neuronal binding partners were examined. α-tubulin was previously identified as a potential syncoilin binding partner by mass spectrometry. This thesis shows that syncoilin and α-tubulin bind via co-immunoprecipitation, but there is no co-localisation between the two proteins in sciatic nerve. Additionally, there is no difference in α-tubulin mRNA expression, protein expression or localisation in the *sync*-/- mouse.

Peripherin was previously identified as a potential syncoilin binding partner and was shown to co-immunoprecipitate with syncoilin. In this thesis, peripherin was shown to co-localise with syncoilin in sciatic nerve. A series of co-transfections in cells without an IF network suggests that syncoilin acts to regulate peripherin filament formation. Interestingly, peripherin and α-tubulin also co-immunoprecipitate.

Finally, a neuronal analysis of the *sync*-/- mouse was performed. A range of behavioural tests such as accelerating rotarod, accelerating treadmill and grip strength showed decreased motor function in the *sync*-/- mouse. A hot plate test for sensory neurons and a static beam test for balance revealed no difference in the *sync*-/- mouse. The impaired motor function tests were confirmed by histology with the discovery that motor neurons in the *sync*-/- mouse have decreased axon calibre when compared to the *sync*+/+ mouse.

8.2 Future Directions

Syncoilin was initially studied because of its connection to the dystrophin associated protein complex (DAPC) and possible link to neuromuscular disease. In muscle, syncoilin is known to bind α-dystrobrevin and desmin, two proteins with strong associations to human disease. Syncoilin has been shown to be upregulated at the

sarcolemma of patients with DMD and congenital muscular dystrophy. In this thesis, syncoilin was shown to be upregulated in muscle undergoing atrophy or regeneration. All of this information suggests that syncoilin has an unknown but potentially important function in muscle.

Howerver, the lack of a strong muscle phenotype in the *sync-/-* mouse indicates that either syncoilin is dispensable or the loss of syncoilin is compensated by another IF protein. In this thesis, the loss of syncoilin was shown to have no effect on muscle cell growth, protein synthesis or drug sensitivity. The search for a phenotype in the *sync-/-* mouse was instead successful in neurons. *Sync-/-* mice have both an observed motor phenotype and a neuronal histological phenotype that potentially explain each other. The hypothesised function of syncoilin in neurons explains why syncoilin is indispensable and why the loss of syncoilin results in these phenotypes. This complete story represents some of the most significant and promising syncoilin research to date; future research should pursue these discoveries.

There are several potential directions for the future of syncoilin research project. Human disease has always been a primary aim of this research. As mentioned in Section 6.4.3, a large screen of patients with neurological diseases returned three syncoilin variations. These variations should be further pursued. Given the association between peripherin and ALS, a close examination of syncoilin in ALS should be undertaken. In particular, does syncoilin co-localise with peripherin aggregates in ALS patients? Are there any changes in the ratios of syncoilin isoforms in ALS patients? Do syncoilin mutations or deletions contribute to ALS in patients with peripherin aggregations but no peripherin mutations? Other neurological disorders

associated with IF proteins such as Charcot-Marie Tooth disease can also be investigated for syncoilin abnormalities.

As mentioned in Section 7.5, little is known about syncoilin expression or function in the brain. Equally unknown is the role of syncoilin in neuronal growth or development. While potentially promising, these fields would also require investments in basic research. In Chapter 5, the interaction between syncoilin and α-tubulin was confirmed by co-immunoprecipitation. Additional insight into α-tubulin and other syncoilin neuronal binding partners could further elucidate the function of syncoilin in neurons and lead to the discovery of neurological diseases associated with syncoilin.

The direction of syncoilin research has changed significantly during the time that the work in this thesis was performed. Syncoilin now has a putative function, and the *sync-/-* mouse has a phenotype confirmed by behavioural tests and histology. There currently exists a stronger foundation than ever for future syncoilin research.

Bibliography

ABRAMOFF, M.D., MAGELHAES, P.J. and RAM, S.J., 2004. Image Processing with ImageJ. *Biophotonics International,* **11**(7), pp. 36-42.

ADAMS, M.E., BUTLER, M.H., DWYER, T.M., PETERS, M.F., MURNANE, A.A. and FROEHNER, S.C., 1993. Two forms of mouse syntrophin, a 58 kd dystrophin-associated protein, differ in primary structure and tissue distribution. *Neuron,* **11**(3), pp. 531-540.

AL-CHALABI, A., ANDERSEN, P.M., NILSSON, P., CHIOZA, B., ANDERSSON, J.L., RUSS, C., SHAW, C.E., POWELL, J.F. and LEIGH, P.N., 1999. Deletions of the heavy neurofilament subunit tail in amyotrophic lateral sclerosis. *Hum Mol Genet,* **8**(2), pp. 157-64.

ALLEN, D.L., HARRISON, B.C., SARTORIUS, C., BYRNES, W.C. and LEINWAND, L.A., 2001. Mutation of the IIb myosin heavy chain gene results in muscle fiber loss and compensatory hypertrophy. *American Journal of Physiology - Cell Physiology,* **280**(3 49-3),.

ANDREANI, C.L., PAYNE, D.W., PACKMAN, J.N., RESNICK, C.E., HURWITZ, A. and ADASHI, E.Y., 1991. Cytokine-mediated regulation of ovarian function. Tumor necrosis factor alpha inhibits gonadotropin-supported ovarian androgen biosynthesis. *The Journal of biological chemistry,* **266**(11), pp. 6761-6766.

ARAISHI, K., SASAOKA, T., IMAMURA, M., NOGUCHI, S., HAMA, H., WAKABAYASHI, E., YOSHIDA, M., HORI, T. and OZAWA, E., 1999. Loss of the sarcoglycan complex and sarcospan leads to muscular dystrophy in beta-sarcoglycan-deficient mice. *Hum Mol Genet,* **8**(9), pp. 1589-98.

BALCI, B., UYANIK, G., DINCER, P., GROSS, C., WILLER, T., TALIM, B., HALILOGLU, G., KALE, G., HEHR, U., WINKLER, J. and TOPALOGLU, H., 2005. An autosomal recessive limb girdle muscular dystrophy (LGMD2) with mild mental retardation is allelic to Walker-Warburg syndrome (WWS) caused by a mutation in the POMT1 gene. *Neuromuscular disorders : NMD,* **15**(4), pp. 271-275.

BARRESI, R., CONFALONIERI, V., LANFOSSI, M., DI BLASI, C., TORCHIANA, E., MANTEGAZZA, R., JARRE, L., NARDOCCI, N., BOFFI, P., TEZZON, F., PINI, A., CORNELIO, F., MORA, M. and MORANDI, L., 1997. Concomitant deficiency of beta- and gamma-sarcoglycans in 20 alpha-sarcoglycan (adhalin)-deficient patients: immunohistochemical analysis and clinical aspects. *Acta Neuropathol (Berl),* **94**(1), pp. 28-35.

BARTON, E.R., 2006. Impact of sarcoglycan complex on mechanical signal transduction in murine skeletal muscle. *American journal of physiology.Cell physiology,* **290**(2), pp. C411-9.

BEAULIEU, J.M. and JULIEN, J.P., 2003. Peripherin-mediated death of motor neurons rescued by overexpression of neurofilament NF-H proteins. *Journal of neurochemistry,* **85**(1), pp. 248-256.

BEAULIEU, J.M., NGUYEN, M.D. and JULIEN, J.P., 1999. Late onset of motor neurons in mice overexpressing wild-type peripherin. *The Journal of cell biology,* **147**(3), pp. 531-544.

BELLIN, R.M., SERNETT, S.W., BECKER, B., IP, W., HUIATT, T.W. and ROBSON, R.M., 1999. Molecular characteristics and interactions of the intermediate filament protein synemin. Interactions with alpha-actinin may anchor synemin-containing heterofilaments. *The Journal of biological chemistry,* **274**(41), pp. 29493-29499.

BELTRAN-VALERO DE BERNABE, D., CURRIER, S., STEINBRECHER, A., CELLI, J., VAN BEUSEKOM, E., VAN DER ZWAAG, B., KAYSERILI, H., MERLINI, L., CHITAYAT, D., DOBYNS, W.B., CORMAND, B., LEHESJOKI, A.E., CRUCES, J., VOIT, T., WALSH, C.A., VAN BOKHOVEN, H. and BRUNNER, H.G., 2002. Mutations in the O-mannosyltransferase gene POMT1 give rise to the severe neuronal migration disorder Walker-Warburg syndrome. *Am J Hum Genet,* **71**(5), pp. 1033-43.

BHOSLE, R.C., MICHELE, D.E., CAMPBELL, K.P., LI, Z. and ROBSON, R.M., 2006. Interactions of intermediate filament protein synemin with dystrophin and utrophin. *Biochemical and biophysical research communications,* **346**(3), pp. 768-777.

BLAKE, D.J. and MARTIN-RENDON, E., 2002. Intermediate filaments and the function of the dystrophin-protein complex. *Trends in cardiovascular medicine,* **12**(5), pp. 224-228.

BONNE, G., DI BARLETTA, M.R., VARNOUS, S., BECANE, H.M., HAMMOUDA, E.H., MERLINI, L., MUNTONI, F., GREENBERG, C.R., GARY, F., URTIZBEREA, J.A., DUBOC, D., FARDEAU, M., TONIOLO, D. and SCHWARTZ, K., 1999. Mutations in the gene encoding lamin A/C cause autosomal dominant Emery-Dreifuss muscular dystrophy. *Nat Genet,* **21**(3), pp. 285-8.

BONNEMANN, C.G., MODI, R., NOGUCHI, S., MIZUNO, Y., YOSHIDA, M., GUSSONI, E., MCNALLY, E.M., DUGGAN, D.J., ANGELINI, C. and HOFFMAN, E.P., 1995. Beta-sarcoglycan (A3b) mutations cause autosomal recessive muscular dystrophy with loss of the sarcoglycan complex [published erratum appears in Nat Genet 1996 Jan;12(1):110]. *Nat Genet,* **11**(3), pp. 266-73.

BROWN, S.C., TORELLI, S., UGO, I., DE BIASIA, F., HOWMAN, E.V., POON, E., BRITTON, J., DAVIES, K.E. and MUNTONI, F., 2005. Syncoilin upregulation in muscle of patients with neuromuscular disease. *Muscle & nerve,* **32**(6), pp. 715-725.

BURKHOLDER, T.J., FINGADO, B., BARON, S. and LIEBER, R.L., 1994. Relationship between muscle fiber types and sizes and muscle architectural properties in the mouse hindlimb. *Journal of Morphology,* **221**(2), pp. 177-190.

CARLSON, C.G. and MAKIEJUS, R.V., 1990. A noninvasive procedure to detect muscle weakness in the mdx mouse. *Muscle & nerve,* **13**(6), pp. 480-484.

CAULIN, C., WARE, C.F., MAGIN, T.M. and OSHIMA, R.G., 2000. Keratin-dependent, epithelial resistance to tumor necrosis factor-induced apoptosis. *The Journal of cell biology,* **149**(1), pp. 17-22.

CHANG, L. and KARIN, M., 2001. Mammalian MAP kinase signalling cascades. *Nature,* **410**(6824), pp. 37-40.

CHARDIN, P., CUSSAC, D., MAIGNAN, S. and DUCRUIX, A., 1995. The Grb2 adaptor. *FEBS letters,* **369**(1), pp. 47-51.

CHENG, J., SYDER, A.J., YU, Q.C., LETAI, A., PALLER, A.S. and FUCHS, E., 1992. The genetic basis of epidermolytic hyperkeratosis: a disorder of differentiation-specific epidermal keratin genes. *Cell,* **70**(5), pp. 811-9.

CHIEN, C.L., LIU, T.C., HO, C.L. and LU, K.S., 2005. Overexpression of neuronal intermediate filament protein alpha-internexin in PC12 cells. *Journal of neuroscience research,* **80**(5), pp. 693-706.

CHING, G.Y., CHIEN, C.L., FLORES, R. and LIEM, R.K., 1999. Overexpression of alpha-internexin causes abnormal neurofilamentous accumulations and motor coordination deficits in transgenic mice. *The Journal of neuroscience : the official journal of the Society for Neuroscience,* **19**(8), pp. 2974-2986.

CHING, G.Y. and LIEM, R.K., 1998. Roles of head and tail domains in alpha-internexin's self-assembly and coassembly with the neurofilament triplet proteins. *Journal of cell science,* **111 (Pt 3)**(Pt 3), pp. 321-333.

CHOU, Y.H., FLITNEY, F.W., CHANG, L., MENDEZ, M., GRIN, B. and GOLDMAN, R.D., 2007. The motility and dynamic properties of intermediate filaments and their constituent proteins. *Exp Cell Res,* **313**(10), pp. 2236-43.

CHUONG, S.D., GOOD, A.G., TAYLOR, G.J., FREEMAN, M.C., MOORHEAD, G.B. and MUENCH, D.G., 2004. Large-scale identification of tubulin-binding proteins provides insight on subcellular trafficking, metabolic channeling, and signaling in plant cells. *Molecular & cellular proteomics : MCP,* **3**(10), pp. 970-983.

COHN, R.D. and CAMPBELL, K.P., 2000. Molecular basis of muscular dystrophies. *Muscle & nerve,* **23**(10), pp. 1456-1471.

COHN, R.D., HENRY, M.D., MICHELE, D.E., BARRESI, R., SAITO, F., MOORE, S.A., FLANAGAN, J.D., SKWARCHUK, M.W., ROBBINS, M.E., MENDELL, J.R., WILLIAMSON, R.A. and CAMPBELL, K.P., 2002. Disruption of DAG1 in differentiated skeletal muscle reveals a role for dystroglycan in muscle regeneration. *Cell,* **110**(5), pp. 639-48.

COMPTON, A.G., COOPER, S.T., HILL, P.M., YANG, N., FROEHNER, S.C. and NORTH, K.N., 2005. The syntrophin-dystrobrevin subcomplex in human neuromuscular disorders. *J Neuropathol Exp Neurol,* **64**(4), pp. 350-61.

COSTA, A.C., WALSH, K. and DAVISSON, M.T., 1999. Motor dysfunction in a mouse model for Down syndrome. *Physiology & Behavior,* **68**(1-2), pp. 211-220.

COSTA, M.L., ESCALEIRA, R., CATALDO, A., OLIVEIRA, F. and MERMELSTEIN, C.S., 2004. Desmin: molecular interactions and putative functions of the muscle intermediate filament protein. *Braz J Med Biol Res,* **37**(12), pp. 1819-30.

COTE, F., COLLARD, J.F. and JULIEN, J.P., 1993. Progressive neuronopathy in transgenic mice expressing the human neurofilament heavy gene: a mouse model of amyotrophic lateral sclerosis. *Cell,* **73**(1), pp. 35-46.

COTE, P.D., MOUKHLES, H. and CARBONETTO, S., 2002. Dystroglycan is not required for localization of dystrophin, syntrophin, and neuronal nitric-oxide synthase at the sarcolemma but regulates integrin alpha 7B expression and caveolin-3 distribution. *J Biol Chem,* **277**(7), pp. 4672-9.

COULOMBE, P.A., HUTTON, M.E., LETAI, A., HEBERT, A., PALLER, A.S. and FUCHS, E., 1991. Point mutations in human keratin 14 genes of epidermolysis bullosa simplex patients: genetic and functional analyses. *Cell,* **66**(6), pp. 1301-11.

COX, G.A., COLE, N.M., MATSUMURA, K., PHELPS, S.F., HAUSCHKA, S.D., CAMPBELL, K.P., FAULKNER, J.A. and CHAMBERLAIN, J.S., 1993. Overexpression of dystrophin in transgenic mdx mice eliminates dystrophic symptoms without toxicity [see comments]. *Nature,* **364**(6439), pp. 725-9.

CROSBIE, R.H., HEIGHWAY, J., VENZKE, D.P., LEE, J.C. and CAMPBELL, K.P., 1997. Sarcospan, the 25-kDa transmembrane component of the dystrophin-glycoprotein complex. *The Journal of biological chemistry,* **272**(50), pp. 31221-31224.

DAVIES, K.E. and NOWAK, K.J., 2006. Molecular mechanisms of muscular dystrophies: old and new players. *Nature reviews.Molecular cell biology,* **7**(10), pp. 762-773.

DE JONGHE, P., MERSIVANOVA, I., NELIS, E., DEL FAVERO, J., MARTIN, J.J., VAN BROECKHOVEN, C., EVGRAFOV, O. and TIMMERMAN, V., 2001. Further evidence that neurofilament light chain gene mutations can cause Charcot-Marie-Tooth disease type 2E. *Ann Neurol,* **49**(2), pp. 245-9.

DEPIANTO, D. and COULOMBE, P.A., 2004. Intermediate filaments and tissue repair. *Exp Cell Res,* **301**(1), pp. 68-76.

DINSDALE, D., LEE, J.C., DEWSON, G., COHEN, G.M. and PETER, M.E., 2004. Intermediate filaments control the intracellular distribution of caspases during apoptosis. *The American journal of pathology,* **164**(2), pp. 395-407.

DRAVIAM, R., BILLINGTON, L., SENCHAK, A., HOFFMAN, E.P. and WATKINS, S.C., 2001. Confocal analysis of the dystrophin protein complex in muscular dystrophy. *Muscle & nerve,* **24**(2), pp. 262-272.

DUNHAM, N.W. and MIYA, T.S., 1957. A note on a simple apparatus for detecting neurological deficit in rats and mice. *Journal of the American Pharmaceutical Association.American Pharmaceutical Association,* **46**(3), pp. 208-209.

ECKES, B., DOGIC, D., COLUCCI-GUYON, E., WANG, N., MANIOTIS, A., INGBER, D., MERCKLING, A., LANGA, F., AUMAILLEY, M., DELOUVEE, A., KOTELIANSKY, V., BABINET, C. and KRIEG, T., 1998. Impaired mechanical stability, migration and contractile capacity in vimentin-deficient fibroblasts. *Journal of cell science,* **111 (Pt 13)**(Pt 13), pp. 1897-1907.

ELDER, G.A., L., F.V.,JR, BOSCO, P., KANG, C., GOUROV, A., TU, P.H., LEE, V.M. and LAZZARINI, R.A., 1998. Absence of the mid-sized neurofilament subunit decreases axonal calibers, levels of light neurofilament (NF-L), and neurofilament content. *J Cell Biol,* **141**(3), pp. 727-39.

EMERY, A.E., 2002. The muscular dystrophies. *Lancet,* **359**(9307), pp. 687-95.

ENGEL, A., EICHNER, R. and AEBI, U., 1985. Polymorphism of reconstituted human epidermal keratin filaments: determination of their mass-per-length and width by scanning transmission electron microscopy (STEM). *Journal of ultrastructure research,* **90**(3), pp. 323-335.

ERVASTI, J.M., 2003. Costameres: the Achilles' heel of Herculean muscle. *The Journal of biological chemistry,* **278**(16), pp. 13591-13594.

ERVASTI, J.M., OHLENDIECK, K., KAHL, S.D., GAVER, M.G. and CAMPBELL, K.P., 1990. Deficiency of a glycoprotein component of the dystrophin complex in dystrophic muscle. *Nature,* **345**(6273), pp. 315-319.

FABRIZI, G.M., CAVALLARO, T., ANGIARI, C., CABRINI, I., TAIOLI, F., MALERBA, G., BERTOLASI, L. and RIZZUTO, N., 2007. Charcot-Marie-Tooth disease type 2E, a disorder of the cytoskeleton. *Brain : a journal of neurology,* **130**(Pt 2), pp. 394-403.

FIGLEWICZ, D.A., KRIZUS, A., MARTINOLI, M.G., MEININGER, V., DIB, M., ROULEAU, G.A. and JULIEN, J.P., 1994. Variants of the heavy neurofilament subunit are associated with the development of amyotrophic lateral sclerosis. *Human molecular genetics,* **3**(10), pp. 1757-1761.

FLIEGNER, K.H., KAPLAN, M.P., WOOD, T.L., PINTAR, J.E. and LIEM, R.K., 1994. Expression of the gene for the neuronal intermediate filament protein alpha-internexin coincides with the onset of neuronal differentiation in the developing rat nervous system. *The Journal of comparative neurology,* **342**(2), pp. 161-173.

FOISNER, R., BOHN, W., MANNWEILER, K. and WICHE, G., 1995. Distribution and ultrastructure of plectin arrays in subclones of rat glioma C6 cells differing in

intermediate filament protein (vimentin) expression. *Journal of structural biology,* **115**(3), pp. 304-317.

GALARNEAU, L., LORANGER, A., GILBERT, S. and MARCEAU, N., 2007. Keratins modulate hepatic cell adhesion, size and G1/S transition. *Experimental cell research,* **313**(1), pp. 179-194.

GAMA SOSA, M.A., L., F.V.,JR, DEGASPERI, R., KELLEY, K., WEN, P.H., SENTURK, E., LAZZARINI, R.A. and ELDER, G.A., 2003. Human midsized neurofilament subunit induces motor neuron disease in transgenic mice. *Exp Neurol,* **184**(1), pp. 408-19.

GEORGIOU, D.M., ZIDAR, J., KOROSEC, M., MIDDLETON, L.T., KYRIAKIDES, T. and CHRISTODOULOU, K., 2002. A novel NF-L mutation Pro22Ser is associated with CMT2 in a large Slovenian family. *Neurogenetics,* **4**(2), pp. 93-6.

GOLDFARB, L.G., PARK, K.Y., CERVENAKOVA, L., GOROKHOVA, S., LEE, H.S., VASCONCELOS, O., NAGLE, J.W., SEMINO-MORA, C., SIVAKUMAR, K. and DALAKAS, M.C., 1998. Missense mutations in desmin associated with familial cardiac and skeletal myopathy. *Nat Genet,* **19**(4), pp. 402-3.

GOLDMAN, R.D., KHUON, S., CHOU, Y.H., OPAL, P. and STEINERT, P.M., 1996. The function of intermediate filaments in cell shape and cytoskeletal integrity. *The Journal of cell biology,* **134**(4), pp. 971-983.

GRADY, R.M., GRANGE, R.W., LAU, K.S., MAIMONE, M.M., NICHOL, M.C., STULL, J.T. and SANES, J.R., 1999. Role for alpha-dystrobrevin in the pathogenesis of dystrophin-dependent muscular dystrophies. *Nature cell biology,* **1**(4), pp. 215-220.

GREWAL, P.K., HOLZFEIND, P.J., BITTNER, R.E. and HEWITT, J.E., 2001. Mutant glycosyltransferase and altered glycosylation of alpha-dystroglycan in the myodystrophy mouse. *Nat Genet,* **28**(2), pp. 151-4.

GRIFFIN, M.A., FENG, H., TEWARI, M., ACOSTA, P., KAWANA, M., SWEENEY, H.L. and DISCHER, D.E., 2005. gamma-Sarcoglycan deficiency increases cell contractility, apoptosis and MAPK pathway activation but does not affect adhesion. *Journal of cell science,* **118**(Pt 7), pp. 1405-1416.

GROS-LOUIS, F., LARIVIERE, R., GOWING, G., LAURENT, S., CAMU, W., BOUCHARD, J.P., MEININGER, V., ROULEAU, G.A. and JULIEN, J.P., 2004. A frameshift deletion in peripherin gene associated with amyotrophic lateral sclerosis. *J Biol Chem,* **279**(44), pp. 45951-6.

GU, Y., MCILWAIN, K.L., WEEBER, E.J., YAMAGATA, T., XU, B., ANTALFFY, B.A., REYES, C., YUVA-PAYLOR, L., ARMSTRONG, D., ZOGHBI, H., SWEATT, J.D., PAYLOR, R. and NELSON, D.L., 2002. Impaired conditioned fear and enhanced long-term potentiation in Fmr2 knock-out mice. *The Journal of neuroscience : the official journal of the Society for Neuroscience,* **22**(7), pp. 2753-2763.

HACK, A.A., LAM, M., CORDIER, L., SHOTURMA, D.I., LY, C.T., HADHAZY, M.A., HADHAZY, M.R., SWEENEY, H.L. and MCNALLY, E.M., 2000. Differential requirement for individual sarcoglycans and dystrophin in the assembly and function of the dystrophin-glycoprotein complex [In Process Citation]. *J Cell Sci,* **113**(Pt 14), pp. 2535-44.

HACK, A.A., LY, C.T., JIANG, F., CLENDENIN, C.J., SIGRIST, K.S., WOLLMANN, R.L. and MCNALLY, E.M., 1998. Gamma-sarcoglycan deficiency leads to muscle membrane defects and apoptosis independent of dystrophin. *J Cell Biol,* **142**(5), pp. 1279-87.

HEDBERG, K.K. and CHEN, L.B., 1986. Absence of intermediate filaments in a human adrenal cortex carcinoma-derived cell line. *Experimental cell research,* **163**(2), pp. 509-517.

HELBLING-LECLERC, A., ZHANG, X., TOPALOGLU, H., CRUAUD, C., TESSON, F., WEISSENBACH, J., TOME, F.M., SCHWARTZ, K., FARDEAU, M. and TRYGGVASON, K., 1995. Mutations in the laminin alpha 2-chain gene (LAMA2) cause merosin-deficient congenital muscular dystrophy. *Nature genetics,* **11**(2), pp. 216-218.

HERRMANN, H. and AEBI, U., 2004. Intermediate filaments: molecular structure, assembly mechanism, and integration into functionally distinct intracellular Scaffolds. *Annual Review of Biochemistry,* **73**, pp. 749-789.

HERRMANN, H. and AEBI, U., 2000. Intermediate filaments and their associates: multi-talented structural elements specifying cytoarchitecture and cytodynamics. *Curr Opin Cell Biol,* **12**(1), pp. 79-90.

HERRMANN, H. and AEBI, U., 1999. Intermediate filament assembly: temperature sensitivity and polymorphism. *Cellular and molecular life sciences : CMLS,* **55**(11), pp. 1416-1431.

HIJIKATA, T., MURAKAMI, T., ISHIKAWA, H. and YORIFUJI, H., 2003. Plectin tethers desmin intermediate filaments onto subsarcolemmal dense plaques containing dystrophin and vinculin. *Histochemistry and cell biology,* **119**(2), pp. 109-123.

HIJIKATA, T., NAKAMURA, A., ISOKAWA, K., IMAMURA, M., YUASA, K., ISHIKAWA, R., KOHAMA, K., TAKEDA, S. and YORIFUJI, H., 2008. Plectin 1 links intermediate filaments to costameric sarcolemma through beta-synemin, alpha-dystrobrevin and actin. *Journal of cell science,* **121**(Pt 12), pp. 2062-2074.

HIROKAWA, N., 1982. Cross-linker system between neurofilaments, microtubules, and membranous organelles in frog axons revealed by the quick-freeze, deep-etching method. *The Journal of cell biology,* **94**(1), pp. 129-142.

HOFFMAN, E.P., H., B.R.,JR and KUNKEL, L.M., 1987. Dystrophin: the protein product of the Duchenne muscular dystrophy locus. *Cell,* **51**(6), pp. 919-28.

HOFFMAN, E.P. and SCHWARTZ, L., 1991. Dystrophin and disease. *Mol Aspects Med,* **12**(3), pp. 175-94.

HOMAN, S.M., MERCURIO, A.M. and LAFLAMME, S.E., 1998. Endothelial cells assemble two distinct alpha6beta4-containing vimentin-associated structures: roles for ligand binding and the beta4 cytoplasmic tail. *Journal of cell science,* **111 (Pt 18)**(Pt 18), pp. 2717-2728.

HORNBERGER, T.A., ARMSTRONG, D.D., KOH, T.J., BURKHOLDER, T.J. and ESSER, K.A., 2005. Intracellular signaling specificity in response to uniaxial vs. multiaxial stretch: implications for mechanotransduction. *American journal of physiology.Cell physiology,* **288**(1), pp. C185-94.

HOWMAN, E.V., SULLIVAN, N., POON, E.P., BRITTON, J.E., HILTON-JONES, D. and DAVIES, K.E., 2003. Syncoilin accumulation in two patients with desmin-related myopathy. *Neuromuscular disorders : NMD,* **13**(1), pp. 42-48.

IBRAGHIMOV BESKROVNAYA, O., ERVASTI, J.M., LEVEILLE, C.J., SLAUGHTER, C.A., SERNETT, S.W. and CAMPBELL, K.P., 1992. Primary structure of dystrophin-associated glycoproteins linking dystrophin to the extracellular matrix. *Nature,* **355**(6362), pp. 696-702.

IBRAGHIMOV-BESKROVNAYA, O., ERVASTI, J.M., LEVEILLE, C.J., SLAUGHTER, C.A., SERNETT, S.W. and CAMPBELL, K.P., 1992. Primary structure of dystrophin-associated glycoproteins linking dystrophin to the extracellular matrix. *Nature,* **355**(6362), pp. 696-702.

IZMIRYAN, A., CHERAUD, Y., KHANAMIRYAN, L., LETERRIER, J.F., FEDERICI, T., PELTEKIAN, E., MOURA-NETO, V., PAULIN, D., LI, Z. and XUE, Z.G., 2006. Different expression of synemin isoforms in glia and neurons during nervous system development. *Glia,* **54**(3), pp. 204-213.

JARRETT, H.W. and FOSTER, J.L., 1995. Alternate binding of actin and calmodulin to multiple sites on dystrophin. *J Biol Chem,* **270**(10), pp. 5578-86.

JOBSIS, G.J., KEIZERS, H., VREIJLING, J.P., DE VISSER, M., SPEER, M.C., WOLTERMAN, R.A., BAAS, F. and BOLHUIS, P.A., 1996. Type VI collagen mutations in Bethlem myopathy, an autosomal dominant myopathy with contractures. *Nat Genet,* **14**(1), pp. 113-5.

JORDANOVA, A., DE JONGHE, P., BOERKOEL, C.F., TAKASHIMA, H., DE VRIENDT, E., CEUTERICK, C., MARTIN, J.J., BUTLER, I.J., MANCIAS, P., PAPASOZOMENOS, S.C., TERESPOLSKY, D., POTOCKI, L., BROWN, C.W., SHY, M., RITA, D.A., TOURNEV, I., KREMENSKY, I., LUPSKI, J.R. and TIMMERMAN, V., 2003. Mutations in the neurofilament light chain gene (NEFL) cause early onset severe Charcot-Marie-Tooth disease. *Brain : a journal of neurology,* **126**(Pt 3), pp. 590-597.

JUNG, D., DUCLOS, F., APOSTOL, B., STRAUB, V., LEE, J.C., ALLAMAND, V., VENZKE, D.P., SUNADA, Y., MOOMAW, C.R., LEVEILLE, C.J., SLAUGHTER,

C.A., CRAWFORD, T.O., MCPHERSON, J.D. and CAMPBELL, K.P., 1996. Characterization of delta-sarcoglycan, a novel component of the oligomeric sarcoglycan complex involved in limb-girdle muscular dystrophy. *The Journal of biological chemistry,* **271**(50), pp. 32321-32329.

KASSIOTIS, C., RAJABI, M. and TAEGTMEYER, H., 2008. Metabolic reserve of the heart: the forgotten link between contraction and coronary flow. *Progress in cardiovascular diseases,* **51**(1), pp. 74-88.

KEMP, M.W., EDWARDS, B., BURGESS, M., CLARKE, W.T., NICHOLSON, G., PARRY, D.A. and DAVIES, K.E., 2008. Syncoilin isoform organization and differential expression in murine striated muscle. *Journal of structural biology,* .

KIM, S., WONG, P. and COULOMBE, P.A., 2006. A keratin cytoskeletal protein regulates protein synthesis and epithelial cell growth. *Nature,* **441**(7091), pp. 362-365.

KOBAYASHI, K., NAKAHORI, Y., MIYAKE, M., MATSUMURA, K., KONDO-IIDA, E., NOMURA, Y., SEGAWA, M., YOSHIOKA, M., SAITO, K., OSAWA, M., HAMANO, K., SAKAKIHARA, Y., NONAKA, I., NAKAGOME, Y., KANAZAWA, I., NAKAMURA, Y., TOKUNAGA, K. and TODA, T., 1998. An ancient retrotransposal insertion causes Fukuyama-type congenital muscular dystrophy. *Nature,* **394**(6691), pp. 388-392.

KOENIG, M., MONACO, A.P. and KUNKEL, L.M., 1988. The complete sequence of dystrophin predicts a rod-shaped cytoskeletal protein. *Cell,* **53**(2), pp. 219-26.

KUHLENBAUMER, G., YOUNG, P., HUNERMUND, G., RINGELSTEIN, B. and STOGBAUER, F., 2002. Clinical features and molecular genetics of hereditary peripheral neuropathies. *J Neurol,* **249**(12), pp. 1629-50.

LANGENBACH, K.J. and RANDO, T.A., 2002. Inhibition of dystroglycan binding to laminin disrupts the PI3K/AKT pathway and survival signaling in muscle cells. *Muscle Nerve,* **26**(5), pp. 644-53.

LARIVIERE, R.C. and JULIEN, J.P., 2004. Functions of intermediate filaments in neuronal development and disease. *J Neurobiol,* **58**(1), pp. 131-48.

LARIVIERE, R.C., NGUYEN, M.D., RIBEIRO-DA-SILVA, A. and JULIEN, J.P., 2002. Reduced number of unmyelinated sensory axons in peripherin null mice. *Journal of neurochemistry,* **81**(3), pp. 525-532.

LE MAREC, N., CASTON, J. and LALONDE, R., 1997. Impaired motor skills on static and mobile beams in lurcher mutant mice. *Experimental brain research.Experimentelle Hirnforschung.Experimentation cerebrale,* **116**(1), pp. 131-138.

LEE, M.K., XU, Z., WONG, P.C. and CLEVELAND, D.W., 1993. Neurofilaments are obligate heteropolymers in vivo. *The Journal of cell biology,* **122**(6), pp. 1337-1350.

LEUNG, C.L., HE, C.Z., KAUFMANN, P., CHIN, S.S., NAINI, A., LIEM, R.K., MITSUMOTO, H. and HAYS, A.P., 2004. A pathogenic peripherin gene mutation in a patient with amyotrophic lateral sclerosis. *Brain pathology (Zurich, Switzerland),* **14**(3), pp. 290-296.

LEVAVASSEUR, F., ZHU, Q. and JULIEN, J.P., 1999. No requirement of alpha-internexin for nervous system development and for radial growth of axons. *Brain research.Molecular brain research,* **69**(1), pp. 104-112.

LEVINE, B.A., MOIR, A.J., PATCHELL, V.B. and PERRY, S.V., 1992. Binding sites involved in the interaction of actin with the N-terminal region of dystrophin. *FEBS letters,* **298**(1), pp. 44-48.

LI, X. and LARSSON, L., 1997. Contractility and myosin isoform compositions of skeletal muscles and muscle cells from rats treated with thyroid hormone for 0, 4 and 8 weeks. *Journal of muscle research and cell motility,* **18**(3), pp. 335-344.

LIM, L.E., DUCLOS, F., BROUX, O., BOURG, N., SUNADA, Y., ALLAMAND, V., MEYER, J., RICHARD, I., MOOMAW, C. and SLAUGHTER, C., 1995. Beta-sarcoglycan: characterization and role in limb-girdle muscular dystrophy linked to 4q12. *Nature genetics,* **11**(3), pp. 257-265.

LONGMAN, C., BROCKINGTON, M., TORELLI, S., JIMENEZ-MALLEBRERA, C., KENNEDY, C., KHALIL, N., FENG, L., SARAN, R.K., VOIT, T., MERLINI, L., SEWRY, C.A., BROWN, S.C. and MUNTONI, F., 2003. Mutations in the human LARGE gene cause MDC1D, a novel form of congenital muscular dystrophy with severe mental retardation and abnormal glycosylation of alpha-dystroglycan. *Human molecular genetics,* **12**(21), pp. 2853-2861.

MADHAVAN, R., MASSOM, L.R. and JARRETT, H.W., 1992. Calmodulin specifically binds three proteins of the dystrophin-glycoprotein complex. *Biochem Biophys Res Commun,* **185**(2), pp. 753-9.

MARCEAU, N., SCHUTTE, B., GILBERT, S., LORANGER, A., HENFLING, M.E., BROERS, J.L., MATHEW, J. and RAMAEKERS, F.C., 2007. Dual roles of intermediate filaments in apoptosis. *Exp Cell Res,* **313**(10), pp. 2265-81.

MARTINEAU, L.C. and GARDINER, P.F., 2001. Insight into skeletal muscle mechanotransduction: MAPK activation is quantitatively related to tension. *Journal of applied physiology (Bethesda, Md.: 1985),* **91**(2), pp. 693-702.

MATSUDA, R., NISHIKAWA, A. and TANAKA, H., 1995. Visualization of dystrophic muscle fibers in mdx mouse by vital staining with Evans blue: evidence of apoptosis in dystrophin-deficient muscle. *J Biochem (Tokyo),* **118**(5), pp. 959-64.

MCCULLAGH, K.J., EDWARDS, B., KEMP, M.W., GILES, L.C., BURGESS, M. and DAVIES, K.E., 2008. Analysis of skeletal muscle function in the C57BL6/SV129 syncoilin knockout mouse. *Mammalian genome : official journal of the International Mammalian Genome Society,* **19**(5), pp. 339-351.

MCCULLAGH, K.J., EDWARDS, B., POON, E., LOVERING, R.M., PAULIN, D. and DAVIES, K.E., 2007. Intermediate filament-like protein syncoilin in normal and myopathic striated muscle. *Neuromuscular disorders : NMD,* **17**(11-12), pp. 970-979.

MCGRAW, T.S., MICKLE, J.P., SHAW, G. and STREIT, W.J., 2002. Axonally transported peripheral signals regulate alpha-internexin expression in regenerating motoneurons. *The Journal of neuroscience : the official journal of the Society for Neuroscience,* **22**(12), pp. 4955-4963.

MCLEAN, J., XIAO, S., MIYAZAKI, K. and ROBERTSON, J., 2008. A novel peripherin isoform generated by alternative translation is required for normal filament network formation. *Journal of neurochemistry,* **104**(6), pp. 1663-1673.

MCNALLY, E.M., DUGGAN, D., GOROSPE, J.R., BONNEMANN, C.G., FANIN, M., PEGORARO, E., LIDOV, H.G., NOGUCHI, S., OZAWA, E., FINKEL, R.S., CRUSE, R.P., ANGELINI, C., KUNKEL, L.M. and HOFFMAN, E.P., 1996. Mutations that disrupt the carboxyl-terminus of gamma-sarcoglycan cause muscular dystrophy. *Hum Mol Genet,* **5**(11), pp. 1841-7.

MENKE, A. and JOCKUSCH, H., 1991. Decreased osmotic stability of dystrophin-less muscle cells from the mdx mouse [see comments]. *Nature,* **349**(6304), pp. 69-71.

MERLINI, L., VILLANOVA, M., SABATELLI, P., MALANDRINI, A. and MARALDI, N.M., 1999. Decreased expression of laminin beta 1 in chromosome 21-linked Bethlem myopathy. *Neuromuscul Disord,* **9**(5), pp. 326-9.

MERSIYANOVA, I.V., PEREPELOV, A.V., POLYAKOV, A.V., SITNIKOV, V.F., DADALI, E.L., OPARIN, R.B., PETRIN, A.N. and EVGRAFOV, O.V., 2000. A new variant of Charcot-Marie-Tooth disease type 2 is probably the result of a mutation in the neurofilament-light gene. *Am J Hum Genet,* **67**(1), pp. 37-46.

METZINGER, L., BLAKE, D.J., SQUIER, M.V., ANDERSON, L.V., DECONINCK, A.E., NAWROTZKI, R., HILTON-JONES, D. and DAVIES, K.E., 1997. Dystrobrevin deficiency at the sarcolemma of patients with muscular dystrophy. *Hum Mol Genet,* **6**(7), pp. 1185-91.

MILTENBERGER-MILTENYI, G., JANECKE, A.R., WANSCHITZ, J.V., TIMMERMAN, V., WINDPASSINGER, C., AUER-GRUMBACH, M. and LOSCHER, W.N., 2007. Clinical and electrophysiological features in Charcot-Marie-Tooth disease with mutations in the NEFL gene. *Archives of Neurology,* **64**(7), pp. 966-970.

MITCHELL, J.D. and BORASIO, G.D., 2007. Amyotrophic lateral sclerosis. *Lancet,* **369**(9578), pp. 2031-2041.

MONTI, R.J., ROY, R.R., HODGSON, J.A. and EDGERTON, V.R., 1999. Transmission of forces within mammalian skeletal muscles. *Journal of Biomechanics,* **32**(4), pp. 371-380.

MOUNKES, L.C., KOZLOV, S.V., ROTTMAN, J.N. and STEWART, C.L., 2005. Expression of an LMNA-N195K variant of A-type lamins results in cardiac conduction defects and death in mice. *Human molecular genetics,* **14**(15), pp. 2167-2180.

MUNOZ-MARMOL, A.M., STRASSER, G., ISAMAT, M., COULOMBE, P.A., YANG, Y., ROCA, X., VELA, E., MATE, J.L., COLL, J., FERNANDEZ-FIGUERAS, M.T., NAVAS-PALACIOS, J.J., ARIZA, A. and FUCHS, E., 1998. A dysfunctional desmin mutation in a patient with severe generalized myopathy. *Proc Natl Acad Sci U S A,* **95**(19), pp. 11312-7.

NDOZANGUE-TOURIGUINE, O., HAMELIN, J. and BREARD, J., 2008. Cytoskeleton and apoptosis. *Biochemical pharmacology,* **76**(1), pp. 11-18.

NEWEY, S.E., HOWMAN, E.V., PONTING, C.P., BENSON, M.A., NAWROTZKI, R., LOH, N.Y., DAVIES, K.E. and BLAKE, D.J., 2001. Syncoilin, a novel member of the intermediate filament superfamily that interacts with alpha-dystrobrevin in skeletal muscle. *The Journal of biological chemistry,* **276**(9), pp. 6645-6655.

NIGRO, V., DE SA MOREIRA, E., PILUSO, G., VAINZOF, M., BELSITO, A., POLITANO, L., PUCA, A.A., PASSOS-BUENO, M.R. and ZATZ, M., 1996. Autosomal recessive limb-girdle muscular dystrophy, LGMD2F, is caused by a mutation in the delta-sarcoglycan gene. *Nat Genet,* **14**(2), pp. 195-8.

NIKOLOVA, V., LEIMENA, C., MCMAHON, A.C., TAN, J.C., CHANDAR, S., JOGIA, D., KESTEVEN, S.H., MICHALICEK, J., OTWAY, R., VERHEYEN, F., RAINER, S., STEWART, C.L., MARTIN, D., FENELEY, M.P. and FATKIN, D., 2004. Defects in nuclear structure and function promote dilated cardiomyopathy in lamin A/C-deficient mice. *The Journal of clinical investigation,* **113**(3), pp. 357-369.

NOGUCHI, S., MCNALLY, E.M., BEN OTHMANE, K., HAGIWARA, Y., MIZUNO, Y., YOSHIDA, M., YAMAMOTO, H., BONNEMANN, C.G., GUSSONI, E. and DENTON, P.H., 1995a. Mutations in the dystrophin-associated protein gamma-sarcoglycan in chromosome 13 muscular dystrophy [see comments]. *Science,* **270**(5237), pp. 819-22.

NOGUCHI, S., MCNALLY, E.M., BEN OTHMANE, K., HAGIWARA, Y., MIZUNO, Y., YOSHIDA, M., YAMAMOTO, H., BONNEMANN, C.G., GUSSONI, E., DENTON, P.H., KYRIAKIDES, T., MIDDLETON, L., HENTATI, F., BEN HAMIDA, M., NONAKA, I., VANCE, J.M., KUNKEL, L.M. and OZAWA, E., 1995b. Mutations in the dystrophin-associated protein gamma-sarcoglycan in chromosome 13 muscular dystrophy. *Science (New York, N.Y.),* **270**(5237), pp. 819-822.

OAK, S.A., RUSSO, K., PETRUCCI, T.C. and JARRETT, H.W., 2001. Mouse alpha1-syntrophin binding to Grb2: further evidence of a role for syntrophin in cell signaling. *Biochemistry,* **40**(37), pp. 11270-11278.

OAK, S.A., ZHOU, Y.W. and JARRETT, H.W., 2003. Skeletal muscle signaling pathway through the dystrophin glycoprotein complex and Rac1. *The Journal of biological chemistry,* **278**(41), pp. 39287-39295.

OHLENDIECK, K. and CAMPBELL, K.P., 1991. Dystrophin-associated proteins are greatly reduced in skeletal muscle from mdx mice. *J Cell Biol,* **115**(6), pp. 1685-94.

PARRY, D.A. and STEINERT, P.M., 1999. Intermediate filaments: molecular architecture, assembly, dynamics and polymorphism. *Q Rev Biophys,* **32**(2), pp. 99-187.

PARRY, D.A., STRELKOV, S.V., BURKHARD, P., AEBI, U. and HERRMANN, H., 2007. Towards a molecular description of intermediate filament structure and assembly. *Exp Cell Res,* **313**(10), pp. 2204-16.

PASSOS-BUENO, M.R., TERWILLIGER, J., OTT, J., VAINZOF, M., LOVE, D.R., DAVIES, K.E. and ZATZ, M., 1991. Linkage analysis in families with autosomal recessive limb-girdle muscular dystrophy (LGMD) and 6q probes flanking the dystrophin-related sequence. *Am J Med Genet,* **38**(1), pp. 140-6.

PATEL, T.J. and LIEBER, R.L., 1997. Force transmission in skeletal muscle: from actomyosin to external tendons. *Exerc Sport Sci Rev,* **25**, pp. 321-63.

PAULIN, D. and LI, Z., 2004. Desmin: a major intermediate filament protein essential for the structural integrity and function of muscle. *Exp Cell Res,* **301**(1), pp. 1-7.

PEKNY, M. and LANE, E.B., 2007. Intermediate filaments and stress. *Exp Cell Res,* **313**(10), pp. 2244-54.

PEREZ-OLLE, R., LOPEZ-TOLEDANO, M.A., GORYUNOV, D., CABRERA-POCH, N., STEFANIS, L., BROWN, K. and LIEM, R.K., 2005. Mutations in the neurofilament light gene linked to Charcot-Marie-Tooth disease cause defects in transport. *Journal of neurochemistry,* **93**(4), pp. 861-874.

PERLSON, E., HANZ, S., BEN-YAAKOV, K., SEGAL-RUDER, Y., SEGER, R. and FAINZILBER, M., 2005. Vimentin-dependent spatial translocation of an activated MAP kinase in injured nerve. *Neuron,* **45**(5), pp. 715-726.

PICCOLO, F., ROBERDS, S.L., JEANPIERRE, M., LETURCQ, F., AZIBI, K., BELDJORD, C., CARRIE, A., RECAN, D., CHAOUCH, M. and REGHIS, A., 1995. Primary adhalinopathy: a common cause of autosomal recessive muscular dystrophy of variable severity [published erratum appears in Nat Genet 1995 Sep 11(1):104]. *Nat Genet,* **10**(2), pp. 243-5.

POON, E., HOWMAN, E.V., NEWEY, S.E. and DAVIES, K.E., 2002. Association of syncoilin and desmin: linking intermediate filament proteins to the dystrophin-associated protein complex. *The Journal of biological chemistry,* **277**(5), pp. 3433-3439.

RANDO, T.A., 2001. The dystrophin-glycoprotein complex, cellular signaling, and the regulation of cell survival in the muscular dystrophies. *Muscle Nerve,* **24**(12), pp. 1575-94.

RAO, M.V., HOUSEWEART, M.K., WILLIAMSON, T.L., CRAWFORD, T.O., FOLMER, J. and CLEVELAND, D.W., 1998. Neurofilament-dependent radial growth of motor axons and axonal organization of neurofilaments does not require the neurofilament heavy subunit (NF-H) or its phosphorylation. *The Journal of cell biology,* **143**(1), pp. 171-181.

REZNICZEK, G.A., KONIECZNY, P., NIKOLIC, B., REIPERT, S., SCHNELLER, D., ABRAHAMSBERG, C., DAVIES, K.E., WINDER, S.J. and WICHE, G., 2007. Plectin 1f scaffolding at the sarcolemma of dystrophic (mdx) muscle fibers through multiple interactions with beta-dystroglycan. *The Journal of cell biology,* **176**(7), pp. 965-977.

ROBERDS, S.L., ANDERSON, R.D., IBRAGHIMOV-BESKROVNAYA, O. and CAMPBELL, K.P., 1993. Primary structure and muscle-specific expression of the 50-kDa dystrophin-associated glycoprotein (adhalin). *The Journal of biological chemistry,* **268**(32), pp. 23739-23742.

ROBERDS, S.L., LETURCQ, F., ALLAMAND, V., PICCOLO, F., JEANPIERRE, M., ANDERSON, R.D., LIM, L.E., LEE, J.C., TOME, F.M. and ROMERO, N.B., 1994. Missense mutations in the adhalin gene linked to autosomal recessive muscular dystrophy. *Cell,* **78**(4), pp. 625-33.

ROBERTSON, J., DOROUDCHI, M.M., NGUYEN, M.D., DURHAM, H.D., STRONG, M.J., SHAW, G., JULIEN, J.P. and MUSHYNSKI, W.E., 2003. A neurotoxic peripherin splice variant in a mouse model of ALS. *J Cell Biol,* **160**(6), pp. 939-49.

ROMMEL, C., BODINE, S.C., CLARKE, B.A., ROSSMAN, R., NUNEZ, L., STITT, T.N., YANCOPOULOS, G.D. and GLASS, D.J., 2001. Mediation of IGF-1-induced skeletal myotube hypertrophy by PI(3)K/Akt/mTOR and PI(3)K/Akt/GSK3 pathways. *Nature cell biology,* **3**(11), pp. 1009-1013.

RUSSO, K., DI STASIO, E., MACCHIA, G., ROSA, G., BRANCACCIO, A. and CORINNA PETRUCCI, T., 2000. Characterization of the beta-dystroglycan-growth factor receptor 2 (Grb2) interaction [In Process Citation]. *Biochem Biophys Res Commun,* **274**(1), pp. 93-8.

SADOULET-PUCCIO, H.M., KHURANA, T.S., COHEN, J.B. and KUNKEL, L.M., 1996. Cloning and characterization of the human homologue of a dystrophin related phosphoprotein found at the Torpedo electric organ post-synaptic membrane. *Human molecular genetics,* **5**(4), pp. 489-496.

SARRIA, A.J., LIEBER, J.G., NORDEEN, S.K. and EVANS, R.M., 1994. The presence or absence of a vimentin-type intermediate filament network affects the shape of the nucleus in human SW-13 cells. *Journal of cell science,* **107 (Pt 6)**(Pt 6), pp. 1593-1607.

SCHEFE, J.H., LEHMANN, K.E., BUSCHMANN, I.R., UNGER, T. and FUNKE-KAISER, H., 2006. Quantitative real-time RT-PCR data analysis: current concepts and the novel "gene expression's CT difference" formula. *Journal of Molecular Medicine (Berlin, Germany),* **84**(11), pp. 901-910.

SCHWEIZER, J., BOWDEN, P.E., COULOMBE, P.A., LANGBEIN, L., LANE, E.B., MAGIN, T.M., MALTAIS, L., OMARY, M.B., PARRY, D.A., ROGERS, M.A. and WRIGHT, M.W., 2006. New consensus nomenclature for mammalian keratins. *J Cell Biol,* **174**(2), pp. 169-74.

SHEA, T.B. and BEERMANN, M.L., 1999. Neuronal intermediate filament protein alpha-internexin facilitates axonal neurite elongation in neuroblastoma cells. *Cell motility and the cytoskeleton,* **43**(4), pp. 322-333.

SJOBERG, G., SAAVEDRA-MATIZ, C.A., ROSEN, D.R., WIJSMAN, E.M., BORG, K., HOROWITZ, S.H. and SEJERSEN, T., 1999. A missense mutation in the desmin rod domain is associated with autosomal dominant distal myopathy, and exerts a dominant negative effect on filament formation. *Hum Mol Genet,* **8**(12), pp. 2191-8.

STONE, M.R., O'NEILL, A., CATINO, D. and BLOCH, R.J., 2005. Specific interaction of the actin-binding domain of dystrophin with intermediate filaments containing keratin 19. *Molecular biology of the cell,* **16**(9), pp. 4280-4293.

SUN, N., CRITCHLEY, D.R., PAULIN, D., LI, Z. and ROBSON, R.M., 2008. Human alpha-synemin interacts directly with vinculin and metavinculin. *The Biochemical journal,* **409**(3), pp. 657-667.

SVITKINA, T.M., VERKHOVSKY, A.B. and BORISY, G.G., 1996. Plectin sidearms mediate interaction of intermediate filaments with microtubules and other components of the cytoskeleton. *The Journal of cell biology,* **135**(4), pp. 991-1007.

TAKAHASHI, M. and ONO, Y., 2003. Pulse-chase analysis of protein kinase C. *Methods in molecular biology (Clifton, N.J.),* **233**, pp. 163-170.

TALTS, J.F., ANDAC, Z., GOHRING, W., BRANCACCIO, A. and TIMPL, R., 1999. Binding of the G domains of laminin alpha1 and alpha2 chains and perlecan to heparin, sulfatides, alpha-dystroglycan and several extracellular matrix proteins. *The EMBO journal,* **18**(4), pp. 863-870.

TER LAAK, H.J., LEYTEN, Q.H., GABREELS, F.J., KUPPEN, H., RENIER, W.O. and SENGERS, R.C., 1998. Laminin-alpha2 (merosin), beta-dystroglycan, alpha-sarcoglycan (adhalin), and dystrophin expression in congenital muscular dystrophies: an immunohistochemical study. *Clin Neurol Neurosurg,* **100**(1), pp. 5-10.

THOMPSON, T.G., CHAN, Y.M., HACK, A.A., BROSIUS, M., RAJALA, M., LIDOV, H.G., MCNALLY, E.M., WATKINS, S. and KUNKEL, L.M., 2000. Filamin 2 (FLN2): A muscle-specific sarcoglycan interacting protein. *The Journal of cell biology,* **148**(1), pp. 115-126.

TICHOPAD, A., PFAFFL, M.W. and DIDIER, A., 2003. Tissue-specific expression pattern of bovine prion gene: quantification using real-time RT-PCR. *Molecular and cellular probes,* **17**(1), pp. 5-10.

TIMMUSK, S., FOSSUM, C. and BERG, M., 2006. Porcine circovirus type 2 replicase binds the capsid protein and an intermediate filament-like protein. *The Journal of general virology,* **87**(Pt 11), pp. 3215-3223.

TOIVOLA, D.M., TAO, G.Z., HABTEZION, A., LIAO, J. and OMARY, M.B., 2005. Cellular integrity plus: organelle-related and protein-targeting functions of intermediate filaments. *Trends Cell Biol,* **15**(11), pp. 608-17.

TROY, C.M., BROWN, K., GREENE, L.A. and SHELANSKI, M.L., 1990. Ontogeny of the neuronal intermediate filament protein, peripherin, in the mouse embryo. *Neuroscience,* **36**(1), pp. 217-237.

TROY, C.M., MUMA, N.A., GREENE, L.A., PRICE, D.L. and SHELANSKI, M.L., 1990. Regulation of peripherin and neurofilament expression in regenerating rat motor neurons. *Brain research,* **529**(1-2), pp. 232-238.

TSURUTA, D. and JONES, J.C., 2003. The vimentin cytoskeleton regulates focal contact size and adhesion of endothelial cells subjected to shear stress. *Journal of cell science,* **116**(Pt 24), pp. 4977-4984.

URSITTI, J.A., LEE, P.C., RESNECK, W.G., MCNALLY, M.M., BOWMAN, A.L., O'NEILL, A., STONE, M.R. and BLOCH, R.J., 2004. Cloning and characterization of cytokeratins 8 and 19 in adult rat striated muscle. Interaction with the dystrophin glycoprotein complex. *The Journal of biological chemistry,* **279**(40), pp. 41830-41838.

VAN DER NEUT, R., KRIMPENFORT, P., CALAFAT, J., NIESSEN, C.M. and SONNENBERG, A., 1996. Epithelial detachment due to absence of hemidesmosomes in integrin beta 4 null mice. *Nature genetics,* **13**(3), pp. 366-369.

VAN HEUSDEN, G.P., 2005. 14-3-3 Proteins: Regulators of Numerous Eukaryotic Proteins. *IUBMB life,* **57**(9), pp. 623-629.

WAGNER, O.I., RAMMENSEE, S., KORDE, N., WEN, Q., LETERRIER, J.F. and JANMEY, P.A., 2007. Softness, strength and self-repair in intermediate filament networks. *Exp Cell Res,* **313**(10), pp. 2228-35.

WELLER, B., KARPATI, G. and CARPENTER, S., 1990. Dystrophin-deficient mdx muscle fibers are preferentially vulnerable to necrosis induced by experimental lengthening contractions. *J Neurol Sci,* **100**(1-2), pp. 9-13.

XIAO, C.W., YAN, X., LI, Y., REDDY, S.A. and TSANG, B.K., 2003. Resistance of human ovarian cancer cells to tumor necrosis factor alpha is a consequence of nuclear factor kappaB-mediated induction of Fas-associated death domain-like interleukin-1beta-converting enzyme-like inhibitory protein. *Endocrinology,* **144**(2), pp. 623-630.

XIAO, S., MCLEAN, J. and ROBERTSON, J., 2006. Neuronal intermediate filaments and ALS: a new look at an old question. *Biochimica et biophysica acta,* **1762**(11-12), pp. 1001-1012.

XIAO, S., TJOSTHEIM, S., SANELLI, T., MCLEAN, J.R., HORNE, P., FAN, Y., RAVITS, J., STRONG, M.J. and ROBERTSON, J., 2008. An aggregate-inducing peripherin isoform generated through intron retention is upregulated in amyotrophic lateral sclerosis and associated with disease pathology. *The Journal of neuroscience : the official journal of the Society for Neuroscience,* **28**(8), pp. 1833-1840.

XU, H., WU, X.R., WEWER, U.M. and ENGVALL, E., 1994. Murine muscular dystrophy caused by a mutation in the laminin alpha 2 (Lama2) gene. *Nature genetics,* **8**(3), pp. 297-302.

XU, Z., CORK, L.C., GRIFFIN, J.W. and CLEVELAND, D.W., 1993. Increased expression of neurofilament subunit NF-L produces morphological alterations that resemble the pathology of human motor neuron disease. *Cell*, **73**(1), pp. 23-33.

XUE, Z.G., CHERAUD, Y., BROCHERIOU, V., IZMIRYAN, A., TITEUX, M., PAULIN, D. and LI, Z., 2004. The mouse synemin gene encodes three intermediate filament proteins generated by alternative exon usage and different open reading frames. *Experimental cell research,* **298**(2), pp. 431-444.

YUAN, A., RAO, M.V., SASAKI, T., CHEN, Y., KUMAR, A., VEERANNA, LIEM, R.K., EYER, J., PETERSON, A.C., JULIEN, J.P. and NIXON, R.A., 2006. Alpha-internexin is structurally and functionally associated with the neurofilament triplet proteins in the mature CNS. *The Journal of neuroscience : the official journal of the Society for Neuroscience,* **26**(39), pp. 10006-10019.

ZHANG, J., BANG, M.L., GOKHIN, D.S., LU, Y., CUI, L., LI, X., GU, Y., DALTON, N.D., SCIMIA, M.C., PETERSON, K.L., LIEBER, R.L. and CHEN, J., 2008. Syncoilin is required for generating maximum isometric stress in skeletal muscle but dispensable for muscle cytoarchitecture. *American journal of physiology.Cell physiology*, **294**(5), pp. C1175-82.

ZHU, Q., COUILLARD-DESPRES, S. and JULIEN, J.P., 1997. Delayed maturation of regenerating myelinated axons in mice lacking neurofilaments. *Experimental neurology,* **148**(1), pp. 299-316.

ZHU, Q., LINDENBAUM, M., LEVAVASSEUR, F., JACOMY, H. and JULIEN, J.P., 1998. Disruption of the NF-H gene increases axonal microtubule content and velocity of neurofilament transport: relief of axonopathy resulting from the toxin beta,beta'-iminodipropionitrile. *The Journal of cell biology,* **143**(1), pp. 183-193.